Coordination Chemistry Reviews 253 (2009) 977–1055

Contents lists available at ScienceDirect

Coordination Chemistry Reviews

journal homepage: www.elsevier.com/locate/ccr

Review

Bonding and structure trends of thiosemicarbazone derivatives of metals—An overview

Tarlok S. Lobana*, Rekha Sharma, Gagandeep Bawa, Sonia Khanna

Department of Chemistry, Guru Nanak Dev University, Amristar 143005, India

Contents

* Corresponding author.
E-mail address: tarlokslobana@yahoo.co.in (T.S. Lobana).

0010-8545/$ – see front matter
doi:10.1016/j.ccr.2008.07.004

ARTICLE INFO

Article history:
Received 20 June 2007
Accepted 4 July 2008
Available online 15 July 2008

Keywords:
Thiosemicarbazones
Metal complexes
Tertiary phosphines
Analytical applications
Biological applications
Structures
X-ray crystallography
Spectroscopy

ABSTRACT

This review describes the coordination chemistry of thiosemicarbazones and covers all the metals for which complexes are reported. The coordination compounds of d-block, p-block and f-block elements are discussed with respect to their bonding and structures. The description of work is group by group and with a given metal, coordination compounds of all the ligands under purview are described. A brief description of synthesis and spectroscopy of complexes is also given. Several of complexes are mononuclear, with distorted tetrahedral, square planar, square pyramid or octahedral as their common geometries. Dimers, trimers, tetramers, as well as complexes of higher nuclearity are also reported. Variable bonding properties, metallation, metal–metal interactions, role of solvents/other factors in stabilization of sulfur-bridging in coinage metals, and the nature of substituents at azomethine carbon are other interesting features of the review. Further, biological and analytical applications of the ligands/complexes are included in brief so as to indicate the importance of ligands under consideration. The literature survey is complete to December 2007, and some papers of more recent origin are included.

1. Introduction

Thiosemicarbazones ($R^1R^2C^2{=}N^3{-}N^2(H){-}C^1(=S)N^1R^3R^4$) constitute an important class of N, S-donor ligands, and their coordination chemistry was initially explored during the early sixties [1]. The synthesis of thiosemicarbazones involves condensation of a ketone, or an aldehyde with a thiosemicarbazide under ambient conditions [2–4]. Akbar Ali and Livingstone in 1974 first reviewed the chemistry of thiosemicarbazones along with other N, S-donor ligands [5], followed by a review by Campbell in 1975 [6]. The subsequent developments in metal-thiosemicarbazone chemistry were reviewed by Padhye and Kauffman in 1985 [7], West et al. in 1991–1993 [8,9], and latest by Casas et al. in 1999–2000 [10,11]. These reviews have described several aspects of thiosemicarbazones such as synthesis of metal complexes, spectroscopic properties, crystal structures, and biological applications [5–9].

Since 1990, much has been published about transition and non-transition metal complexes with thiosemicarbazones, and a review appears timely, and may be of considerable usefulness. The focus of this review is three-fold: bonding and structures of complexes, biological applications of complexes, and analytical applications such as ion sensors, metal ion extractants, etc. A brief account of synthetic aspects, and spectroscopic properties are given. This review provides a comprehensive account of structurally characterized complexes, and it neither attempts to duplicate information already reviewed, nor lower their importance [5–10]. The original X-ray figures of selective complexes are also given, and figures of all other structurally characterized complexes are given using Chemdraw programme. The biological applications only of structurally characterized complexes are described. The review by West et al. in 1991 gave an earlier account of biological applications [8]. In short, the review attempts to provide an overview of the status of chemistry of thiosemicarbazones. The literature survey is complete to December 2007.

2. Ligands

In this section, a brief account of complexes of thiosemicarbazone ligands with various transition and main group metals is described.

2.1. Types of ligands

Thiosemicarbazones are basically Schiff bases obtained by the condensation of an aldehyde, or a ketone with a thiosemicarbazide, and are broadly classified as mono-thiosemicarbazones and bis-thiosemicarbazones.

$$R_2CO + H_2N{-}NH{-}C(=S){-}NH_2 \rightarrow R_2C{=}N{-}NH{-}C(=S){-}NH_2$$

2.1.1. Mono-thiosemicarbazones

The basic mono-thiosemicarbazone ligand (structure I, Scheme 1) has different, R^1, R^2, R^3 and R^4 substituents, and depending upon the substituents, various sub-classes of ligands are formed. Thiosemicabazones based on aldehydes have hydrogen atom as one of the substituents (R^2) at C^2 carbon, while second substituent R^1 may be an alkyl, an aryl or a heterocyclic group. Similarly, substituents at N^1 nitrogen may be both hydrogen atoms, or one hydrogen, and second alkyl, or aryl group, and finally N^1

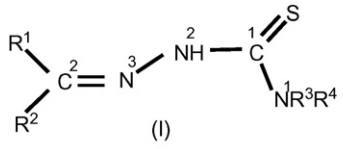

(I)

R^1	R^2	NR^3R^4	
Ph	H	N^1H_2	benzaldehyde thiosemicarbazone (II)
py	H	N^1HMe	N^1-methyl- 2-formylpyridine carbaldehyde thiosemicarbazone (III)
py	H	N^1Me_2	N^1-dimethyl-2-formylpyridine carbaldehyde thiosemicarbazone (IV)
py	H		N^1-hexmethyleneiminyl-2-formylpyridine carbaldehyde thiosemicarbazone (V)

Scheme 1.

Nomenclature

bipy	2,2′-bipyridine
4,4′-bpy	4,4′-bipyridine
dppb	1,4-bis(diphenylphosphino)butane
dppm	1,1-bis(diphenylphosphino)methane
DMF	dimethyl formamide
DMSO	dimethyl sulfoxide
Fc	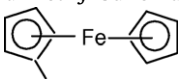
Hbtsc	benzaldehyde thiosemicarbazone
Hbzptsc	benzophenone thiosemicarbazone
Hchtsc	cyclohexanone thiosemicarbazone
Hcptsc	cyclopentanone thiosemicarbazone
Hftsc	furan-2-carbaldehyde thiosemicarbazone
Hmbtsc	*p*-methoxy benzaldehyde thiosemicarbazone
Hptsc	pyrrole-2-carbaldehyde thiosemicarbazone
Hpytsc	pyridine-2-carbaldehyde thiosemicarbazone
Httsc	thiophene-2-carbaldehyde thiosemicarbazone
H_2stsc	salicylaldehyde thiosemicarbazone
pyz	pyrazine
Ph_3P	triphenyl phosphine
thf	tetrahydrofuran

may be a part of the cyclic ring. Some examples (II–V) are shown in Scheme 1 below.

The second category of mono-thiosemicarbazone ligands depends upon the parent ketonic group, and thus both the substituents at C^2 carbon may be same or different alkyl, or aryl groups (VI). Further, in type VII, the parent ketone is cyclic and thus C^2 carbon is part of the ring. The pattern of substituents at N^1 nitrogen is similar to the above type of ligands. Some ligands based on ketones are exemplified here.

Table 1
Metals in a group forming complexes with thiosemicarbazones.

5	6	7	8	9	10	11	12	13	14	15
								Al		
V	Cr	Mn	Fe	Co	Ni	Cu	Zn	Ga		
	Mo	Tc	Ru	Rh	Pd	Ag	Cd	In	Sn	
	W	Re			Pt	Au	Hg	Tl	Pb	Bi
U										

2.1.2. Bis-thiosemicarbazones

Bis-thiosemicarbazones have two arms connected via a ring, or a C—C bond, as for example, shown in structures VIII and IX below, and for more examples one can refer to the text.

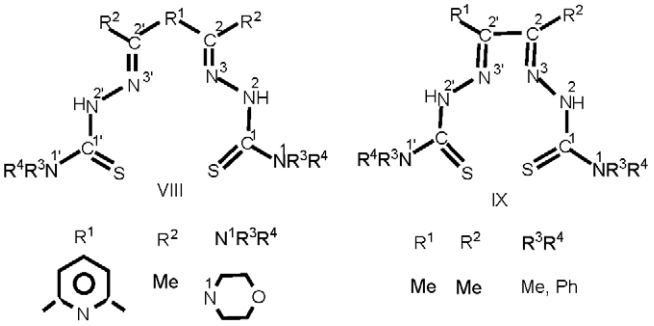

2.2. Bonding modes of ligands

Thiosemicarbazone ligands exist as thione–thiol tautomers (Xa–Xb), and can bind to a metal center in the neutral (Xa), or the anionic forms (Xc). The anionic form is generated after loss of —N^2H (Xa) or —SH (Xb) hydrogen ions. A number of bonding modes have been observed for the thiosemicarbazones in their neutral or anionic forms.

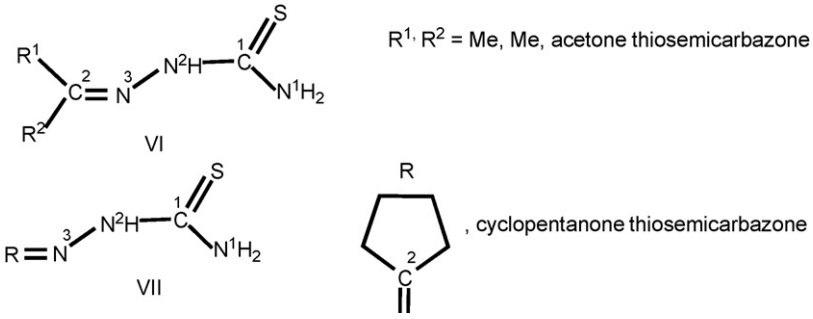

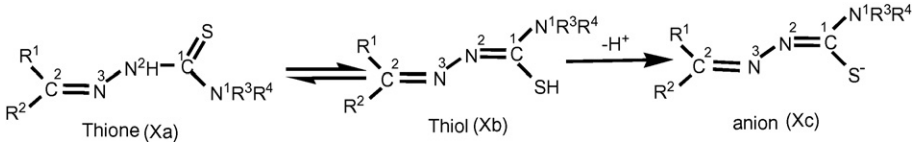

2.2.1. Bonding modes in neutral form

In neutral form, the binding occurs via only S atom in η^1-S (XI), μ_2-S (XII), η^2-N^3, S-chelation (XIII), η^3-N^3, S-chelation and S-bridging (XIV) modes. However, if the substituent at C^2 has a donor atom, and engages in bonding, the additional bonding modes observed are, η^3-X, N^3, S-chelation (XV), η^4-X, N^3, S-chelation and S-bridging (XVI), and η^4-X, N^3, S-chelation and X-bridging (XVI) (e.g. X = N, O) [12–21].

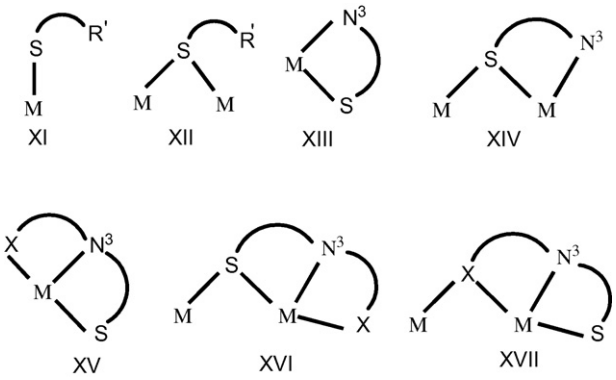

2.2.2. Bonding modes in anionic form

The modes (XI–XVII) shown by the neutral ligands are also exhibited by the anionic ligands, viz. η^1-S, μ_2-S, η^2-N^3, S-chelation, η^2-N^3, S-chelation and S- bridging, η^3-X, N^3, S-chelation, η^3-X, N^3, S-chelation-cum-S-bridging, η^3-X, N^3, S-chelation and X-bridging [22–29]. In addition, η^2-N^2, S (XVIII) and N^2, S-bridging and S-bridging modes (XIX) are identified [30,31]. A rare example of pentacoordination (XX) by a thiosemicarbazone ligand has also been reported [32].

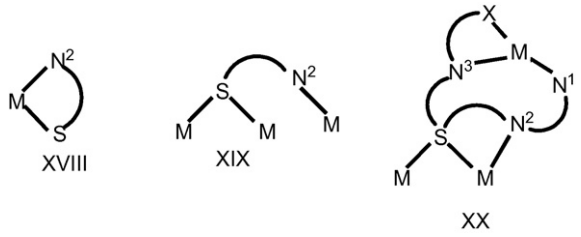

2.2.3. Bonding modes of bis-thiosemicarbazones

Bis-thiosemicarbazones can bind in neutral as well as anionic forms using their both arms. The common coordination modes are XXI and XXII depending on the participation of the central ring connecting the two arms [33–35].

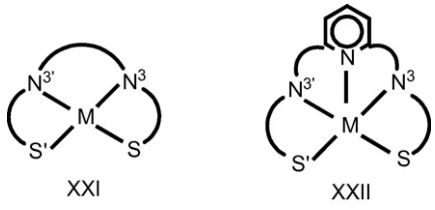

All the modes described above have been characterized by X-ray crystallography, and in some cases the structural description is also confirmed by DFT (density functional theory) calculations [36–44].

2.3. Synthesis of ligands

The preparative methods for thiosemicarbazones were well described by Klayman et al. [45,46], Scovill [47] and Blanksma [48]. In general, a thiosemicarbazide was dissolved in methanol by refluxing for half an hour, however some times a few milliliter of distilled water is added to completely dissolve it. After addition of a given aldehyde or ketone, the reaction mixture is refluxed for 8–10 h and evaporation gave crude sample. It is recrystallized from methanol. For the synthesis of some substituted thiosemicarbazones like 2-ethoxy-4-nitrobenzaldehyde thosemicarbazone, a modification of procedure described by Blanksma [48] is used. In this procedure, 2-ethoxy-4-nitrotoluene was reacted with chromyl chloride (in chloroform) and then treated with thiosemicarbazide (in water) [49]. Another modification involves the use of molecular sieves to induce reaction between an aldehyde or ketone with a thiosemicarbazide in DMF [50]. In some cases to make thiosemicarbazide completely soluble, 1–2 ml of concentrated HCl [51,52] or acetic acid is added [53] to ensure the complete condensation.

3. Survey of literature

3.1. General

Table 1 gives a list of metals whose complexes with thiosemicarbazones have been reported. More complexes are reported with Ru, Co, Ni–Pt, Cu, Zn–Hg, and Sn metals, and relatively fewer with V, Mo, Mn, Re, Fe, Au, Tl, and Pb metals, and finally with Cr, W, Tc, Rh, Ag, Al, Ga, In and Bi metals, only a small number of complexes are known. Generally complexes are mononuclear or dinuclear, and with only a few complexes of higher nuclearity. There are only a few polymeric species. Organometallic complexes are also incorporated.

The structures of complexes characterized using X-ray crystallography are given as Chemdraw figures, and only a few original X-ray structures are incorporated. Table 2 shows NMR data of complexes of some representative ligands, as discussed in Section 3.3. Table 3 shows important bond parameters of some representative complexes, and a brief commentary of the same appears in Section 3.4.10.

3.2. Synthesis

Complexes of 3d metals (Mn^{II}, Fe$^{II,\ III}$, Co^{II}, Ni^{II}, Cu^{II} and Zn^{II}) were generally prepared by the reaction of a metal halide, nitrate, acetate, sulfate, or perchlorate with a thiosemicarbazone in an organic solvent, followed by either refluxing, or room temperature stirring [22,54–71]. However, for some metals, different starting materials have been used. For example, for the preparation of vanadium complexes, the starting materials [$VOCl_2(thf)_2$] [72] and NH_4VO_3 [73] have been used, and likewise Cr^{III} complexes were formed by the reaction of $CrCl_3{\cdot}6H_2O$ with a thiosemicarbazone in presence of solid $NaHCO_3$ in aqueous medium [74–76].

Complexes of 4d and 5d transition metals have been prepared by different routes, which depend on the metal. For molybdenum, $MoO_2(acac)_2$ is used as a starting material, the acac anion is replaced by the thiosemicarbazone ligand during complexation [77–79]. For W, Tc and Re complexes, metal carbonyls, $W(CO)_6$ [80,81], $(NEt_4)_2Tc(CO)_3Cl_3$ [82], and $ReX(CO)_3(CH_3CN)_2$ [83,84], have been used as precursors. For example, tungsten complexes were prepared by the reaction of a thiosemicarbazone with $W(CO)_6$ in presence of trimethyl amine-*N*-oxide in acetone [80,81]. Further, some Re complexes were prepared using [$ReOCl_3(Ph_3P)_2$] [85].

Ruthenium(II) complexes have been prepared from $RuCl_2(PPh_3)_3$ [69–74], $RuCl_2(bipy)_2$ [91], or $Ru_2Cl_4(dppb)_3$ [30], and a thiosemicarbazone, generally in the presence of Et_3N base in toluene/methanol medium. Similarly, Rh^{I}, Pd^{II} and Pt^{II}

Table 2
^{1}H and ^{13}C NMR data (δ, ppm) of thiosemicarbazone ligands and their complexes[a].

Complex	N^2H	C^2H	N^1H_2	Ring protons	References
^{1}H NMR data					
$[Ru(btsc)_2(Ph_3P)_2]$ **59**	–	8.88s	5.03s	6.97–7.90 (m, $C^{2,4-6,8}H$ + Ph)	[25]
$[Ru(pytsc)_2(dppb)]$ **60**	–	8.80s	5.46s	8.52 (d, C^7H); 7.10–7.65 (m, $C^{4,5,6}H$ + Ph)	[25]
$[Pd(pytsc)(Ph_3P)]$ **195**	–	8.25d	4.71s	6.60–6.69 (m, C^5H); 7.40–7.78 (m, $C^{4,6}H$ + Ph)	[22]
$[Pd(Hstsc)(Ph_3P)]$ **192**	–	5.65s	–	5.80 (q, C^5H); 6.49 (dd, C^4H); 7.18 (d, C^6H)	[22]
$[CuX(Hbzptsc)_2]$ **232**	8.78s	–	8.06sbr	7.28–7.60 (m, N^1H_2 + Ph)	[218]
$[CuX(Hbzptsc)(Ph_3P)_2]$ **246**	9.11sbr	–	8.57s, 6.91s	7.29–7.69 (m, Ph + Ph_3P)	[218]
$[CuX(Hftsc)(Ph_3P)]_2$ **250**	10.47sbr	7.98s	7.25br	6.90 (d, C^4H); 6.57 (dd, C^5H); 7.64 (d, C^6H)	[12]
$[CuX(Hptsc)(Ph_3P)]_2{\cdot}2H_2O$ **258**	9.86s; 11.58s(N^4H)	8.02s	7.26sbr	6.93 (d, C^6H); 6.53 (d, C^4H); 6.21 (dd, C^5H)	[12]
$[CuX(Httsc)(Ph_3P)]_2{\cdot}2CH_3CN$ **261**	12.78s	8.36s	6.97s	7.49 (d, C^6H); 7.43 (d, C^4H); 7.06 (dd, C^5H)	[219]
[PhHg(cptsc)] **482**	–	–	5.00sbr	2.60(t, $C^{3,6}H_2$); 2.45 (t, $C^{3,6}H_2$); 1.72(m,$C^{4,5}H_2$)	[98]
[PhHg(mbtsc)] **483**	–	8.11s	5.92sbr	8.16 (d, $C^{5,7}H$); 6.54 (m, $C^{4,8}H$); 3.70 (s, C^9H)	[98]
(PhHg(ptsc)] **484**	11.27s(N^4H)	7.46s	5.21sbr	7.01 (d, C^6H); 6.57 (sbr, C^4H); 6.27 (dd, C^5H)	[98]
[2-pyPh)Hg(Hstsc) **488**	–	7.77s	5.54sbr	7.22 (m, C^6H); 7.01 (dd, C^5H); 6.93 (d, C^8H); 6.83 (d, C^7H)	[309]
$[TlPh_2(cptsc)]$ **504**	–	–	5.02sbr	2.51 (t, $C^{3,6}H_2$); 2.20 (b, $C^{3,6}H_2$); 1.61 (m,$C^{4,5}H_2$)	[105]
$[TlPh_2(pytsc)]$ **507**	–	8.43s	5.51s	8.59 (s, C^7H); 7.79 (t, C^5H); 7.11 (s, C^6H)	[105]
$[SnEt_2(pytsc)(S_2PPh_2)]$ **531**	–	8.75s	7.82s	7.89 (d, C^4H); 8.15 (d, C^5H); 7.68 (m, C^6H); 9.01 (d, C^7H)	[325]

Complex	C^1	C^2	Ring carbon atoms	References
^{13}C NMR data				
$[Ru(btsc)_2(Ph_3P)_2]$ **65**	179.46	147.28	136.06 (C^3); 128.49 ($C^{4,8}$); 127.23 (C^5)	[25]
$[Ru(pytsc)_2(dppb)]$ **60**	182.0	145.2	149.0 (C^7); 155.3 (C^3); 135.8 (C^5); 122.4 (C^6); 120.7 (C^4)	[25]
$[CuX(Hbzptsc)(Ph_3P)_2]$ **246**	176.9	157.9	136.3, 131.1 (C^3); 130.4 (C^6); 129.8, 127.8 ($C^{4,8}$); 128.6 ($C^{5,7}$)	[218]
$[CuX(Httsc)(Ph_3P)]_2{\cdot}2CH_3CN$ **261**	173.8	142.2	137.6 (C^3); 129.3 (C^4); 127.9 (C^5)	[219]
[PhHg(cptsc)] **482**	176.23	167.0	34.37, 31.52, 31.31 ($C^{3,6}$); 24.33, 20.05 ($C^{4,5}$)	[98]
[PHg(mbtsc)] **483**	169.46	165.48	161.81, 161.51 (C^6); 134.45 (C^3); 114.50, 114.14 ($C^{4,8}$)	[98]
(PhHg(ptsc)] **484**	168.93	156.58	138.05 (C^3); 110.35 (C^5); 117.14 (C^6); 123.06 (C^4)	[98]
$[TlPh_2(cptsc)]$ **504**	174.8	172.5	34.9, 34.1, 31.6 (C^3); 25.4, 25.2, 24.8 ($C^{4,5}$)	[105]
$[TlPh_2(pytsc)]$ **507**	181.9	145.5	151.0 (C^3); 148.9 (C^7); 138.8 (C^5); 124.8 (C^4); 126.5 (C^6)	[105]
$[SnEt_2(pytsc)(S_2PPh_2)]$ **531**	175.51	144.74	148.35 (C^3); 125.55 (C^4) 138.57 (C^5); 125.21 (C^6); 156.32 (C^7)	[325]

[a] For ligand NMR, see references [25,98,218].

complexes were prepared using $[RhCl(PPh_3)_3]$ [92], M_2PdCl_4, M_2PtCl_4 (M = Li, K) [22,93–109] and $PdCl_2(PPh_3)_2$ [26] in ethanol. Copper(I) complexes have been generally prepared by the direct reaction of a copper(I) halide with a thiosemicarbazone in presence of PPh_3 as co-ligand [12–16,109–114], or by the treatment of $[Cu(MeCN)_4]PF_6$ with a ligand in the basic medium [31]. There is only one report of electrochemical method for the preparation of Cu^I-thiosemicarbazone complexes [18]. A hexameric Ag(I)-thiosemicarbazone complex has been prepared by reacting $AgBF_4$ with a thiosemicarbazone ligand in DMF using Et_3N base [31]. Gold(I) and gold(III) complexes require precursors such as, $[AuCl(PEt_3)]$ [115], and dichloro[2-(dimethylaminomethyl)phenyl-C′,N)]gold(III), and $[Au(damp\text{-}C,N)Cl_2]$ [116,117]. Mercury(II) complexes have been prepared by treating HgX_2 (X = halide) [118,119], or RHg(OAc) with a thiosemicarbazone in an alcohol [13,120–123].

Organometallic thiosemicarbazone complexes of Al and Ga have been prepared by reacting a trialkyl metal salt, R_3M (M = Al, Ga), with a thiosemicarbazone ligand in toluene [124–126]. Indium(III) complexes were generally prepared using indium(III) halide/nitrate [127], while thallium(III) complexes were prepared using $R_2Tl(OH)$ [R = CH_3, phenyl] [25,128,129]. Tin(IV) complexes were prepared using $SnMe_2O$, $SnMe_2Cl_2$, or Ph_2SnO [130–133]. For lead complexes, $PbPh_2Cl_2$ has been used as a precursor [134,135], however, electrochemical methods are also reported [136]. In case of bismuth, $BiCl_3$, or $Bi(NO_3)_3$ were reacted with a thiosemicarbazone used in acetone [137,138].

3.3. Spectroscopic techniques

The techniques such as NMR, UV–visible, etc. have been used for the characterization of compounds, however, only a brief account of NMR (^{1}H, ^{13}C), IR and ESR spectroscopic trends are given in this section. The ^{31}P and metal nuclei NMR spectroscopic data find mention in the text where applicable.

3.3.1. NMR spectroscopy

The basic component of thiosemicarbazone ligand system can be represented by the moiety: $>C^2{=}N^3{-}N^2H{-}C^1(=S)N^1H_2$; here, C^2 carbon may be forming the part of the ring as discussed in ligand section. NMR (^{1}H and ^{13}C) data of rings at C^2 carbon of some ligands, and of the active thiosemicarbazone moiety as depicted above are only briefly delineated for demonstrating the usefulness of NMR to the metal–ligand bonding (Table 2).

The hydrazinic protons ($-N^2H$) of free ligands appear as single broad peaks in a fairly wide range, δ 8.74–11.57 ppm, depending on the nature of the substituents at C^2 carbon [30,120,121,139]. The interaction of a thiosemicarbazone with a metal substrate induces changes in the position of this signal. For example, the presence of this band at lowfield in Cu^I complexes, namely, $[CuI(Hbzptsc)_2]$ **232**, $[CuX(Hbzptsc)(Ph_3P)_2]$ **246**, $[CuX(Hftsc)(Ph_3P)]_2$ **250**, $[CuX(Hptsc)(Ph_3P)]_2{\cdot}2H_2O$ **258** and $[CuX(Httsc)(Ph_3P)]_2{\cdot}2CH_3CN$ **261** (Table 2), suggested the coordination of a thiosemicarbazone to the metal center in neutral form (XXIIIa). The absence of N^2H proton in the complexes, as listed in Table 2, revealed its deprotonation. The presence of N^4H proton of pyrrole group at δ, 11.58 and 11.27 ppm in complexes $[CuX(Hptsc)(Ph_3P)]_2{\cdot}2H_2O$ **258** and (PhHg(ptsc)] **484**, respectively, showed no coordination of N^4H group [13], whereas its absence in complex [Pd(Hstsc)(Ph_3P)] **192** supports deprotonation of N^4H and its subsequent coordination to the metal center [26].

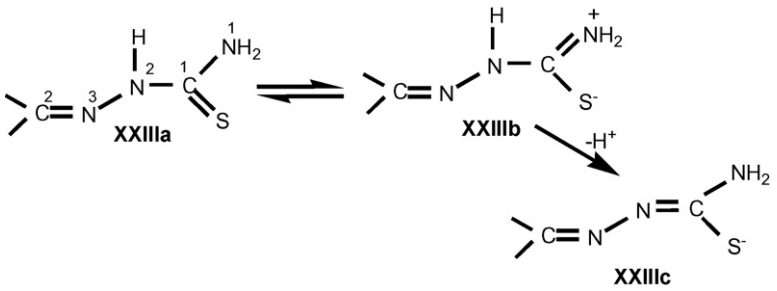

Table 3
Bond parameters of some representative complexes.

Compound [references]	M—S	M—N^3 (N^2)	S—M—N^3(N^2)	M—X X	N^3—M—X
[V^{IV}OCl(L)] **1** [72]	2.358 (1)	2.087 (3)	80.69 (7)	1.914 (2) (O)	99.57 (11)
[Cr(HL)(L)] **8** [75]	2.378 (1)	2.018 (3)	81.9 (1)	1.941 (2) (O)	79.4 (1)
[$Mo^{VI}O_2$(L)(CH_3OH)] **11** [78]	2.442 (1)	2.304 (4)	74.6 (1)	2.402 (1) (S)	80.3 (1)
[$W(CO)_5$(HL)] **21** [81]	2.568 (2)	–	–	–	–
[$Tc(CO)_3$Cl (HL)] **30** [82]	–	2.000 (3)	–	2.194 (3) ($N^{4\prime}$)	–
[ReL_2]Cl **37** [85]	2.284 (1)	2.059 (3)	–	–	–
[FeL_2](ClO_4) **42** [141]	2.224 (2)	1.924 (4)	84.30 (15)	1.966 (4) (N^4)	80.0 (2)
[RuL($bpy)_2$]·(ClO_4) **62** [91]	2.352 (1)	2.115 (3)	80.83 (10)	–	–
[Ru(HL)($PPh_3)_2$Cl]Cl **65** [90]	2.386 (2)	1.984 (5)	83.3 (1)	2.085 (5) (N^4)	77.4 (2)
[$Ru(L)_2PPh_3)_2$] **59** [30]	2.411 (2)	2.145 (5) (N^2)	65.80 (14)	–	–
[$CoL_2]_2$[$CoCl_4$] **111** [185]	2.196 (5)	1.867 (13)	94.7 (4)	2.034 (10) (O)	94.5 (5)
[Co(HL)(L)] **106** [181]	2.203 (1)	1.886 (2)	87.2 (1)	1.963 (2) (O)	83.5
[Co(L)N_3(bpy)] **110** [184]	2.218 (1)	1.901 (2)	87.68 (6)	1.907 (2) (O)	94.9 (1)
[NiL_2] **136** [206]	2.208 (1)	1.934 (4)	84.9 (1)	–	–
[NiL(NCS)] **117** [189]	2.290 (2)	2.131 (5)	83.4 (2)	–	–
[Ni($HL)_2$] **154** [221]	2.373 (2)	2.001 (6)	82.9 (2)	2.062 (6) (N^4)	75.8 (2)
[Pd(L)Br] **190** [22]	2.245 (4)	1.941 (9)	84.9 (3)	2.073 (11) (N^4)	80.6 (4)
[PdL_2] **205** [239]	2.241 (1)	2.105 (1)	80.97 (5)	–	–
[Pd_2L_2(dppm)] **212** [103]	2.348 (2)	2.028 (7)	82.27 (19)	2.046 (7) (C)	81.5 (3)
[Pd_3L_3] **215** [28]	2.259 (1)	2.012 (4)	85.64 (11)	2.000 (3) (O)	93.27 (14)
[Pd_4L_4] **219** [103]	2.377 (10)	2.004 (6)	82.9 (1)	1.997 (7) (C)	81.69 (3)
[Pt(L)Cl] **221** [97]	2.244 (3)	1.962 (8)	85.2 (3)	2.106 (9) (N^4)	80.3 (3)
[$Cu^I(HL)_2$I] **232** [139]	2.229 (1)	–	–	–	–
[$Cu^I(HL)_2$]Cl **248** [18]	2.267 (1)	2.134 (1)	85.71 (4)	–	–
[$Cu^I_6L_6$] **269** [31]	2.447 (7)	2.005 (2) (N^2)	–	–	–
[Cu^{II}(L)(SH)] **276** [257]	2.257 (7)	1.977 (18)	84.80 (2)	2.027 (19) (N^4)	80.44 (7)
[Cu^{II}(HL)Cl] **285** [266]	2.217 (1)	1.967 (3)	85.8 (1)	1.906 (3) (O)	92.9 (1)
[Cu^{II}(HL)Cl_2] **309** [279]	2.275 (3)	1.972 (7)	82.9 (3)	2.038 (8) (N^4)	80.8(3)
[Cu^{II}L(bpy)] **330** [288]	2.260 (1)	1.962 (3)	84.74 (8)	1.941 (2) (O)	92.49 (10)
[$Ag^I_6L_6$] **393** [31]	2.495 (1)	2.274 (4) (N^2)	–	–	–
[Au^{III} (L)Cl(damp-Cl)] **398** [116]	2.247 (2)	2.115 (6)	84.5 (2)	–	–
[Zn($HL)_2Cl_2$] **404** [66]	2.361 (1)	–	–	–	–
[ZnL_2]·H_2O **416** [320]	2.263 (1)	2.053 (2)	–		–
[Zn ($HL)_2$] **432** [323]	2.474 (2)	2.120 (4)	80.2 (1)	2.167 (6) (O)	73.3 (2)
[CdI_2HL] **446** [337]	2.546 (2)	–	–		–
[CdI_2(HL)] **457** [19]	2.591 (2)	2.398 (9)	73.9 (2)	2.350 (8) (N^4)	66.3 (2)
[PhHgL] **482** [120]	2.382 (2)	2.489 (6)	75.69 (13)	–	–
[Hg(HL)Br_2] **480** [19]	2.560 (3)	2.547 (7)	71.5 (2)	2.475 (7) (N^4)	62.9 (2)
[Ga($CH_3)_2$L] **496** [125]	2.328 (3)	2.089 (7)	84.1 (2)	–	–
[InL_2]PF_6 **500** [127]	2.519 (1)	2.230 (4)	78.10 (11)	2.283 (4) (N^4)	71.56 (14)
[$TlPh_2$L] **507** [128]	2.779 (3)	2.547 (7)	68.39 (18)	2.657 (7)	–
[$Tl_2L_2Me_4$] **514**[25]	2.720 (2)	2.657 (4)	66.16 (9)	–	–
[$TlPh_2$L] **505** [356]	2.991 (4)	2.56 (1) (N^2)	55.7 (3)	–	–
[$SnMe_2$(L)L′] **520** [130]	2.456 (2)	2.371 (5)	75.7 (1)	2.822 (5) (O)	66.0 (2)
[Sn(L)R_2] **548** [334]	2.692 (2)	2.437 (5)	71.62 (11)	2.415 (6) (N^4)	66.88 (10)
[PbLPh_2Cl] **554** [134]	2.583 (1)	2.494 (4)	72.31 (9)	–	–

Compound	M···M	[References]	Compound	M···M	[References]
Metal–metal distances in poly-nuclear complexes[a]					
$Ni^{II}(\mu$-O)$_2Ni^{II}$ **175**	2.729	[29]	Pd^{II} (μ-S)$_2Pd^{II}$ **215**	3.412 (1)–3.653 (1)	[28]
$Pd^{II}(\mu$-S)$_2Pd^{II}$ **215**	3.404–4.171	[28]	$Pd^{II}(\mu$-S)$_nPd^{II}$ n = 1, 2, **219**	3.375 (9)–3.434 (9)	[103]
$Cu^{II}(\mu$-O)$_2Cu^{II}$ **361**	3.000 (2)	[298]	Cu^I (μ-S)$_2Cu^I$ **259**	2.99	[13]
$Cu^I(\mu$-I)$_2Cu^I$ **349**	3.097	[12]	Cu^I (μ-S)$_2Cu^I$ **260**	3.232	[13]
$Cu^I(\mu$-I)$_2Cu^I$ **250**	2.980	[13]	$Cu^I(\mu$-S)$_2Cu^I$ **258**	3.008	[13]
$Cu^I(\mu$-I)$_2Cu^I$ **251**	3.224	[13]	$Cu^I(\mu$-S)$_2Cu^I$ **261**	2.7719	[13]
$Cu^I(\mu$-Br)$_2Cu^I$ **257**	3.054	[13]	[$Cu^I(\mu$-S)$_2Cu^I$ **262**	2.8131	[13]
[Cu_6L_6] **269**	3.226(6)[b], 2.8501(5)[c]	[31]	[Ag_6L_6] **393**	3.391 (1)[b], 2.934 (1)[c]	[31]

[a] Mostly bridging cores are shown.
[b] Within ring.
[c] Inter ring.

The amino groups ($-N^1H_2$) of the free thiosemicarbazones show a pair of two broad signals in the ranges, δ 7.17–8.12 and 6.29–7.79 ppm, respectively, due to the restricted rotation of this group about C^1—N^1 bond axis caused by the delocalization of the lone pair of electrons on the N^1H_2 nitrogen (XXIIIa and b) [30,120,139]. In neutral complexes, two bands are observed; however, if a co-ligand like PPh_3 is present, one of the peaks is generally obscured by its phenyl ring protons. Alternatively, the presence of an aromatic ring at C^2 carbon also obscures one of the peaks in some cases. Thus except for complex **246**, which showed two signals for the $-N^1H_2$ group, other complexes of the neutral ligands showed one signal each in the range, δ 6.97–8.06 ppm, for the reasons just outlined. Complexes having anionic thiosemicarbazones, showed a single signal each due to $-N^1H_2$ group at high field in the range, δ 4.71–5.92 ppm. This is attributed to the formation of XXIIIc after deprotonation of $-N^2H$ with the reduction of the double bond character of C^1—N^1 bond, and it leads to the free rotation of N^1H_2 group at room temperature. However, at low temperature, two signals again appear due to a slow or nearly stopping of C^1—N^1 bond rotation at that temperature [120]. The azomethine C^2H protons in the free ligands occur in the range, δ 5.65–9.26 ppm [30,120,139], and these protons show irregular trends in their complexes. In some cases, these were obscured by the ring peaks at C^2 carbon or by the presence of the co-ligands.

In ^{13}C NMR, the signals of C^1 and C^2 carbon atoms of thiosemicarbazones appear in the ranges, δ 177.40–178.86 and δ 132.56–163.43 ppm, respectively [30,120,139]. The C^1 carbon showed an upfield shift (δ 168.93–182.0 ppm) and C^2 carbon showed downfield shift (δ 142.52–172.5 ppm) on complexation. The other ring carbon atoms did not show significant shifts (Table 2).

3.3.2. IR spectroscopy

Thiosemicarbazones ($R^1R^2C^2{=}N^3{-}N^2H{-}C^1(=S)N^1H_2$) exhibit characteristic bands corresponding to various groups in specific energy regions. Like NMR, important information can be derived from the IR spectra of complexes regarding the bonding behavior of the ligands.

The ν(N—H) signals play an important role in evaluating the nature of the bonding in thiosemicarbazone complexes. The bands assigned to ν(N—H) can be split into two regions: (i) 3450–3210 cm^{-1} due to $-N^1H_2$ group, (ii) 3180–3150 cm^{-1} due to $-N^2H$ group. The presence of a band corresponding to $-N^2H$ group, suggests the coordination of a thiosemicarbazone to the metal center in a neutral form, while its absence, is suggestive of deprotonation of hydrazinic $-N^2H$ proton in the complexes. Generally, a high-energy shift is observed in the bands appearing in the region, 3490–3200 cm^{-1} (due to $-N^1H_2$ group), and a slightly lower energy shift in the bands in the region, 3160–3120 cm^{-1} (due to $-N^2H$ group) in case of the spectra of the neutral complexes. However, the anionic complexes (with deprotonated $-N^2H$ group) exhibit vibrational modes due to the $-N^1H_2$ group only, in the range of 3500–3260 cm^{-1}, slightly lower in energy relative to those of the free ligands.

Medium to broad peaks in the region of 1635–1470 cm^{-1} corresponding to $\delta(N^1H_2)$, ν(C=N) and ν(C=C) in the free ligands are shifted slightly to higher or lower energy upon complexation and occur in the range, 1630–1500 cm^{-1}. Coordination of

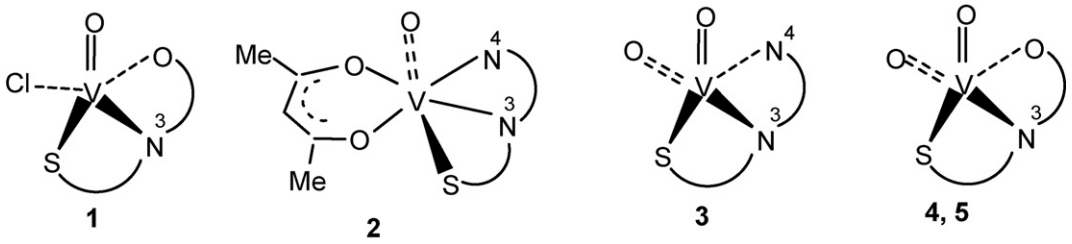

$R^1R^2C{=}N\text{-}NH\text{-}C(=S)NR^3R^4$

R^1	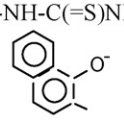			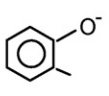	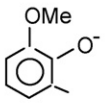
R^2	H	Me	Me	H	H
R^3, R^4	H, H	H, Ph		H, Ph	H, Et
	1 [72]	**2** [141]	**3** [142]	**4** [73]	**5** [143]

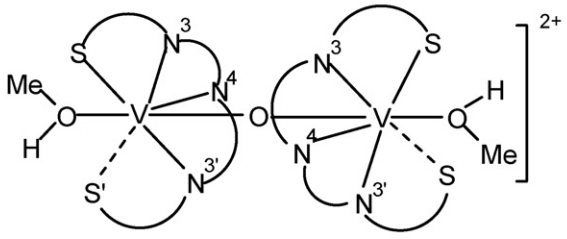

6

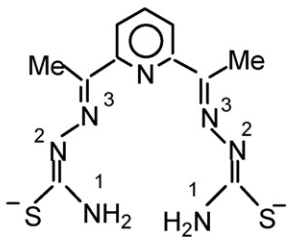

6 [144]

Chart 1.

thiosemicarbazones in neutral form to a metal through its sulfur-donor atom exhibits insignificant shifts in ν(C=S) bands in the region, 850–800 cm^{-1} while anionic complexes show shift to lower energy in the region, 820–790 cm^{-1}. The characteristic bands due to $\nu(P{-}C_{Ph})$ in the region 1098–1095 cm^{-1} are indicative of the presence of coordinated PPh_3 in the complexes [13,30,139,140].

3.3.3. ESR spectroscopy

There is only a limited use of this technique for complexes, and mostly complexes of iron and copper have been studied for their ESR spectra. The relevant information is given in the text where applicable.

3.4. Trends in bonding and structures of complexes

3.4.1. Groups 5–6 elements (V, Cr, Mo, W)

3.4.1.1. Vanadium. Chart 1 depicts complexes of vanadium with thiosemicarbazones in its tetravalent and pentavalent oxidation states, namely, $[V^{IV}OLCl]$ **1** [72], $[V^{IV}O(acac)L]$ **2** [141], $[V^{V}O_2L]$, **3** [142], and $[R_4N]^+[V^{V}O_2L]^-$ {R=H, **4** [73], Et, **5** [143]}. The ligands are uninegative with deprotonation of OH group of R^1 at C^2 carbon (**1**), or $-N^2H$-group (**2** and **3**), and dinegative with deprotonation of both hydroxyl (–OH) and N^2H groups (**4** and **5**). The ligands are tridentate (via O, N^3, S or N^4, N^3, S) and the geometry is distorted square pyramidal for **1**, **3**–**5** and distorted octahedral for **2**, with one oxo group in apical position *trans* to sulfur atom.

A dimeric V^{IV} complex, $[\{V_2L_2(MeOH)_2(\mu\text{-}O)](ClO_4)_2$ **6** [144], was obtained by the reaction of VO^{2+} with an equivalent amount of a bis-thiosemicarbazone, in the presence of excess perchlorate in MeOH. Two octahedral units, {VL(MeOH)} are linked by a μ-O bridge with a linear V–O–V axis (180°). The ligand is dinegative and the geometry of complex is distorted pentagonal bipyramidal with all the donor atoms in the pentagonal plane. The methanol molecules occupy axial positions (Fig. 1).

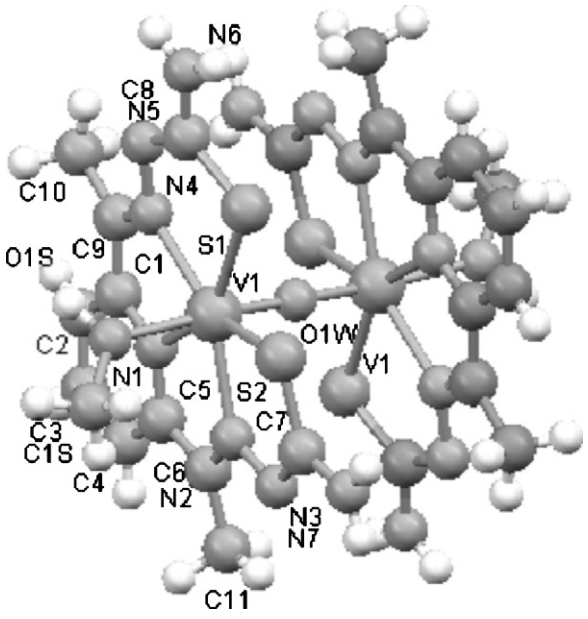

Fig. 1. Structure of $[\{V_2L_2(MeOH)_2(\mu\text{-}O)]^{2+}$ **6** (adapted from reference [144]).

3.4.1.2. Chromium. Chromium(III) complexes, namely, $[Cr(HL)_2](ClO_4)$ **7** [74], and [Cr(HL)(L)] **8**, **9** [75,76] are paramagnetic ($\mu \approx 4.34$ BM) (Chart 2), Ligands undergo deprotonation of –OH protons (**7–9**), as well as loss of $-N^2H$ proton for one ligand in **8** and **9** and are tridentate binding via O, N^3, S-donor atoms, and each complex has distorted *trans*-octahedral geometry.

3.4.1.3. Molybdenum. A series of mononuclear Mo compounds (in VI oxidation state) viz., **10–17**, as well as dimers, **18** and **19** have been reported (Chart 3) [77–79,145,146]. These were prepared by reacting $MoO_2(acac)_2$ or MoO_2Cl_2 with a thiosemicarbazone in ethanol. The ligand is uninegative tridentate in **10** and **11** {deprotonation of R^1—OH group, **10** and R^1—SH group, **11**}, and are dinegative tridentate in other complexes **12**–**17** (deprotonation of —OH/SH and $-N^2H-$ groups). Water and methanol present are coordinated to the metal center in the complexes. The geometry is distorted octahedral for **10**–**12** with *cis*-MoO_2 moiety. In dinuclear complex **18** [78], the ligand is tridentate dinegative (deprotonation of —SH and $-N^2H$ groups), and the geometry is distorted square pyramidal with anti-$Mo^{V}_2O_3$ group. Dichloromethane is present as a solvent of crystallization. Dimer **19** is similar with distorted octahedral geometry around each Mo^{VI} center [145].

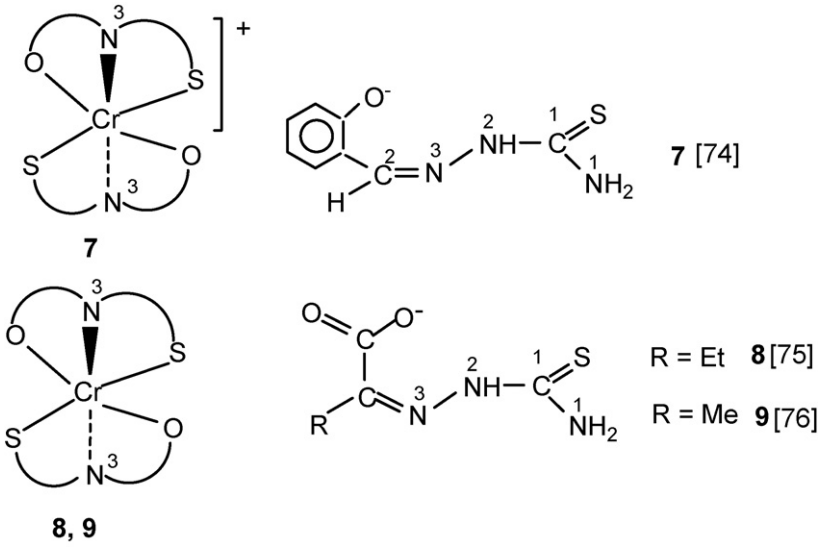

Chart 2.

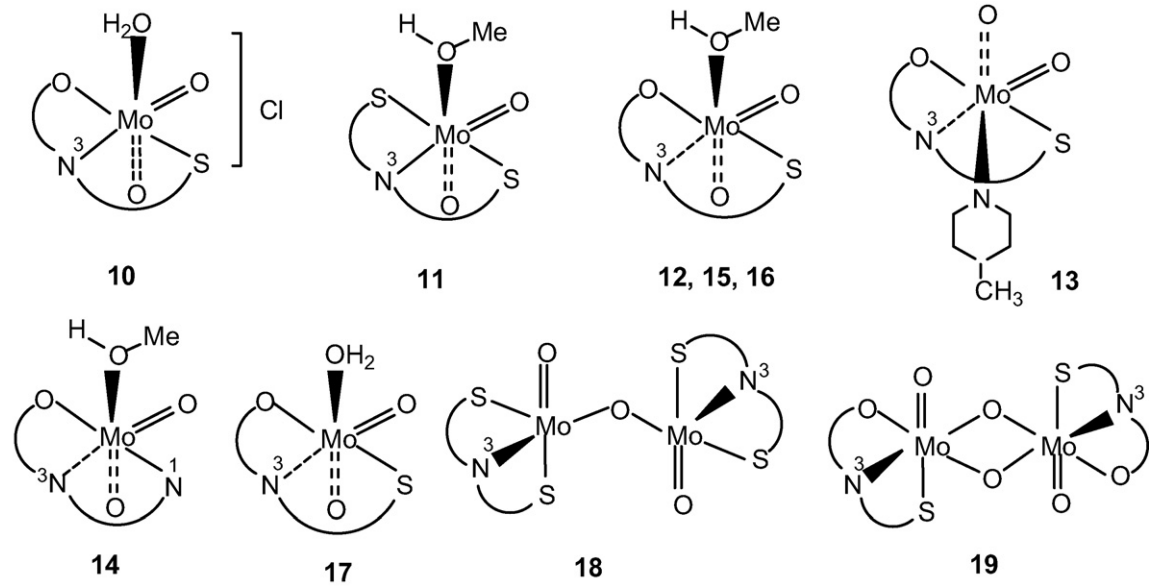

$R^1R^2C{=}N\text{-}NH\text{-}C(=S)NR^3R^4$

R^1	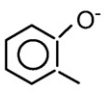	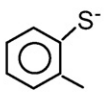	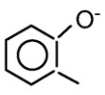	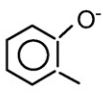	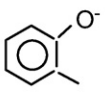	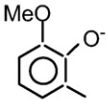	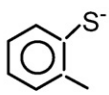
R^2	H	Me	H	H	H	H	Me
R^3	H	CPh_3	H	H	H	H	CPh_3
R^4	H	H	H	H	H	Me	H
	10 [77]	**11** [78]	**12** [79]	**13** [78]	**14** [145], **15** [146] **19** [145]	**16**, **17** [146]	**18** [78]

Chart 3.

3.4.1.4. Tungsten. The substitution of CO by a thiosemicarbazone in $W(CO)_6$ yielded $W(CO)_5(HL)$ **20** [80] and **21** [81] (Chart 4). The neutral ligands coordinate via the S-donor atom only; the W—C bond distance *trans* to S is shorter than the other W—C distances, due to the better π acceptor properties of CO vis-à-vis that of S-donor atom.

3.4.2. Groups 7–8 elements (Mn, Tc, Re, Fe, Ru)

3.4.2.1. Manganese(II). Chart 5 depicts Mn^{II} complexes, namely, $[Mn(HL)_2Cl_2]$ **22** [147], $[Mn(HL)Cl(OH_2)]Cl$ **23** [148], $[MnL_2]\cdot 0.25H_2O$ **24** [55], $[Mn(HL)_2](ClO_4)_2\cdot 0.25H_2O$ **25** (Fig. 2) [56], and $[MnL_2]$ **26**, **27** [54,57] (Chart 5). In octahedral complexes, the ligands are neutral (**22**, **25**) or uninegative (**24**, **26**, **27**) and neutral in the square pyramidal complex (**23**).

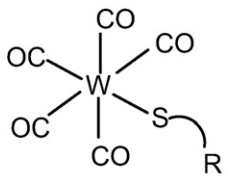

R^1	R^2	R^3	R^4	
Me	Me	H	Me	**20** [80]
Me	Me	H	H	**21** [81]

20, 21

Chart 4.

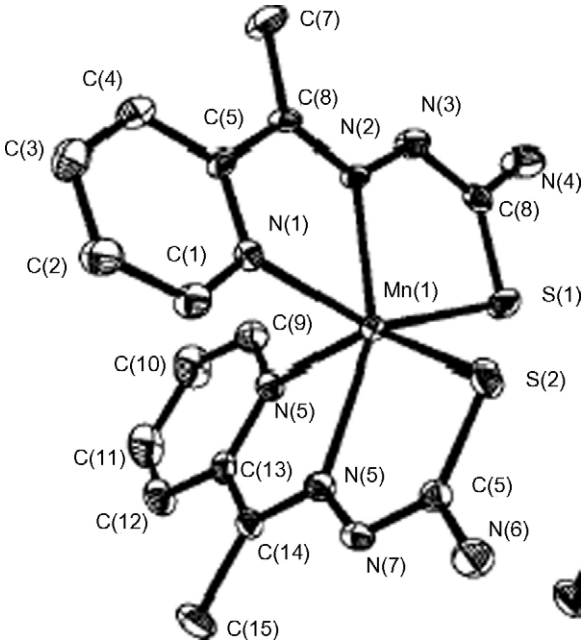

Fig. 2. Structure of $[Mn(HL)_2]^{2+}$ **25** {adapted from reference [56]}.

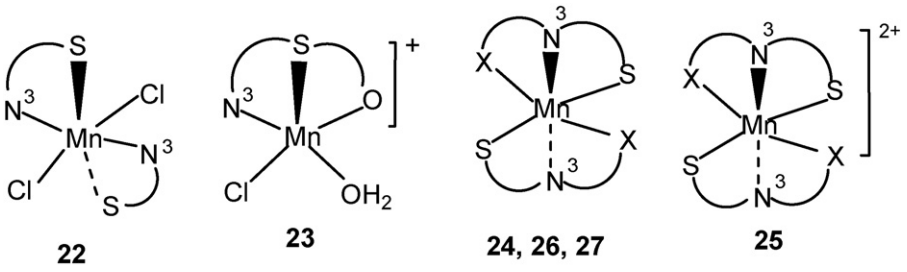

$R^1R^2C{=}N{-}NH{-}C(=S)NR^3R^4$

R^1	Ph	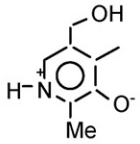	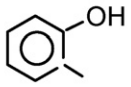		
R^2	H	H	Me	Me	Me
R^3	H	H	H	H	H
R^4	H	H	H	H	Ph
X	-	-	O	N^4	N^4
	22 [147]	**23** [148]	**24** [55]	**25** [56]	**26** [54], **27** [57]

Chart 5.

Bis-thiosemicarbazone ligands form the seven-coordinate pentagonal bipyramidal complexes, $[Mn(HL)(OH_2)_2](ClO_4)_2$ **28** [149], and $[MnL(C_2H_5OH)_2]$ **29** [34]. The ligand is dianionic (deprotonation of $-N^2H$ group) in **29** (Chart 6).

3.4.2.2. Technetium. Only Tc^I forms complexes with neutral thiosemicarbazone ligands, namely, $[Tc(CO)_3Cl(HL)]$ **30**, and $[Tc_2(CO)_6Cl_2(HL)_2]$ **31** [82]. Only the pyridyl groups at the C^2 carbon coordinate to the Tc(I) metal center in **32** and pyridyl nitrogen and thione sulfur atoms coordinate in **31** (Chart 7).

3.4.2.3. Rhenium. Chart 8 depicts a series of octahedral Re^I and Re^{III} complexes, $[Re^IBr(HL)(CO)_3]$ **32–34** [83,84], $[Re^IL(CO)_3]$ **35** (Fig. 3) [150] and $[Re^{III}L_2]Cl$ **36–38** [85]. The ligands are neutral N^3, S-chelating in **32–34**, and uninegative N^4, N^3, S-chelating after loss of N^2H proton in complexes **35–38**. It is unusual that in $[Re^IBr(CO)_3(HL)]$ **39** (Fig. 3) [150], the neutral thiosemicarbazone coordinates through pyridyl N^4 and N^3 atoms only.

Dinuclear Re^I complexes, $Re_2L_2(CO)_6$ **40** and **41** [83] (Chart 9) have uninegative ligands in N^3, S-chelating and S-bridging modes; the geometry around each center is distorted octahedral as before.

3.4.2.4. Iron. A series of octahedral Fe^{III} complexes, namely, $[FeL_2]X$ {X=ClO_4, **42** [144]; **43** [151]; **44** [56], PF_6, **45** [152], NO_3, **46** [151], BF_4 **47** [56]} and $[A][FeL_2]$ {A=NH_4^+, **48** [153], K^+, **49** [154]} have been reported (Chart 10). In complexes **42–47**, the uninegative ligands coordinate to the metal center via N^4, N^3, S-donor atoms, and the dinegative ligands coordinate via O, N^3, S-donor atoms in **48** and

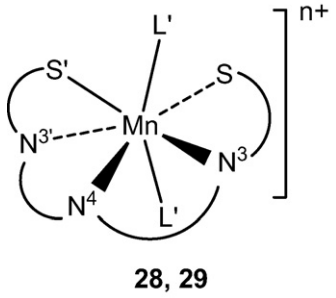

28, 29

R	n	L’	
H	2	OH_2	**28** [149]
Me	0	C_2H_5OH	**29** [34]

L = 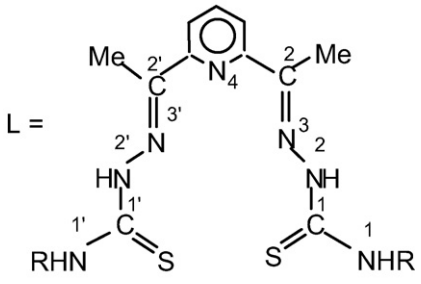

Chart 6.

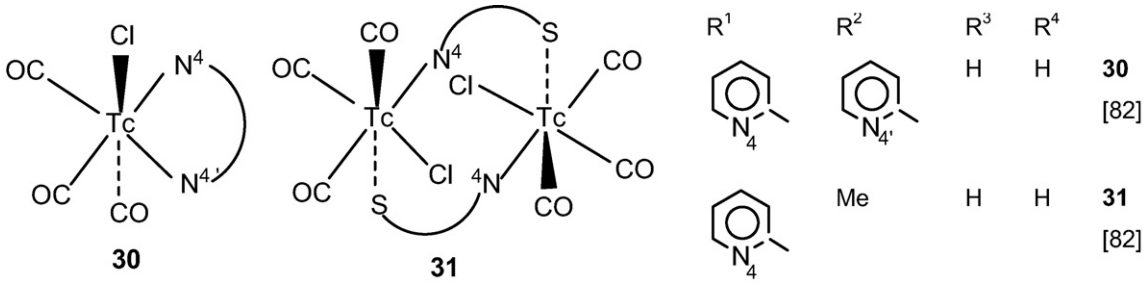

Chart 7.

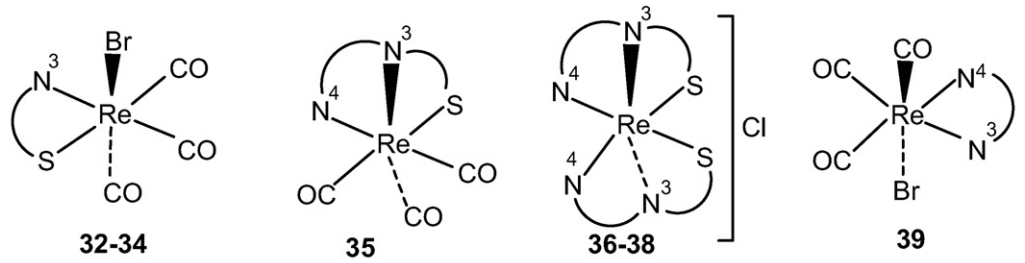

R^1R^2C=N-NH-C(=S)NR^3R^4; Fc = ferrocenyl

R^1	Fc	Fc	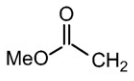					
R^2	H	H	Me	Me	Me	Me	Me	H
R^3	H	H	H	H	H	H	H	H
R^4	Me	H	H	Ph	H	Me	Et	H
	32 [83]	**33** [83]	**34** [84]	**35** [150]	**36** [85]	**37** [85]	**38** [85]	**39** [150]

Chart 8.

49. The cations of $[FeL_2](ClO_4)\cdot H_2O$ **44** [56] (Fig. 4), $[FeL_2](PF_6)$ **45** [152] and $[FeL_2](BF_4)\cdot C_7H_8N_4$ **47** [56] have structures similar to that of **42**. A few Fe^{II} complexes, namely, square pyramidal $[Fe(HL)_2Cl]Cl$ **50** [156], and octahedral $[FeL_2]$ **51** [155], **52** [157], have also been reported. The ligand is neutral (N^3, S-donor) in **50**, uninegative O, N^3, S-donor (deprotonation of —OH group) in **51**, and N^4, N^3, S-donor (deprotonation of $—N^2H$ group) in **52** (Chart 10).

In the solid state, these low spin complexes exhibit axial ESR spectra ($g_{||} = 2.153$, $g_{\perp} = 1.944$, **42**; $g_{||} = 2.097$, $g_{\perp} = 1.982$, **43**; 298 K), but in frozen condition, they show well-defined rhombic spectra with three g values ($g_1 = 2.160$, $g_2 = 2.142$, $g_3 = 1.997$, **42**; $g_1 = 2.162$, $g_2 = 2.145$, $g_3 = 1.994$, **43**; 77 K) [141,151]. The deviation of g values from 2.0037 indicates that the unpaired electron is in d_{xy} orbital with $d^2_{xz}d^2_{yz}d^1_{xy}$ configuration of the low spin iron(III) cations.

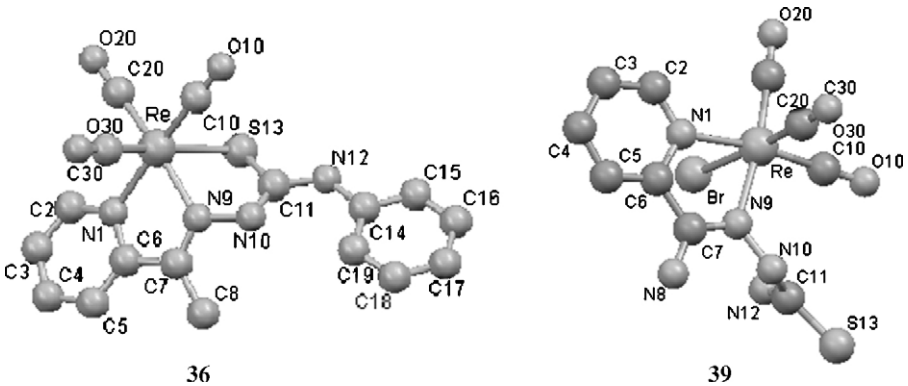

Fig. 3. Structures of complexes $[Re^IL(CO)_3]$ **36** and $[Re^IBr(CO)_3(HL)]$ **39**{adapted from reference [150]}.

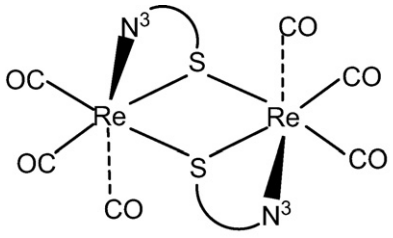

40, 41

R^1	R^2	R^3	R^4	
Fc	H	H	Me	**40** [83]
Fc	H	H	H	**41** [83]

Chart 9.

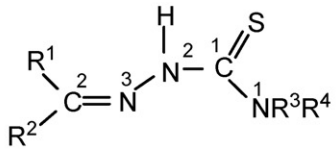

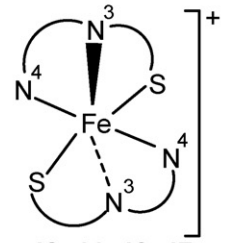

42–44, 46, 47

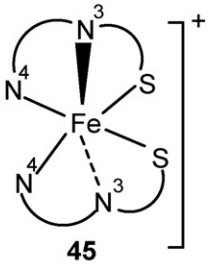

45

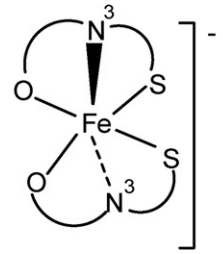

48, 49

R^1	R^2	NR^3R^4	
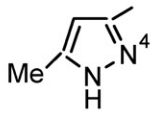	H		**42** [144]
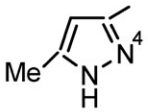	H	$(^nBu)_2N$	**43** [151]
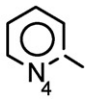	Me	NH_2	**44** [56]
	H	NH_2	**45** [152]
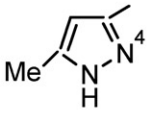	H	$(^nPr)_2N$	**46** [151]
	Me	NH_2	**47** [56]
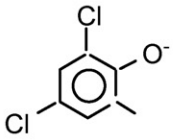	H	NH_2	**48** [153]
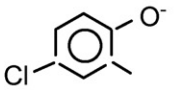	H	NH_2	**49** [154]

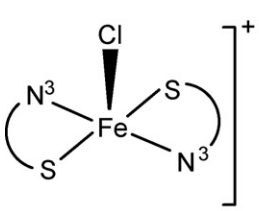

50

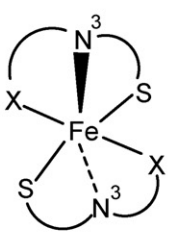

X= O, **51**, N^4, **52**

Me	Me	H	H	**50** [156]
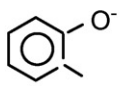	H	H	H	**51** [155]
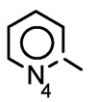	H	H	H	**52** [157]

Chart 10.

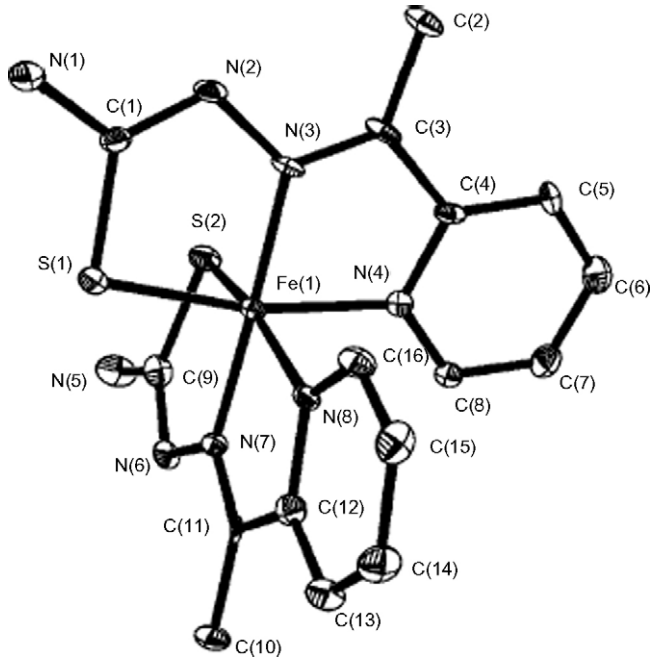

Fig. 4. Structure of complex $[FeL_2](ClO_4)\cdot H_2O$ **44** {adapted from reference [56]}.

A bis-thiosemicarbazone ligand forms the seven-coordinate pentagonal bipyramidal complex, $[Fe(H_2L)(SCN)_2]$ **53** [158] (Chart 11). An octahedral Fe^{II} carbonyl complex **54**, and a mixed valent (Fe^{I}/Fe^{II}) tetranuclear cluster **55** have also been reported [159]. The ligand is uninegative in both these compounds. The C–S bond has broken in one ligand, and the sulfur generated is tetradentate as shown in **55**.

3.4.2.5. Ruthenium. Chart 12 depicts a series of Ru^{II} complexes, namely, **56–64**, with uninegative N^2, S-chelating ligands in $[RuL_2(PPh_3)_2]$ **56–59** (Fig. 5, **59**) [30,86,87,39], $[RuL_2(dppb)]$ **60** {dppb = $Ph_2P–(CH_2)_4–PPh_2$} [30] (Fig. 6, **60**), $[RuL(bpy)_2)](ClO_4)$ **61** [91], and uninegative N^3, S-chelating in $[RuL(bpy)_2](ClO_4)$ **62** [91], and O, N^4, N^3, S-tetradentate in $[RuL(PPh_3)_2)](ClO_4)$ **63** (acetyl oxygen at pyridyl ring is also coordinating) [88]. The ligands are neutral binding via N^3, S-donor atoms in $[Ru(HL)_2(PPh_3)_2](ClO_4)_2\cdot 2H_2O$ **64** [89], and N^4, N^3, S-donor atoms in $[RuCl(HL)(PPh_3)_2]Cl\cdot CH_2Cl_2$ **59** [30]. These bonding modes depend on the substituents at C^2 carbon, and the geometry around each metal center is distorted octahedral. The ^{31}P NMR spectra of complexes **59** and **60** showed single peaks which support that the environment in solution state remain unchanged [30]. The sulfur atoms are usually *trans* when two thiosemicarbazones coordinate to the Ru^{II} center.

An organometallic dinuclear complex $[Ru_2(HL)_2(CO)_4]$ **66** [160] involves which metallation of the cyclopentadienyl ring of the ferrocenyl moiety. The ligand is N^2, S-chelating to Ru^{II} in $[\{Ru(bpy)_2(stsc)\}_4Ni_4](ClO_4)_4$ **67** [32] with four other sites occupied by chelating bipyridine ligands, and the pendant donor atoms, O, N^3, N^1 (as imino moiety $–N^1H–$) {after deprotonation of amino group, $–N^1H_2$} bind to Ni^{II} centers forming repeat unit, $\{(bpy)_2Ru(N^2, S)(Ni(O, N^3, N^1)\}$. Four such repeat units are bridged by coordinate sulfur forming the octanuclear cluster **67**; the ligand is trinegative hexadentate.

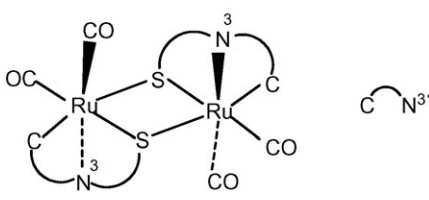

66

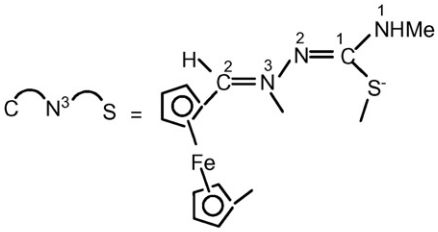

66 [162]

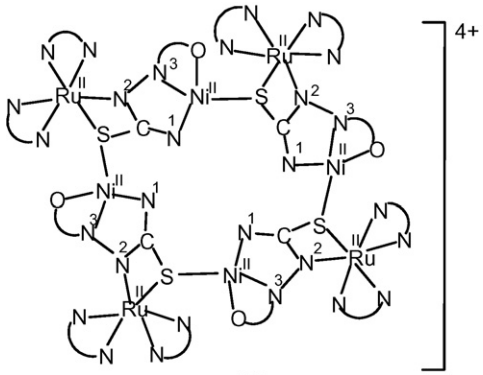

67

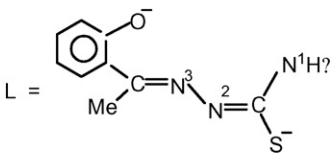

67 [32]

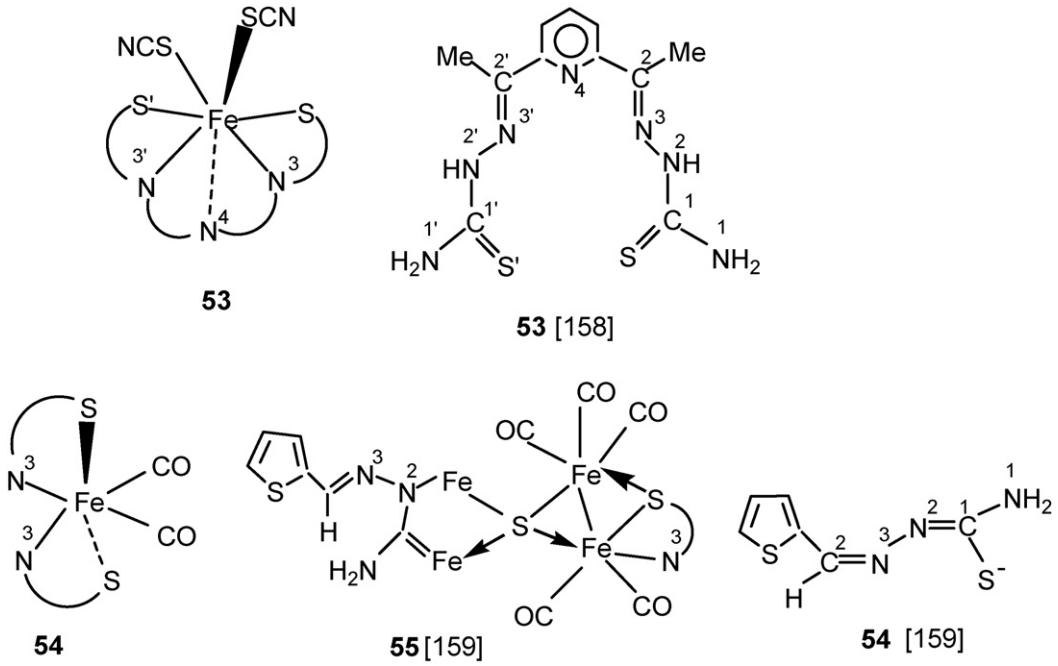

53 **53** [158] **54** **55** [159] **54** [159]

Chart 11.

Reaction of *trans*-[Ru(dppm)$_2$Cl$_2$] (dppm) with thiophene-2-carbaldehyde thiosemicarbazone (HL^1) in the presence of Et$_3$N forms [Ru(η^3-C, N^3, S-L^1)(η^2-P,P-dppm)(η^1-P-dppm)] **68** (Fig. 7), with an unprecedented cyclometalation of a heterocyclic ring in Ru^{II}-thiosemicarbazone chemistry. In contrast, the thiophene ring did not undergo cyclometalation in complexes of monotertiary phosphines of stoichiometry [Ru(η^2-N^2,S-HL^1)$_2$(PR′)$_3$] (R′ = phenyl, **69**; *p*-tolyl, **70**). Benzaldehyde thiosemicarbazone (HL^2) with *trans*-[Ru(dppm)$_2$Cl$_2$] displayed cyclometalation and yielded an organometallic complex [Ru(η^3-C, N^3, S–L^2)(η^2-P,P-dppm)(η^1-P-dppm)] **71** [161]. The cyclometalation in complexes **68** and **71** is attributed to the presence of two types of coordination modes of dppm, namely, both η^1-P-dppm and chelating η^2-P,P-dppm in the same complex.

Pyridine-2-carbaldehyde thiosemicarbazones and its N^1 substituted thiosemicarbazones with Ru(PPh$_3$)$_3$Cl$_2$ form mononuclear Ru^{II} precursors [Ru(N^3,S–HL)$_2$(PPh$_3$)$_2$] **72**–**74** for the generation of trinuclear complexes with copper(I) halides, [(Ph$_3$P)$_2$Ru^{II}(L)$_2$Cu$^{II}_2$X$_2$] **75**–**80** [162] (Fig. 8, **75**). In complexes **75**–**80**, the pendant amino group (–N^{4}H$_2$) loses one hydrogen atom along with the oxidation of Cu^{I} to Cu^{II}. Cyclic voltammetry support the Ru^{II}/Ru^{III} redox behavior of this metal in trinuclear complexes.

3.4.3. Group 9 elements (Co, Rh)

3.4.3.1. Cobalt. Most of these complexes contain Co^{III}, but a few complexes are known in the Co^{II} state. Cobalt(II) halide/perchlorate complexes are of stoichiometry, [CoI$_2$(HL)$_2$] **81** [163], [CoX(HL)$_2$]X (X = Cl, **82**, Br, **83**) [164,165], [Co(HL)(L)]ClO$_4$·H$_2$O **84** and [Co(HL)(L)]ClO$_4$·1.5 MeOH **85** [56] (Chart 13). The ligands bond to the metal center in η^1-S-bonding mode in **81**, and as N^3, S-chelating in **82** and **83** trigonal bipyramidal. In complexes **84** and **85**, one ligand is neutral and second is uninegative.

The *S*-methylated ligand, acetone *S*-methylisothiosemicarbazone shows different bonding properties in, [Co(HL)$_2$Cl]I **86**, and [Co(HL)Br$_2$] **87** [166] complexes, and coordinates via N^1, N^3-donor atoms. The former has distorted trigonal bipyramidal geometry, and the latter has distorted tetrahedral geometry.

Chart 14 shows a series of Co^{III} octahedral complexes, [Co^{III}L$_2$]X **88**, **91**–**94**, **97**–**102** [167–169,171–177], where a uninegative thiosemicarbazone coordinates to the Co center via, N^4, N^3, S, or O, N^3, S-donor atoms (N^4 or O belong to R^1 group, pyrazolyl, pyridine, or uracil moiety at C^2 carbon atom). Fig. 9 shows structure of [Co^{III}(HL)$_2$]$_2$[Fe(CN)$_5$(NO)]·8H$_2$O **96** [178] (Fig. 9), the cation has octahedral structure with nitroprusside anion and water as solvent of crystallization.

Chart 15 depicts another category of octahedral Co^{III} complexes, namely, [Co^{III}(HL)$_2$]Cl **103** [179], [Co^{III}(HL)$_2$](BF$_4$) **104** [180], [Co^{III}(HL)(L)] **105**–**108** (Chart 14) [75,181–183]. In octahedral compound [Co^{III}(HL)$_2$](BF$_4$) **104** [180], there is deprotonation of the –N^{2}H group, while in compound [Co^{III}(HL)$_2$]Cl **103** [179], only the –OH group deprotonates, and thus ligands are uninegative tridentate in both these cases. In **103**–**108**, one ligand ionizes its –OH hydrogen and the second ionizes both its –N^{2}H and –OH hydrogen atoms, and these complexes are similar to Cr^{III} complexes discussed earlier. Interestingly, in complex [Co(H$_2$L)(HL)]·H$_2$O **109** [183], one ligand loses one OH proton with neutral R group, and second loses both OH protons with anionic R group, and there is no deprotonation of –N^{2}H hydrogen.

The azide complex [Co^{III}L(bipy)(N$_3$)] **110** [184] also has an octahedral geometry with the dinegative tridentate thiosemicarbazone ligand (O, N^3, S-donor atoms). The mixed valent complexes, [Co^{III}L$_2$]$_2$[Co^{II}Cl$_4$]·2C$_2$H$_5$OH **111**, **112** [185,186] (Chart 16), have octahedral cations, and ligands are uninegative tridentate (–N^{2}H deprotonation) coordinating via O, N^3, S-donor atoms.

3.4.3.2. Rhodium(III). Only a few rhodium complexes in its trivalent state, namely, [Rh(PPh$_3$)$_2$LX] **113** [92], **114** and **115** [187] (Chart 17) (Fig. 10) are reported. A thiosemicarbazone ligand acts as a dinegative tridentate coordinating via O, N^3, S-donor atoms in **113** and via C, N^3, S-donor atoms in **114** and **115**, with two PPh$_3$ ligands in *trans* positions. In complex [Rh(Ph$_3$P)$_2$LH] **116** [188] (Fig. 11), the thiosemicarbazone ligand undergoes oxidation at the sulfur center where it changes into sulfone and coordinates to rhodium as dianionic tridentate C, N^3, S-donor.

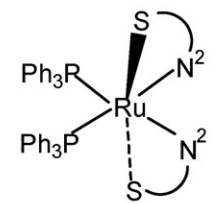

56–59

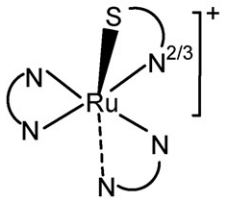

61 (N^2), **62** (N^3)

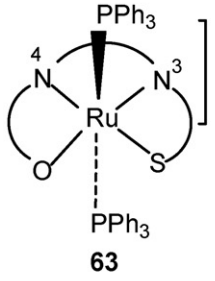

63

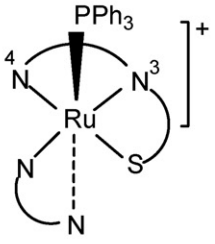

65

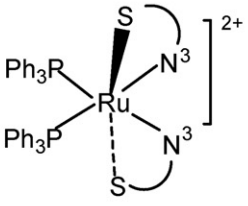

64

	R^1	R^2	R^3, R^4	
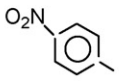		H	H, H	**56** [86]
		H	H, H	**57** [87]
		H	H, Ph	**58** [39]
		H	H, H	**59** [30]
		H	H, H	**60** [30]
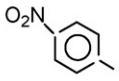		H	H, H	**61** [91]
	Me	Me	H, H	**62** [91]
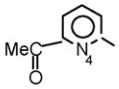		Me	p-tolyl p-tolyl	**63** [88]
		H	H, Cy	**64** [89]
		Me	p-tolyl p-tolyl	**65** [90]

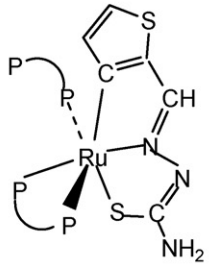

68

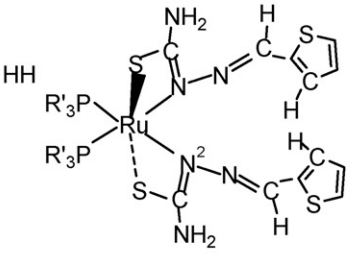

R' = Ph **69** ; p-tolyl **70**

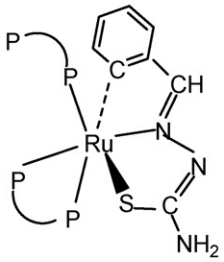

71

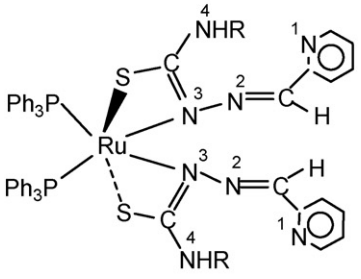

R = H, **72**; Me, **73**; Et, **74**

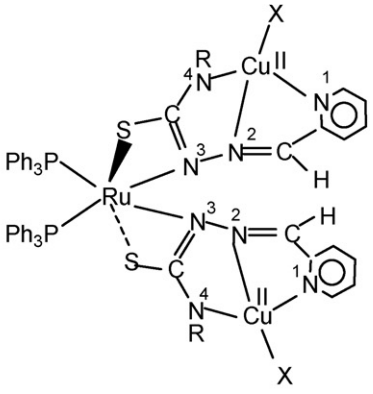

R, X = H, Cl **75**; H, Br **76**; Me, Cl **77**;
R, X = Me, Br **78**; Et, Cl **79**; Et, Br **80**

Chart 12.

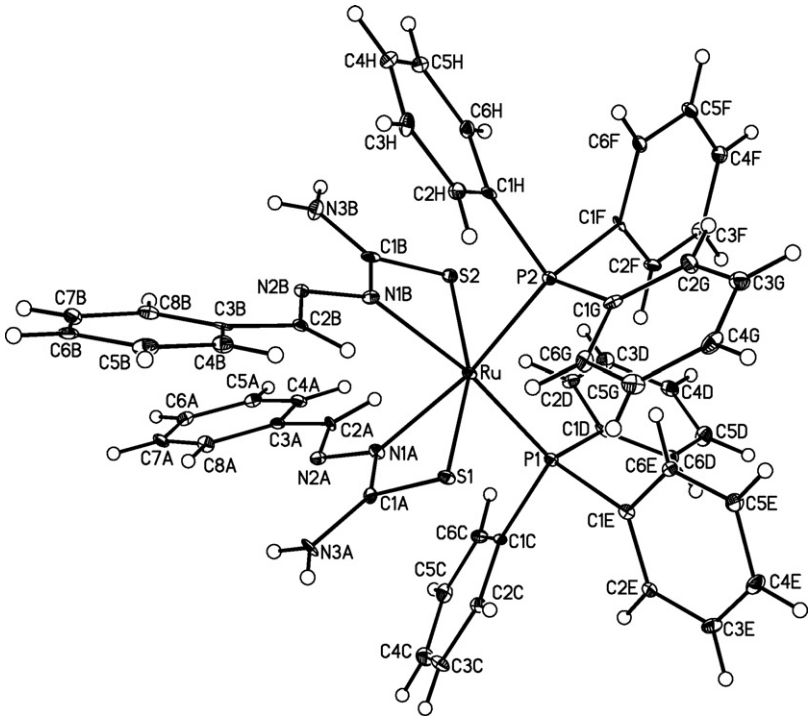

Fig. 5. Structure of complex $[RuL_2(PPh_3)_2]$ **59** {adapted from reference [30]}.

3.4.4. Group 10 elements (Ni, Pd, Pt)

3.4.4.1. Nickel(II). Nickel metal forms many divalent compounds which are monomers, dimers and trimers. The ligands are neutral as well as uninegative or dinegative bidentate or tridentate ligands and involve bridging via O or S-donor atoms.

3.4.4.1.1. Monomers. Chart 18 shows several tetracoordinate Ni^{II} monomeric complexes of type, [NiL(Y)] **117–133** having tridentate ligands [189–204]. In complexes **117–126**, the $-N^2H$, group deprotonates and the ligands bind via N^4, N^3, S-donor atoms, and in complexes **127–132**, the of —OH group deprotonates, and ligands bind via O, N^3, S-donor atoms. The geometry is square planar with the fourth site occupied by Cl, Br, NCS (N-bonding), $MeCO_2$ (**117–126**), or by PPh_3 or NH_3 (**127–132**). The ligand is uninegative tridentate (P, N^3, S-donor atoms) in complex $[Ni(L)Y]NO_3$ **133** [204].

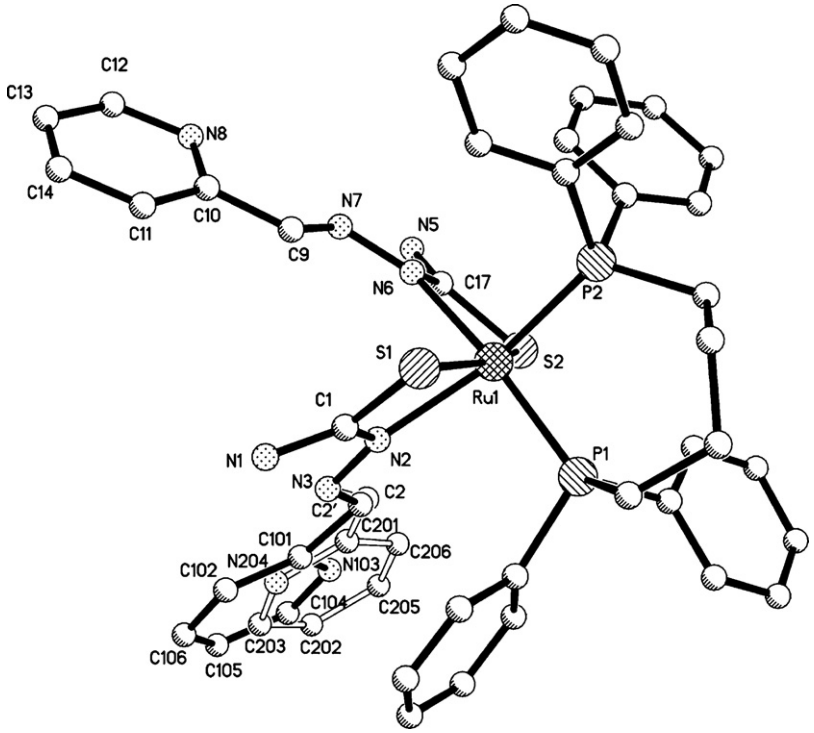

Fig. 6. Structure of complex $[RuL_2(dppb)]$ **60** {adapted from reference [30]}.

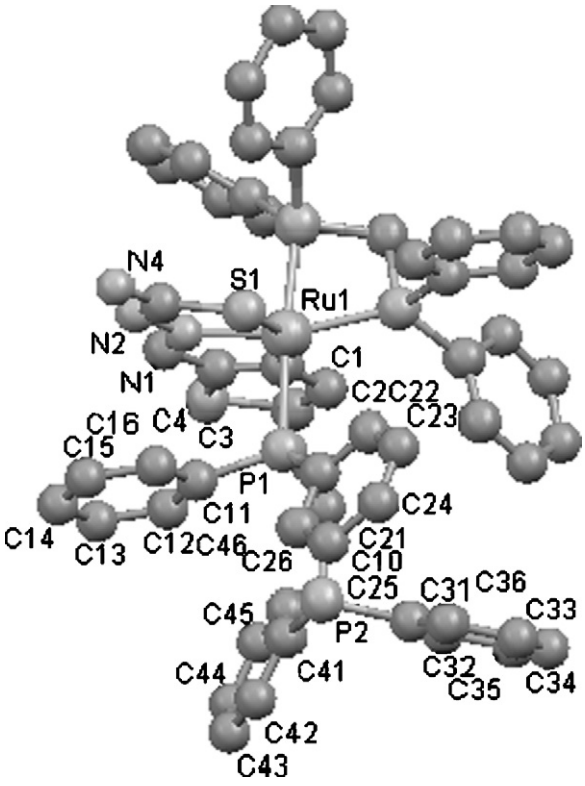

Fig. 7. Structure of complex [Ru(η^3-C, N^3, S–L^1)(η^2-P,P-dppm)(η^1-P-dppm)] **68** {adapted from reference [161]}.

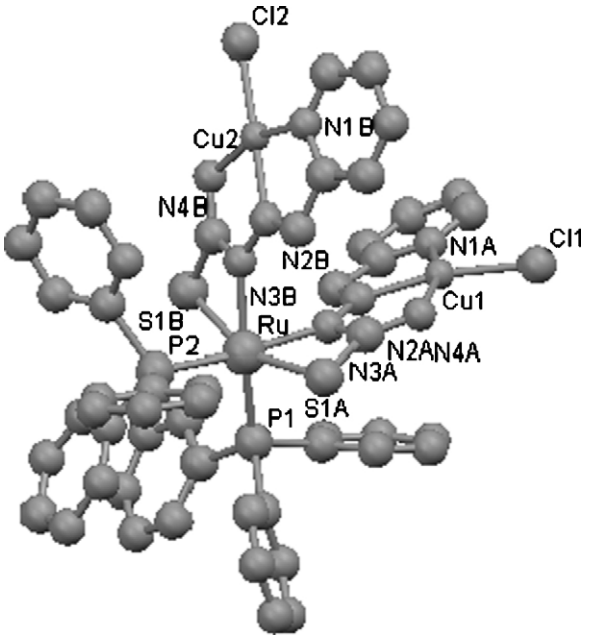

Fig. 8. Structure of complex [$(Ph_3P)_2Ru^{II}(L)_2Cu^{II}{}_2Cl_2$] **75** {adapted from reference [162]}.

Another category of square planar complexes, namely, [NiL_2] **134–144** [24,205–214], have two anionic thiosemicarbazone ligands binding via N^3 and S-donor atoms (Chart 19). The donor atoms are in *trans* positions in centrosymmetric complexes, **134–141** and **144**, while they are in *cis* positions in complexes **142–143**, possibly due to the more bulky groups at C^2 carbon.

In octahedral [NiL_2] **145–150** [185,215–218] and [NiL_2]·$2H_2O$ **151** [219] complexes, the uninegative tridentate ligands (deprotonation of –N^2H) coordinate via X, N^3, S-donor atoms (X = O, N^4, Chart 20).

The neutral ligands coordinate to the metal center, via N^4, N^3, S-donor atoms in the ionic complexes, [$Ni(HL)_2$]X_2 (X = Cl, ClO_4, NO_3) **152–158** [176,217,143,220–223], and via O, N^3, S-donor atoms (oxygen is from neutral –OH group) in complexes **159** [224] and **160** [225] (Chart 21). Similarly there is N^3, S-chelation in the ionic complexes [$Ni(HL)_2X]^+X^-H_2O$ (X = O_2NO, **161**; Cl **162**) [226]. The cations have octahedral (**161**) or trigonal bipyramidal (**162**) structures and N^3 atoms are axial in the latter.

A series of bis-thiosemicarbazone complexes, [NiL] **163–174** are shown in Chart 22 [33,217,227–233]. Bis-ligands are dinegative after deprotonation of the –N^2H group, and bind in a variety of modes. For example, in square planar compound **163**, it is the N^2 nitrogen of one arm, N^3 and S atoms of second arm, along with pyridyl nitrogen (N^4), which bind to the metal center. In compound **164**, Ni^{II} has a pseudooctahedral coordination with *cis*-S_2 (thioether), *trans*-N^3 and *cis*-S_2 (thiolate) donor atoms, while in **165** and **166**, there is symmetrical N^3, S-coordination from both arms of the bis ligand. Complexes **167**–**174** are similar to **165** [228] in bonding and structure.

3.4.4.1.2. Dimers and trimers. The di- and tri-nuclear complexes **175**–**179** [29,234,201] are shown in Chart 23. The ligands coordinate to the Ni^{II} center via O, N^3, S-donor atoms in dimeric Ni_2L_2 **175**, **176** complexes – dimerization occurring through the oxygen atom. The geometry around each metal center is distorted square planar. The dimerization in **177**, **178** is via N^4O oxygen rather than through the phenolic oxygen. The only known trimeric com-

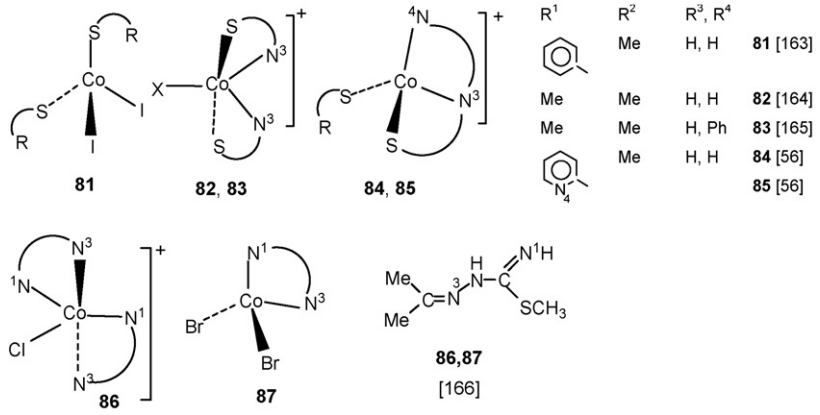

Chart 13.

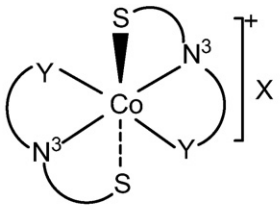

88-90, 94-102

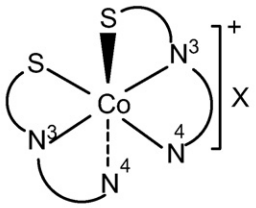

91 - 93

R^1							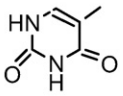		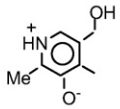
R^2	H	Me	Me	H	H	H	H	H	H
R^3, R^4	H, H	H, Me	H,n- Pr	H, H	H, H	H, H	H, H	H, Me	H, H
Y	N^4	N^4	N^4	N^4	N^4	N^4	O	O	O
X	SCN	BF_4	BF_4	ClO_4	NO_3	Cl	SO_4	BF_4	$[Fe(CN)_5(NO)]^-$
	88	**89**	**90**	**91**	**92**	**93**	**94**	**95**	**96**
	[167]	[174]	[172]	[177]	[169]	[169]	[176]	[175]	[178]

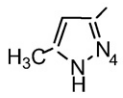

R^2	H	H	H	H	H	H
NR^3R^4	NH Cy	$N(Pr^n)_2$	NEt^2	NEt_2		$N(Bu^n)_2$
X	Cl	NO_3	ClO_4	BF_4	Br	NO_3
	97	**98**	**99**	**100**	**101**	**102**
	[168]	[171]	[172]	[172]	[173]	[176]

Chart 14.

plex **179**, has two Ni atoms with distorted square planar geometry, while the third Ni atom is octahedral.

3.4.4.2. Palladium(II). Square planar mono-, di-, tri-, and tetra-nuclear complexes of Pd^{II} have been reported. The ligands are deprotonated and act as mono-, bi-, tri- or tetradentate.

3.4.4.2.1. Monomers. Chart 24 depicts mononuclear [PdLX] complexes, {X = Cl, **180–189**; Br, **190**, **191**; Ph_3P, **192** (Fig. 12)}, [22,26,93–95,97–101], [PdLX] {X = Cl **193** [96]; py, **194** [235]; Ph_3P,

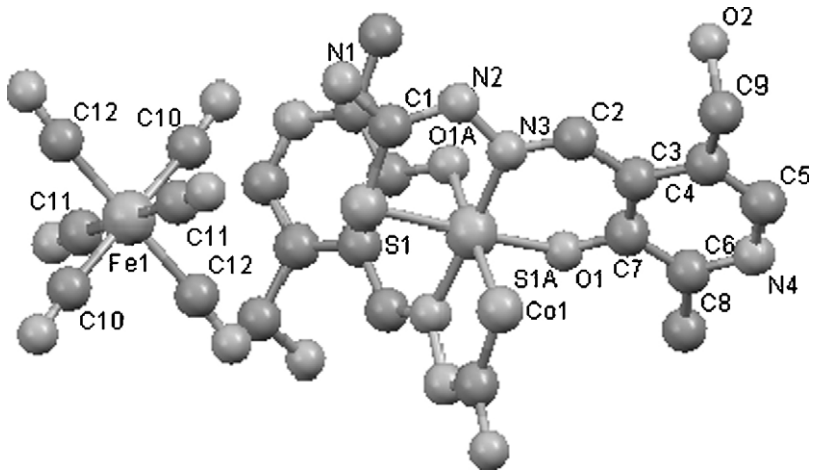

Fig. 9. Structure of complex $[Co(HL)_2][Fe(CN)_5(NO)]\cdot 8H_2O$ **96** {adapted from reference [178]}.

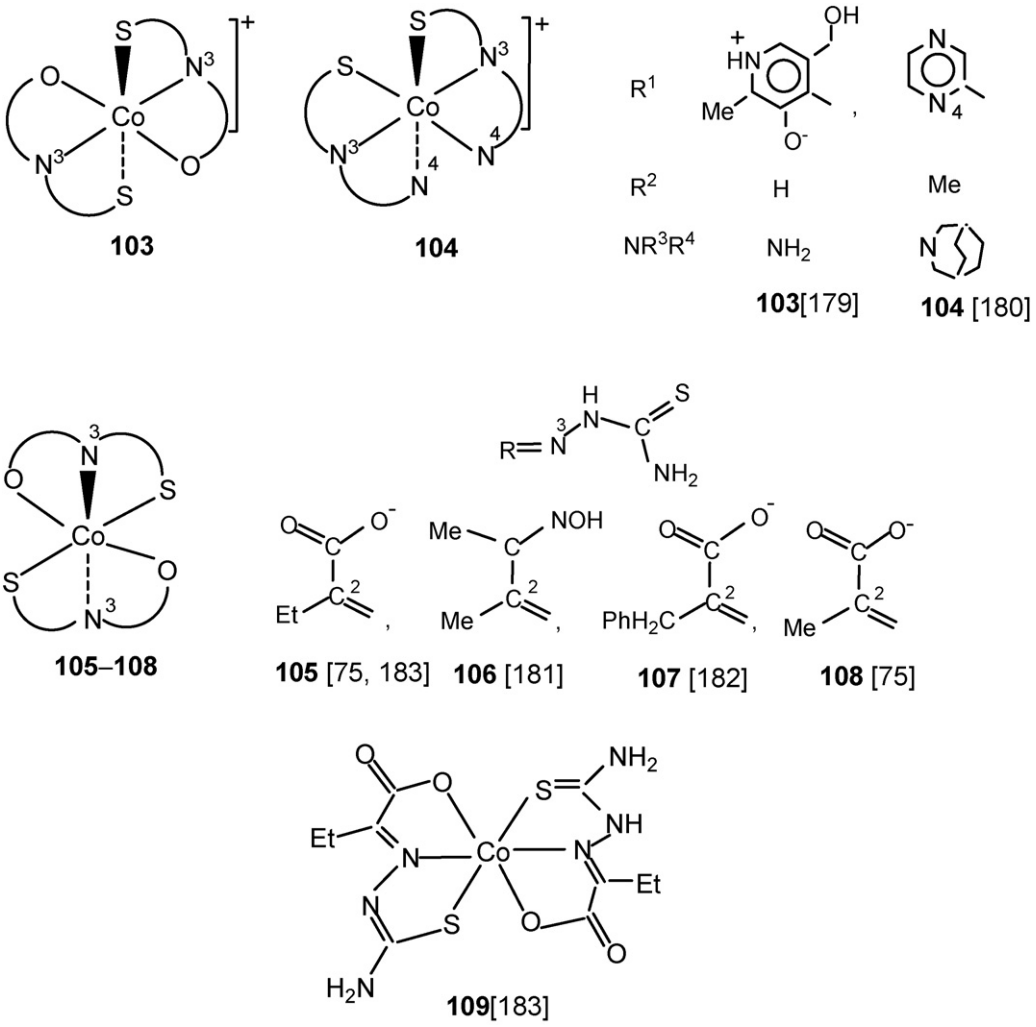

Chart 15.

195 (Fig. 13), **196** (Fig. 14) [26,27], [PdL′] {L′ = $MePh_2P$, **197** [102], Ph_3P, **198** [103], dppm, **199**–**200** [236]}. The ligands are uninegative N^4, N^3, S-donors in **180**–**192**; uninegative O, N^3, S-donor in **193**, and dinegative O, N^3, S-donor in **194** and **194** (one site occupied deprotonated –OH group). In complex **192**, an unusual deprotonation of –N^4H– of pyrrole ring takes place and the ligand is dinegative tridentate (Fig. 12). Finally, in **197–198**, the ligands are again dinegative with one site occupied by the carbon atom of a ring at C^2. In

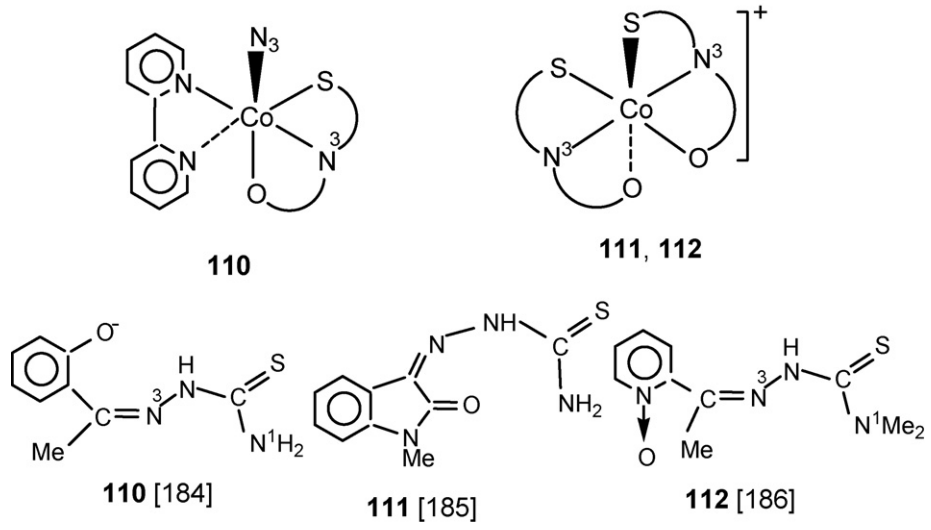

Chart 16.

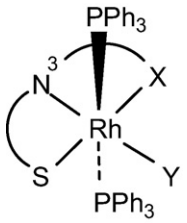

113–115

	R^1			
	R^2	H	H	H
	NR^3R^4	NH_2	NH_2	NH_2
	X	O	S	S
	Y	Cl	H	Cl
		113	**114**	**115**
		[92]	[187]	[187]

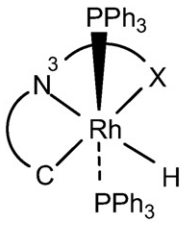

116

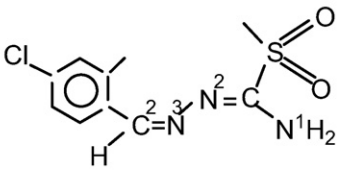

116 [188]

Chart 17.

these complexes, metallation of phenyl rings occurs in the presence of tertiary phosphines. The ^{31}P NMR spectra of complexes **192** and **195** showed that the solid state structures are intact in the solution state ($\Delta\delta$, 33.9, **192**; 30.1 ppm, **195**).

The uninegative ligands chelate through N^3, S-donor atoms in *trans* square planar complexes, $[PdL_2]$ **201–204** [208,209,237,238] (Chart 25), while in $PdL_2{\cdot}3H_2O$ **205** [239], $[PdL_2]{\cdot}CH_3OH$ **206** [58] and $[PdL_2]{\cdot}CHCl_3$ **207** [59] complexes, there is *cis*-disposition of S-donor atoms. Inter- and intra-molecular stacking interactions contribute to the *cis*-structure of complexes **205–207**. One ligand is X, N^3, S-donor in [PdLL′] {X = N^4, **208** [22], **209** [60]; O, **210** [240] (Fig. 15)} and the second is bonded only via the S-donor atom. The ligand is dianionic tetradentate complex [PdL] **211** [61].

3.4.4.2.2. Dimers. The phenyl rings at C^2 carbon involve metallation in the dinuclear complexes $[Pd_2L_2(dppm)]{\cdot}CH_3COCH_3$ **212** [103] (dppm = $Ph_2PCH_2PPh_2$), and $[Pd_2LCl_2(dppm)]$ **213** [241]. The former has bridging dppm and the latter has both sulfur and dppm as bridging moieties. Dimeric complex, $[Pd_2L_2]{\cdot}$DMSO **214** with a dianionic bis-thiosemicarbazone ligand [242] has three coordination sites of a metal center occupied by S, N^3, N^4-donor atoms of one ligand, while the fourth site is occupied by the sulfur-donor atom of the second ligand. An interesting feature is that the deprotonation of —N^2H— takes place only from one arm of the bis ligand and the second proton loss occurs from the central ring (Chart 26).

3.4.4.2.3. Trimers and tetramers. In the trinuclear complexes, $[Pd_3L_3]{\cdot}$DMSO **215** [28], and $[Pd_3L_3]{\cdot}$DMF **216** [243], the dinegative ligand coordinates to a Pd^{II} center via O, N^3, S-donor atoms forming a neutral repeat species Pd(O, N^3, S), and three such species combine via S atoms to form trinuclear complexes, with the central six-membered Pd_3S_3 ring adopting chair conformation (Chart 27). Tetranuclear complexes $[Pd_4L_4]$ **217** and **218** involve binding via C, N^3, and S-donor atoms [103,244] and complex **219** binds via N^4, N^3, S-donor atoms [245]. The coordinate sulfur bridges Pd centres, and the central core Pd_4S_4 is an eight-membered twisted ring of

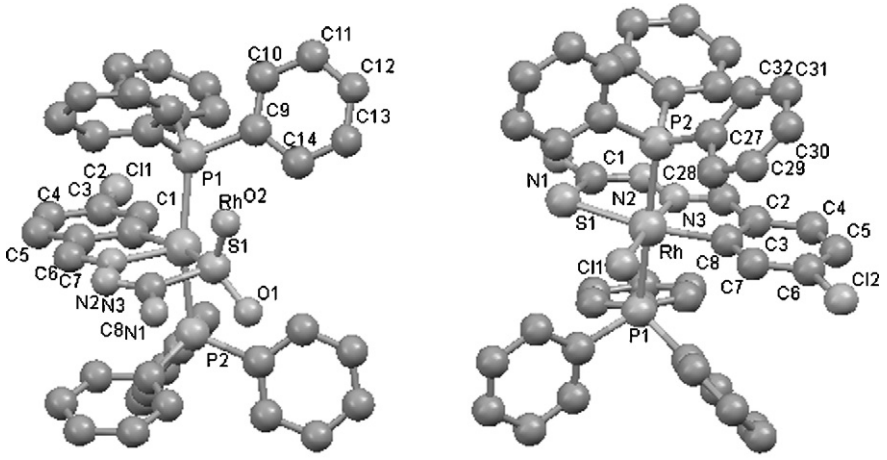

114 **115**

Fig. 10. Structure of complexes $[Rh(PPh_3)_2LH]$ **114** and $[Rh(PPh_3)_2LCl]$ **115** {adapted from reference [187]}.

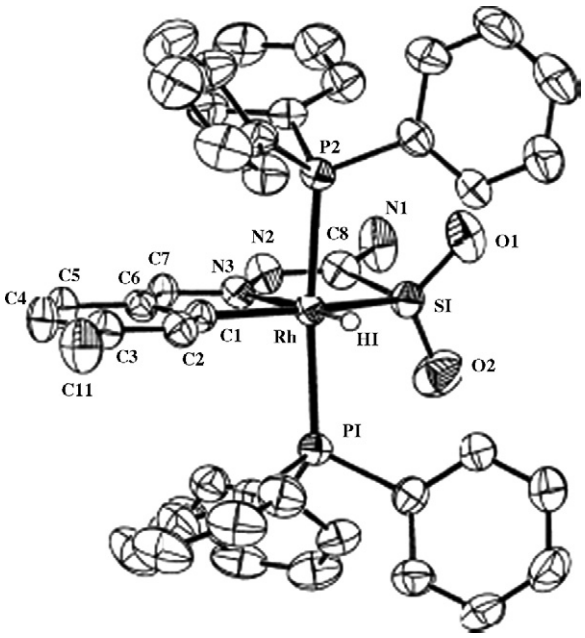

Fig. 11. Structure of complex [Rh(Ph$_3$P)$_2$LH] **116** {adapted from reference [188]}.

alternate Pd and S atoms. As in compounds **197** and **198**, the Pd—C bond formation occurs in **217** and **218**, involving a pendant phenyl group at C^2 carbon for metallation.

3.4.4.3. Platinum. Chart 28 depicts mononuclear distorted square planar Pt^{II}complexes with the general formulae, [PtLCl] **220–225** [97,105–108], and [PtL$_2$] **226** [109]. In complexes **220**, **223**, and **225**, the ligand L is uninegative tridentate coordinating via N^4, N^3, S or P, N^3, S-donor atoms. In complex, [PtL(H$_2$L)] **227** [240] (Fig. 16), one ligand is dinegative tridentate coordinating via O, N^3, S-donor atoms, and the second ligand is neutral monodentate coordinating via S-donor atom only. Complex **224** [107] is a case of metallation by the aromatic ring at C^2 carbon of the R^1group and the ligand is dinegative tridentate coordinating via C, N^3, S-donor atoms. Bis-thiosemicarbazones also form square planar complexes, [PtL] **228**, **229** [246,247], in which the ligand is tetradentate (N^3, S, N^3, S-donor atoms). In addition, a tetranuclear complex [Pt$_4$L$_4$] **230**, similar to that of Pd is known [244].

3.4.5. Group 11 elements (Cu, Ag, Au)

Copper complexes of different nuclearity occur with both Cu^I and Cu^{II} oxidation states. Copper(I) forms monomeric, dimeric, tetrameric, and hexameric complexes, and likewise, copper(II) forms monomers, dimers, tetramers and polymers. The coordina-

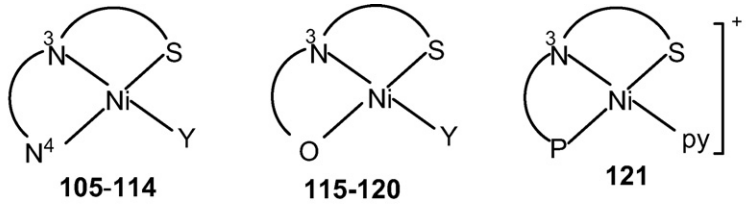

R^1									
R^2	Me	Me	Ph	Me	Me			H	Me
NR^3R^4	NH_2	NMe_2	NH_2				NMe_2		
Y	NCS	Cl	Cl	NCS	OCO_2Me	Cl	Cl	Br	Br
	117	**118**	**119**	**120**	**121**	**122**	**123**	**124**	**125**
	[189]	[190]	[191]	[192]	[193]	[194]	[195]	[196]	[196]

R^1								PPh_2
R^2	Me	H	H	H	H	H	H	H
NR^3R^4	NMe_2	NH_2	NH_2	NHPh	NH_2		NHMe	NH_2
Y	Cl	PPh_3	NH_3	NH_3	NH_3	NH_3	NH_3	Py
	126 [197]	**127** [198]	**128** [200]	**129** [201]	**130** [199]	**131** [202]	**132** [203]	**133** [204]

Chart 18.

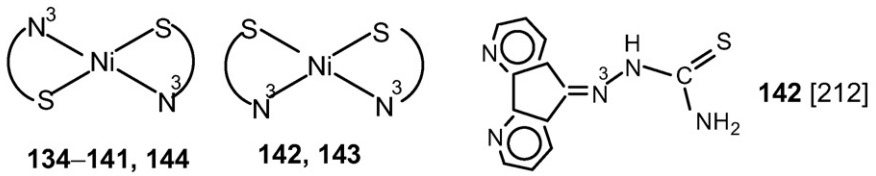

R^1	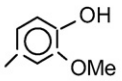			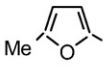	
R^2	H	H	H	H	H
R^3, R^4	H, H	H, H	H, H	H, H	H, Me
	134 [205]	**135** [24]	**136** [206]	**137** [207]	**138** [209]

R^1			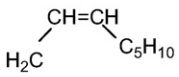	Fc	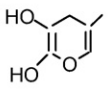
R^2	H	H	H	Me	H
R^3, R^4	H, H	H, H	H, Ph	H, H	H, H
	139 [209]	**140** [210]	**141** [211]	**143** [213]	**144** [214]

Chart 19.

tion number around Cu center varies from 3 to 6, and the geometries are distorted trigonal planar, tetrahedral, square planar, square pyramid, or octahedral. Only a few compounds with Ag^{I} and $Au^{I,III}$ have been reported.

3.4.5.1. Copper(I).

3.4.5.1.1. Monomers and dimers. Chart 29 depicts copper(I) halide mononuclear complexes, $[Cu(\eta^1\text{-S–HL})_2X]$ {X = Cl, **231** [110]; I, **232** [249]} (Fig. 17, **232**), $[CuX(\eta^1\text{-S–HL})(Ph_3P)_2]$ {**233–244** [13,112–114,248] (Fig. 18, **241**), and $[Cu(HL)_2]Cl$ **248** [18]. Neutral thiosemicarbazone ligands coordinate via a S-donor atom in complexes **231**–**247**. Complexes have either trigonal planar (**231**, **232**) or distorted tetrahedral geometry (**233**–**249**). The geometry of N^3, S-chelated complex **248** is more distorted.

A series of dimeric complexes are also reported with two types of central cores, $Cu(\mu\text{-}X)_2Cu$ (**249–258**), (Fig. 19, **257**)

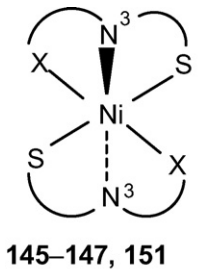

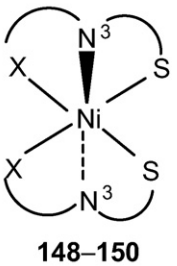

R	NR^3R^4	X	
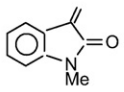	NH_2	O	**145** [185]
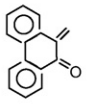	NH_2	O	**146** [215]
R^1, R^2	NR^3R^4	X	
 , H	NH_2	N^4	**147** [216]
 , Me		N^4	**148** [217]
 , Me	NH_2	N^4	**149** [217] **151** [219]
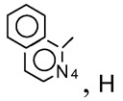 , H	NH_2	N^4	**150** [218]

Chart 20.

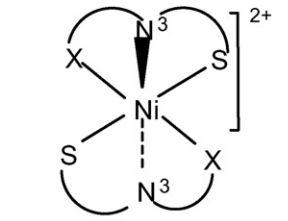

152–155, 159, 160

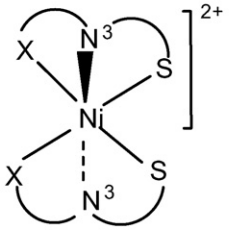

156–158

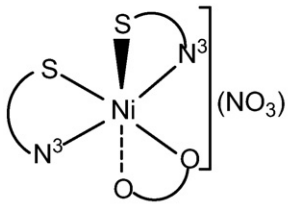

161 [226]

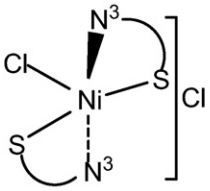

162 [226]

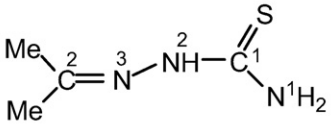

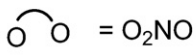

R^1	R^2	NR^3R^4	X	Y	
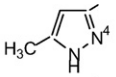	H	$N(Bu^n)_2$	N^4	ClO_4	**152** [176]
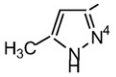	H	NHMe	N^4	NO_3	**153** [220]
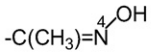	Me	NHPh	N^4	NO_3	**154** [221]
	Me		N^4	ClO_4	**155** [143]
	Me	NH_2	N^4	NO_3	**156** [217]
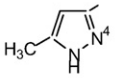	H	NH_2	N^4	Cl	**157** [222]
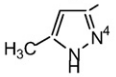	H	NH_2	N^4	Cl	**158** [223]
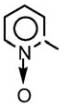	H	NH_2	O	NO_3	**159** [224]
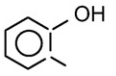	H	NH_2	O	Cl	**160** [225]

Chart 21.

[12–15], or Cu(μ-S)$_2$Cu core (**258–262**, (Fig. 20, **262**; Fig. 21, **258**) [13,248] (Chart 30). Sulfur-bridging was not favored theoretically and stabilization needed hydrogen bonding between halogen atom and water, or solvent of crystallization (**258–262**) [13,248]. For example, Fig. 22 shows the presence of water–halogen hydrogen bonding (compound **258**) and Fig. 23 shows that the presence of CH_3CN–halogen hydrogen bonding (compound **262**). Fig. 24 shows the case in which acetonitrile binds to isatin (–NH) and does not participate in bonding to halogen in complex **239**.

The dinuclear complex $[Cu_2(\mu_2\text{-N, S–HL})_2(CH_3CN)_2]\cdot 2BF_4$ **263** has N^3, S-chelation-and-S-bridging [250], while in complex $[Cu_2L_2](PF_6)_2$ **264** [251], the bis-thiosemicarbazone ligands act as bidentate N, S-donors and copper atom is in a severly distorted tetrahedral N_2S_2 environment.

The ^{31}P spectra of mononuclear $[CuX(HL)(Ph_3P)_2]$, **240**, **243** and **244**, the halogen bridged dinuclear, $[Cu_2(\mu\text{-}X)_2(HL)_2(Ph_3P)_2]$ **250** and **257** and sulfur-bridged dinuclear, $[Cu_2(\mu\text{-S–HL})_2(HL)_2(Ph_3P)_2]$ **259** complexes revealed that there is no change in their solid state structures in the solution state [13]. However, the complexes **260** and **261**, showed conversion of S-bridged dimers into monomers and the complex, **251** showed isomerization of iodo-bridged dimer into a S-bridged dimer in the solution state [13].

A novel heterobridged dimer $[Cu_2(\mu\text{-}I)_2(\mu\text{-S–HL})(PPh_3)_2]$ **265** (Fig. 25) exists with two iodine and one sulfur atom bridging two copper(I) atoms [15]. Another interesting asymmetric dimer, $[(Ph_3P)Cu(\mu\text{-Br})(\mu_3\text{-S,N-Hcptsc})CuBr(PPh_3)]$ **266** with a new {Cu(μ-Br)(μ$_3$-S,N)Cu} bonding core is also known [16].

3.4.5.1.2. Poly-nuclear compounds. There are two tetranuclear and one hexanuclear compounds known. Tetranuclear Cu^I complexes are $[Cu_2(HL)_2Cl_2]_2$ **267** [18], and $[Cu_4L_4]$ **268** (Fig. 26) [31]. Complex **267** has two types of tetrahedral copper centers with CuN_2S_2 and CuS_2Cl_2 cores, and two copper(I) centers are bridged by sulfur atoms to form an eight-membered ring. In complex **268**, the ligand is deprotonated, and each copper has a CuS_2N coordination core. Two Cu atoms are bridged by S atoms forming a four-membered ring, and two such rings are interconnected via N^2-donor atom forming a tetranuclear complex.

The structure of the hexanuclear complex $[Cu_6L_6]$ **269** is shown in Fig. 27. It was prepared by reacting salicylaldehyde thiosemicarbazone (H_2L) with $[Cu(MeCN)_4]\cdot PF_6$ in DMF in the presence of triethylamine base [31]. In this complex, three Cu atoms and

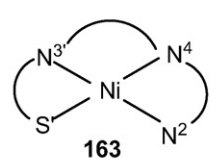

163

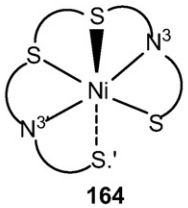

164

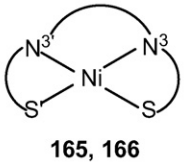

165, 166

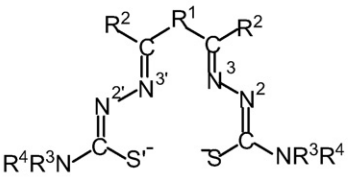

R^1	R^2	NR^3R^4	
	Me		**163** [217]
	Me	NH_2	**164** [227]
	H	NHMe	**165** [228]
$-CH_2-CH_2-$	Me	NHPh	**166** [229]

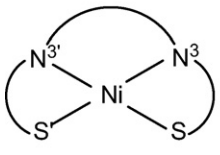

167–171

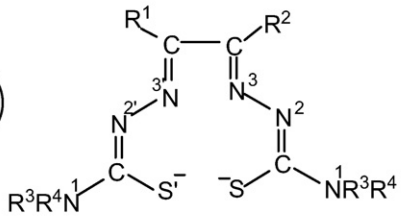

R^1	R^2	NR^3R^4	
Me	Me	NMe Ph	**167** [230]
py	py	NEt_2	**168** [33]
py	py	$N(Pr^n)_2$	**169** [33]
py	py		**170** [33]
py	py		**171** [33]

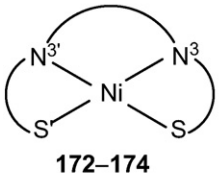

172–174

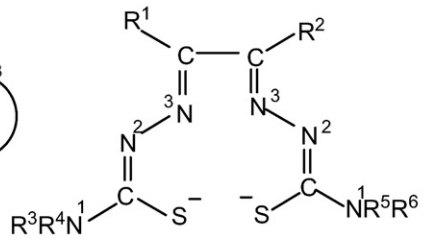

R^1	R^2	R^3, R^4	R^5, R^6	
H	Ph	Et, Et	Et, Et	**172** [231]
Me	H	H, Et	Me, Et	**173** [232]
H	Ph	Et, Et	Et, Et	**174** [233]

Chart 22.

three S atoms from three deprotonated ligand moieties form a six-membered Cu_3S_3 ring, and two such rings are interconnected by N^2 nitrogen of the ligand to form an hexanuclear complex. The geometry around each Cu center is trigonal planar.

3.4.5.2. Copper(II). Copper(II) has been extensively studied and forms a wide variety of complexes with neutral or anionic thiosemicarbazones of nuclearity ranging from mono- to poly-nuclear with distorted tetrahedral, square planar, square pyramidal or octahe-

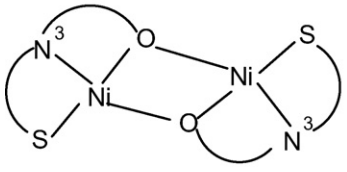

175, 176

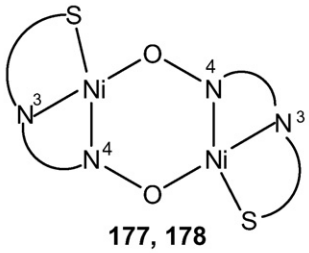

177, 178

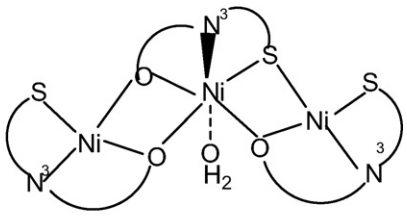

179

R^1	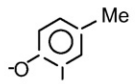	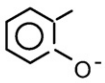	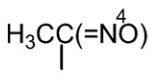	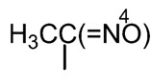	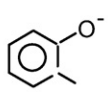
R^2	Me	Me	Ph	Ph	H
R^3, R^4	Me, Me	Me, Me	H, Et	H, Me	Me, Me
	175 [29]	**176** [29]	**177** [234]	**178** [234]	**179** [201]

Chart 23.

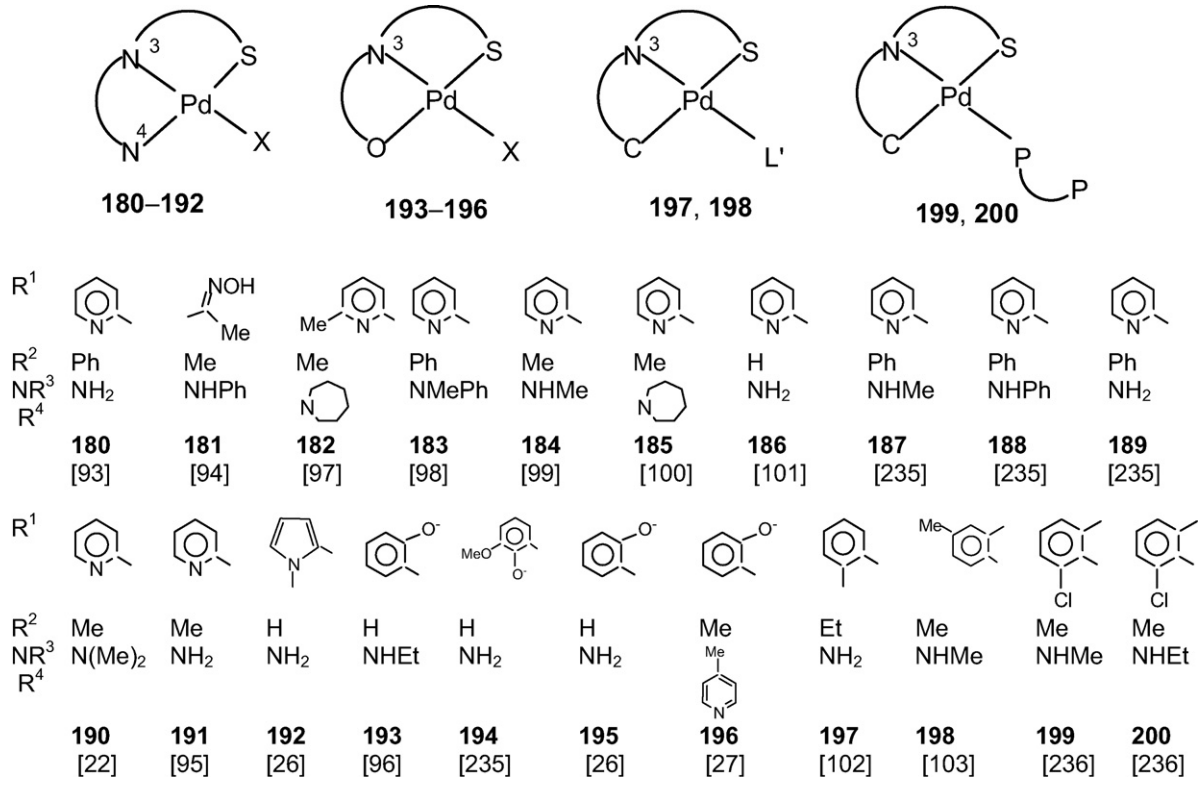

Chart 24.

dral geometries. The preparations generally involve direct reaction of a copper(II) salt such as $CuCl_2$, $CuBr_2$, $Cu(OAc)_2$, etc. with a thiosemicarbazone in an organic solvent such as methanol or ethanol, and rarely via template procedure by reacting a thiosemicarbazide with an aldehyde in presence of a metal salt.

3.4.5.2.1. Mononuclear complexes. Most of the Cu^{II} complexes are mononuclear, and are listed in Charts 31–38. Tetrahedral geometry is observed in $[CuL_2]$ **270–272** [252–255], and $[Cu(HL)Cl_2]$ **273** [17] complexes, with N^3, S-chelated ligands (Chart 31). In $[Cu(HL)_2]\cdot NO_3\cdot CH_3OH$ **274** complex, one ligand is P, N, S-donor and the second is only P-donor [256].

In square planar complexes, [CuXL] **275–283** (Chart 32) [257–264], the uninegative ligands bind via N^4, N^3, S-donor atoms. The presence of pyridyl substituents at C^2 carbon favours tricoordination, and the geometry is restricted to tetracoordination with

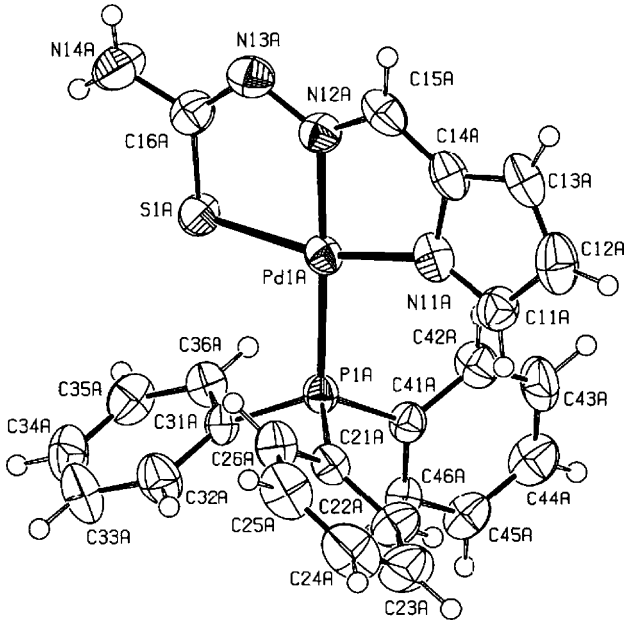

Fig. 12. Structure of complex [PdL(Ph3P)] **192** {adapted from reference [26]}.

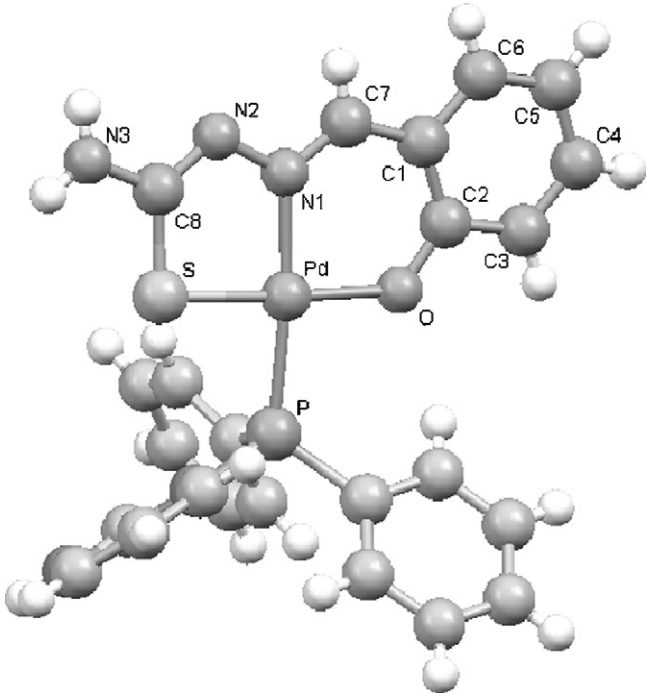

Fig. 13. Structure of complex [PdL(Ph3P)] **195** {adapted from reference [26]}.

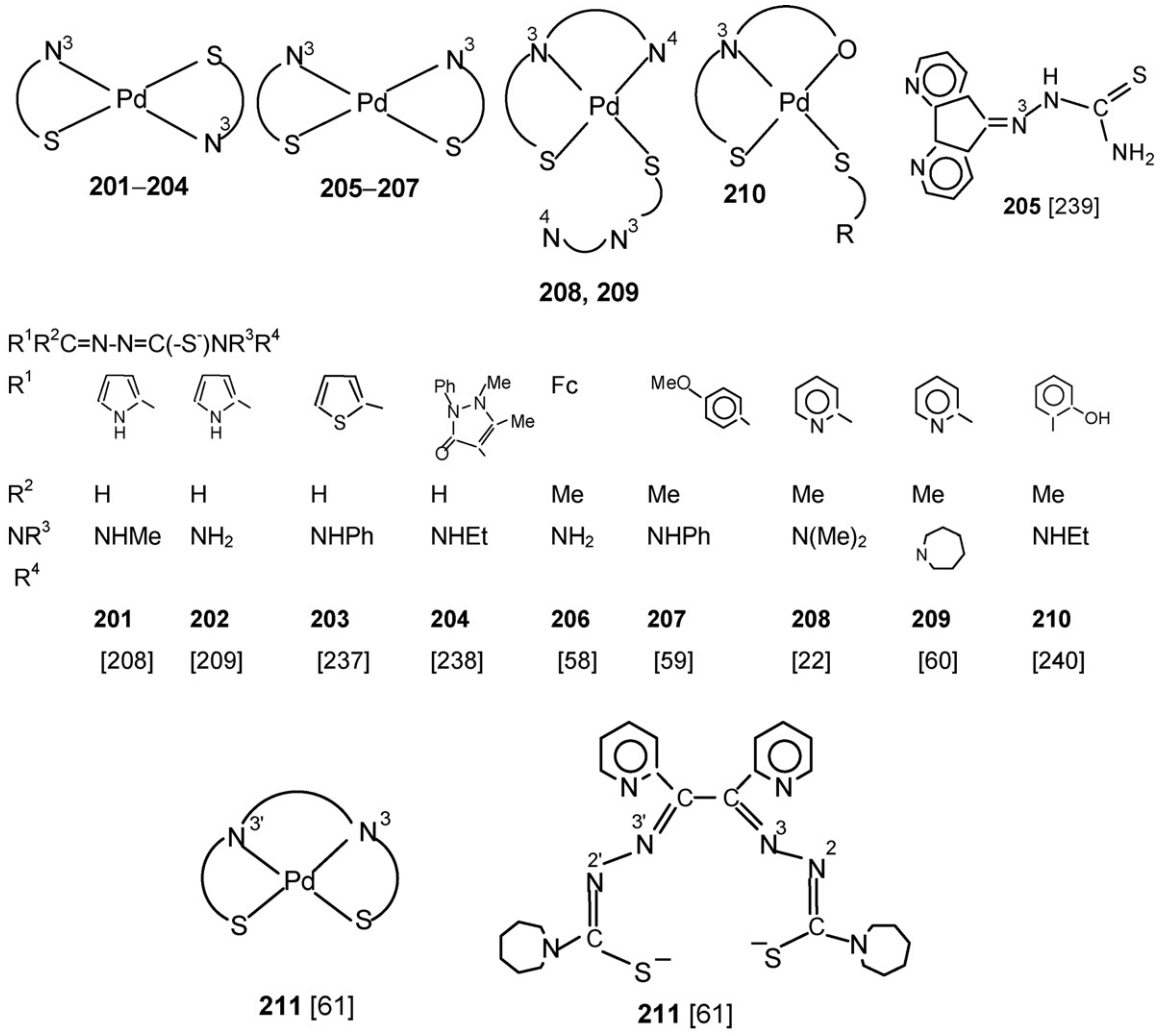

Chart 25.

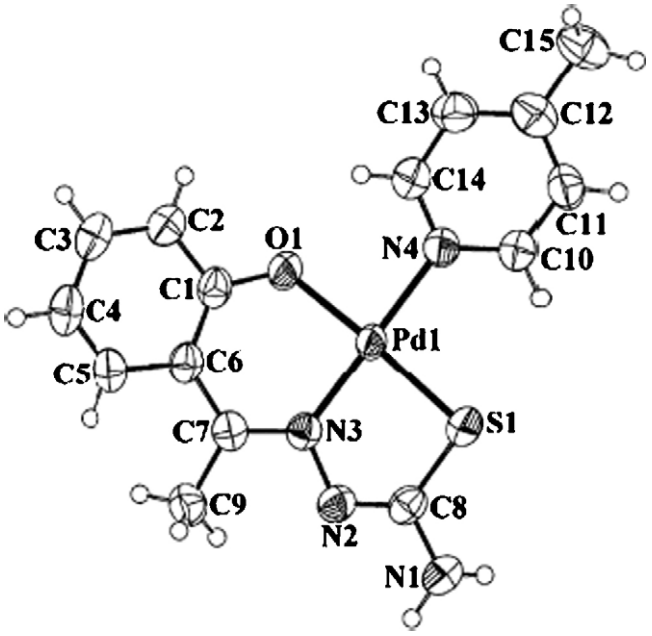

Fig. 14. Structure of complex [PdL(Ph_3P)] **196** {adapted from reference [27]}.

one site occupied by a halogen, or a thiol group (–SH). A few other thiosemicarbazones without a pyridyl substituent also form square planar complexes, viz., [CuLCl] **284** [265] (N^4, N^3, S-donor atoms), and [CuLCl] (**285**, **286**) [266,267] (N^3, S, O-donor atoms). Complex **285** has three water molecules as solvent of crystallization. The ligand is uninegative tridentate (deprotonation of –OH group) in [Cu(HL)Cl] **287** [268] and **288** [269] (Chart 33).

Bis-thiosemicarbazones entrap a metal ion in view of their geometry, and invariably formed square planar [CuL] complexes, **289–305** [251,270–277] (Chart 34). In complexes **289–304**, the bis-ligands are dinegative tetradentate coordinating via N_2S_2 donor atoms, whereas in complex **305**, the bis-ligand is neutral. The substituents at the terminal nitrogen (N^1) atoms do not affect the coordination sphere. However, the alkylation/arylation at the backbone of carbon atoms (C^2, $C^{2'}$) increases the backbone C–C bond length, allowing the metal to fit better into the ligand cavity with shorter Cu–S bonds. The increase in C–C bond length may be attributed to the steric effect of the substituents [270]. Another square planar complex [Cu(HL)]·NO_3 **306** has a uninegative tetradentate ligand with N_2SO donor atoms (deprotonation of OH group) [278].

Square pyramidal geometry is also common for copper metal, and as Chart 35 depicts, there is a pyridyl substituent at C^2 carbon in each of the complexes, [Cu(HL)XY] **307–313**, [Cu(HL)X(ONO_2)](NO_3) **314** [262,279–284], and [CuLXY] **315–318**

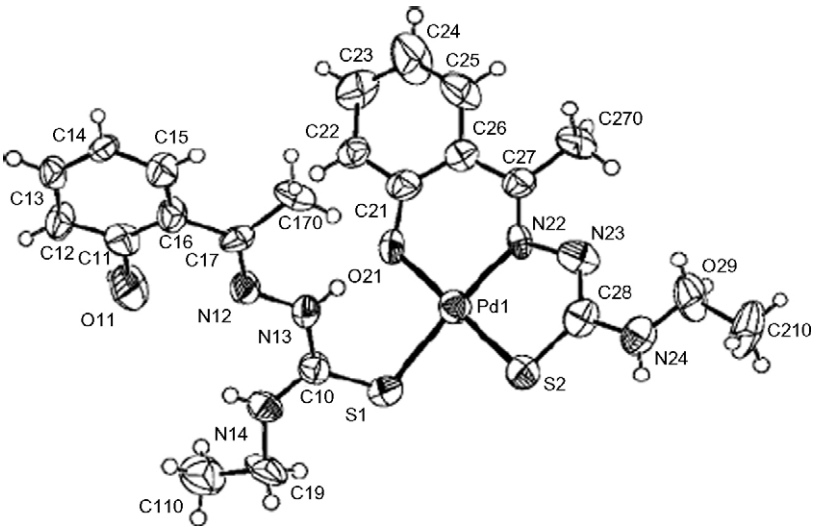

Fig. 15. Structure of complex [PdLL'] **210** {adapted from reference [240]}.

[284–287]. Complexes **307–315** have neutral N^4, N^3, S-donor atoms and **316–318** have tridentate anionic ligands. In complex $[Cu(HL)X(ONO_2)](NO_3)$ **313**, the N^4 donor atom originates from the aniline as a substituent at the C^2 carbon [281]. In complex $[CuL_2]$ **314**, both ligands are uninegative, one is tridentate and second is bidentate [283].

Other square pyramidal complexes, [Cu(HL)XY] and [CuLXY], **319–325** with N^3, S, O-donor atoms from uracil based and other related thiosemicarbazones are shown in Chart 36 [62–65,170]. The pyridoxal ligand is zwitter ionic in complexes **321** and **322**. Water tends to occupy coordination sites as in complexes **321–325**. Most of these complexes are EPR active and their signals corre-

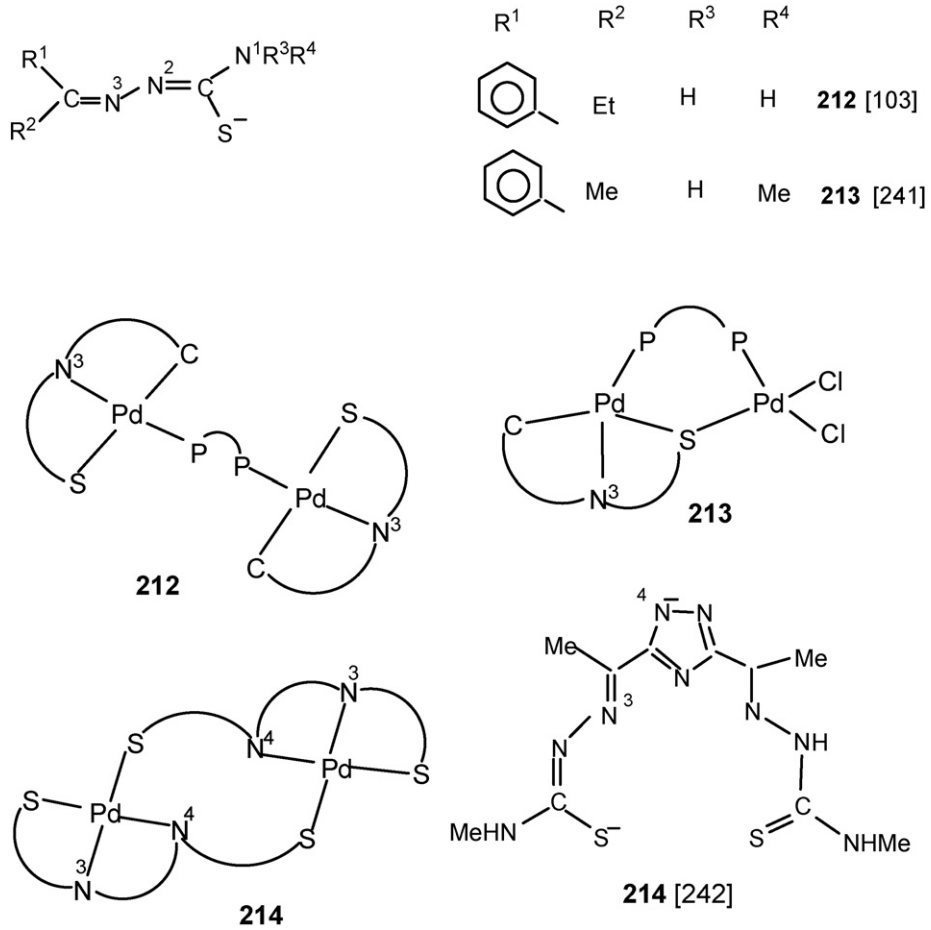

Chart 26.

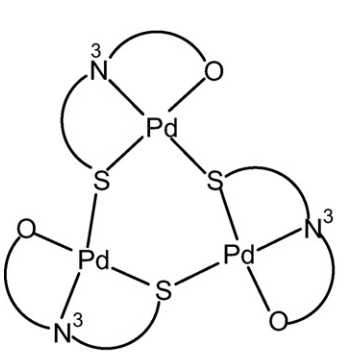

215–217

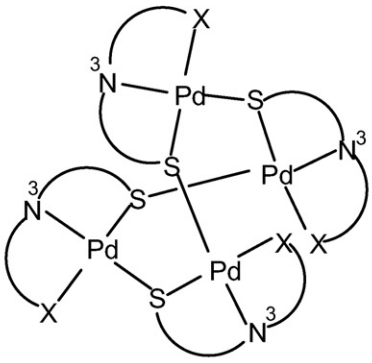

218, 219

$R^1R^2C{=}N{-}N{=}C(-S^-)NR^3R^4$

R^1	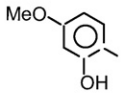		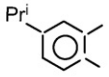		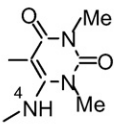
R^2	Me	Me	H	Et	H
R^3, R^4	Me, Me	H, Et	H, H	H, H	H, H
X	-	-	C	C	O
	215	**216**	**217**	**218**	**219**
	[28]	[243]	[244]	[103]	[245]

Chart 27.

spond to rhombic type with d_{x2-y2} ground state [281,286]. There is still another type of square pyramidal complexes, [CuLL′], **326–335** [288–291], in which pyridine based ligands are coordinate in plane along with two donor atoms of a thiosemicarbazone (Chart 37). In all these complexes, the thiosemicarbazone ligand is dinegative except complex **333**, in which it is uninegative.

Only a few octahedral Cu^{II} complexes are reported, namely, $[CuL_2]$ **336**, **337** [285,293], $[Cu(HL)(OClO_3)_2(OH_2)]$ **338** [294], [Cu(HL)(L)]NCS **339** [294] and $[Cu(HL)(ONO_2)(OH_2)]{\cdot}NO_3$ **340** [62] (Chart 38). The N^4, N^3, S-donor ligand is anionic in **336**, **337** neutral in **338** and both neutral as well as anionic in complex **339**. However in complex **340**, the ligand is neutral, O, N^3, S-donor.

3.4.5.2.2. Di- and tetra-nuclear complexes. Thiosemicarbazones with a pyridyl group at C^2 carbon have yielded several dimeric complexes, $[Cu_2X_2L_2]$ ($X_2 = C_2O_4^{2-}$, O_3SO^{2-}, $2RCOO^-$, $2Cl^-$, $2N_3^-$) **341–343** (Fig. 28), **344–347** [257,264,286,295–298] and $[Cu_2X_2(HL)_2]X_2$ ($X = H_2PO_3O^-$, CF_3COO^-) **348**, **349** $[Cu_2(OSO_3)_2(HL)_2]$ **350** [292], involving N^4, N^3, S-binding by anionic or neutral thiosemicarbazones (Chart 39). Four oxygen atoms of oxalate group bridge two square pyramidal. Cu atoms in **341**, whereas in complexes **342–344**, **348**, and **349**, one oxygen atom of a bridging group coordinates to two metal centers. In complexes **344**, **345** and **347**, the bridging atom is chlorine, whereas in complex **346**, a nitrogen atom of an azide group is bridged between two copper centers.

Chart 40 depicts another series of square pyramid sulfur-bridged dimers, $[Cu_2L_2X_2]$ **351–358** [398], (**356**, **357**, Fig. 29) [20,281,298–300], with terminal X groups (halogen, or other anions). In all these complexes, a thiosemicarbazone is mono anionic, coordinating in N^3, S-chelation and S-bridging mode.

Thiosemicarbazones with 2-hydroxyphenyl as a substituent at C^2 carbon act as dinegative tridentate N^3, S-chelation and O-bridging ligands (deprotonation of –OH and $-N^2H$ groups) in $[Cu_2L_2]$ **359**, **360** [21,298], and uninegative N^3, S-chelation and O-bridging in $[Cu_2L_2(OH_2)]{\cdot}2NO_3{\cdot}H_2O$ **361** [301,302] (Chart 41). The geometry of complexes **359** and **360** is distorted square planar, and cation of **361** is square pyramidal.

Other dimeric complexes, $[Cu_2L_2Cl_2]$ **362** [269], $[Cu_2L_2(O_2SO_2)]$ **363**, $[Cu_2L_2(4, 4\text{-bpy})]$ (4,4-bpy = 4,4′-bipyridine) **364**, $[Cu_2L_2X_2]$ **365**, **366**, **370** $[Cu_2L_2]$ **367**, **368**, $[Cu_2(HL)_2(OH_2)_2(O_2SO_2)]$ **371** and $[Cu_2(HL_2)Cl_2]Cl_2$ **372** with different kinds of bridges are shown in Charts 42 and 43 [64,270,271,275,303–305]. The geometry of complex **362** is trigonal bipyramidal formed by anionic thiosemicarbazone ligand (deprotonation of –OH group) [269]. The ligands are uninegative in complex **371** (deprotonation of –OH group) as well as in complexes **363**, **365–368** (deprotonation of $-N^2H$ group). Complexes **363** and **371** have two oxygen atoms from sulfate anion bridging two Cu atoms. Dimerization in complexes **365**, **366** and **370** occurs via one pyridyl group at C^2 carbon, and finally in complexes **367** and **368**, the bridging occurs via coordinate sulfur atoms. Each copper atom in these complexes is either square planar (**363**), or square pyramidal (**365–368**, **371**). In complex **372**, two copper atoms are bridged via hydroxyl (deprotonated) group of pyridoxal substituent of thiosemicarbazone. In complex **368** one azomethine nitrogen and one thiolate sulfur of bis-thiosemicarbazone bind to one copper atom and the other N^3, S-donor atoms of this ligand coordinate to second copper center [270].

Two tetranuclear complexes, $[Cu_4L_4(P_2O_7)]{\cdot}9H_2O$ **373** [306] and $[CuL(SO_4)]_4$ **374** [307] are known. In complex **373**, four Cu atoms are connected by a pyrophosphate group $(P_2O_7)^{4-}$ and two coordinate S atoms act as bridges for adjacent Cu atoms. Two Cu centers

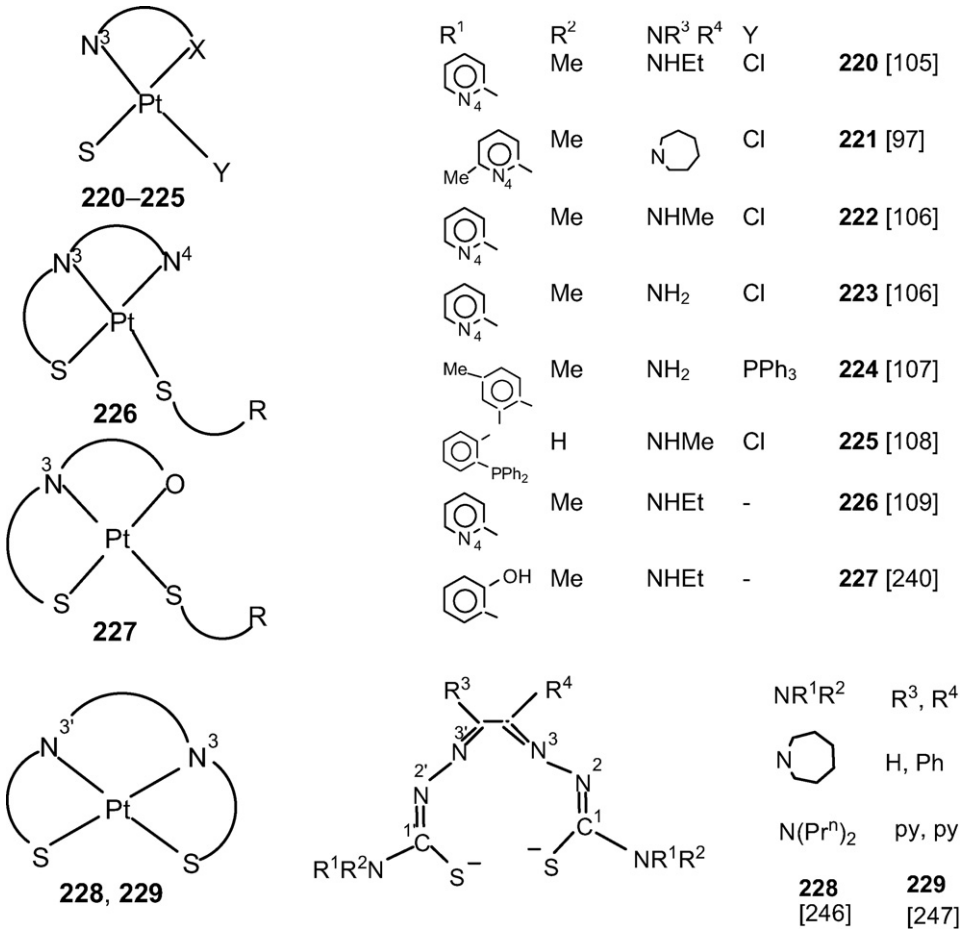

Chart 28.

are five coordinate and the other two are four coordinate. In **374**, the basic unit consists of CuN_2S atoms, which is dimerized via two oxygen atoms of a sulfate group. The two dimeric units are interconnected by one of the pyridyl groups to form the tetramer. Two copper atoms are four coordinate, whereas other two are five coordinate.

3.4.5.2.3. Polymeric complexes. Copper(II) forms polymeric complexes, $[Cu(L)Cl]_n$ **375** [187], $[Cu(H_2L)_n]\cdot 3nH_2O$ **376** [269], $\{[Cu(HL)Cl]_2(H_2O)_2\}_n$ **377** [110] (Chart 44, arrows show the donor atoms of the ligands involved in coordination and are marked for clarity) and $[CuL]_n$ **378**. The ligand is uninegative in complexes **375–377** and dinegative in **378**. In **375**,

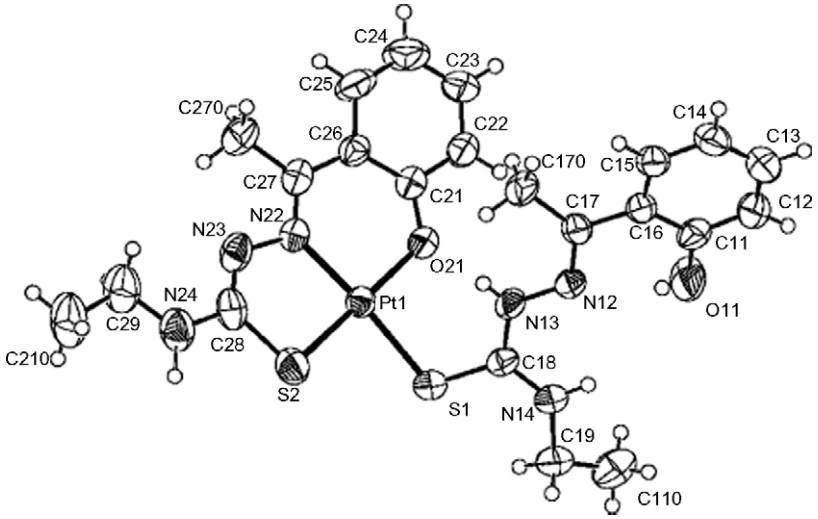

Fig. 16. Structure of complex, $[PtL(H_2L)]$ **227** {adapted from reference [240]}.

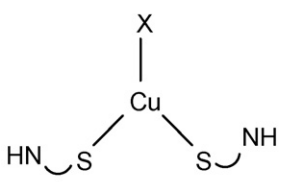

231, **232**

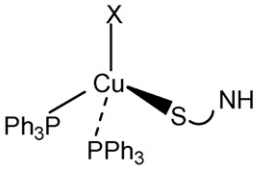

233–235, 237–247

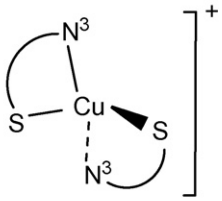

235

$R^1R^2C{=}N{-}NH{-}C(=S)NH_2$

R^1, R^2	Ph, Ph	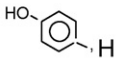	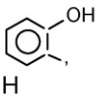	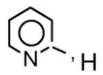		Ph, Ph	Me, Me
X	I	I, Br	Br	I, Br, Cl	I, Br	Br, Cl	-
	232	**233, 234**	**235**	**240-242**	**243, 244**	**246, 247**	**248**
	[139]	[112]	[112]	[13]	[13]	[139]	[18]

$R{=}N{-}NH{-}C(=S)NH_2$

R	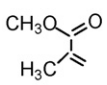	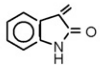	
X	Cl	I, Br, Cl	I
	231 [110]	**237–239**[114, 248]	**232** [249]

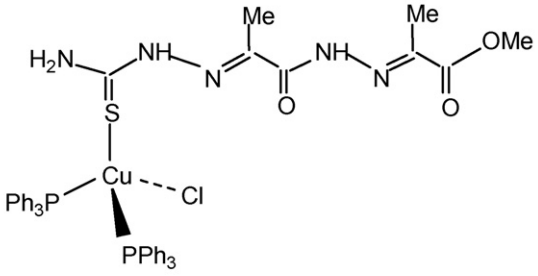

236 [113]

Chart 29.

ligand is coordinating via O, N, S-donor atoms. The contact distance (Cu···S) between two monomeric units is 2.825(8) Å. The species (CuONSCl) dimerizes via O-donor atoms and formation of polymer **376** occurs through participation of pendant $-N^1H_2$ groups. The formation of polymer **377** occurs through the coordinate sulfur and chlorine atoms and interaction is weak {Cu···S, 3.207(1); Cu···Cl, 2.957(1) Å; Cu···Cu, 3.790 Å} [110].

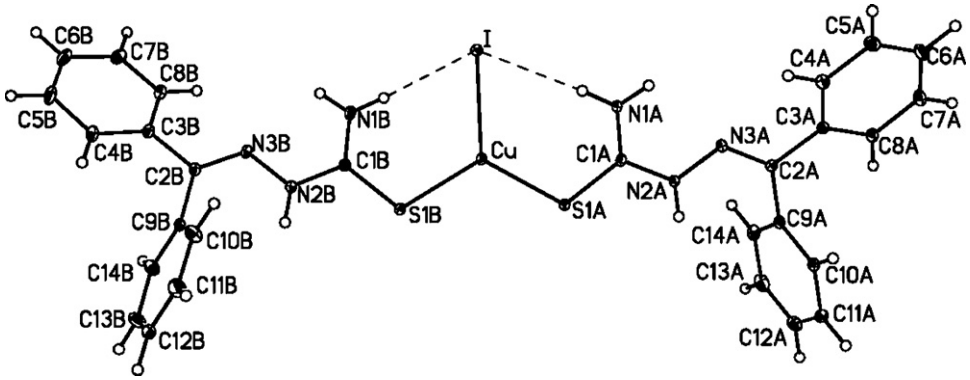

Fig. 17. Structure of $[Cu(\eta^1\text{-S-HL})_2I]$ **232** {adapted from reference [139]}.

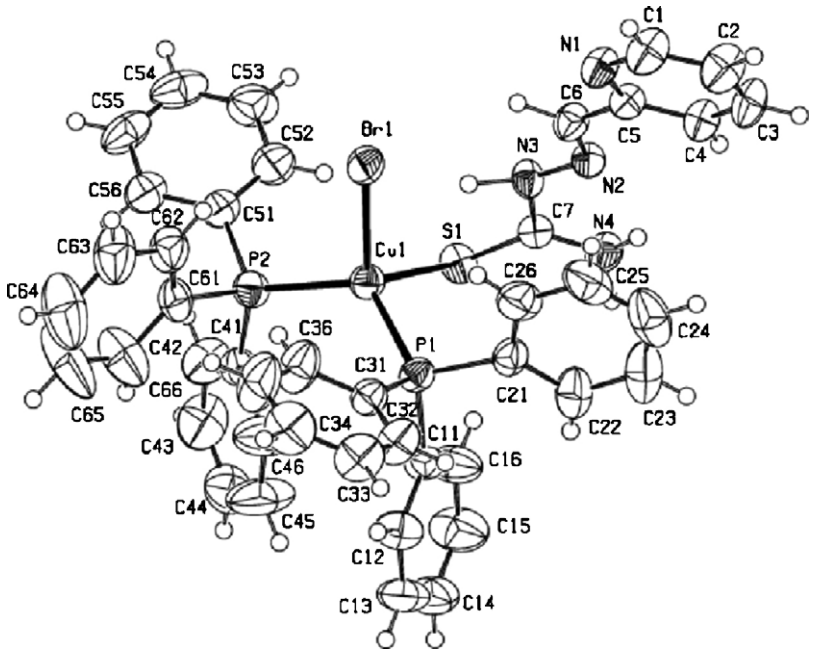

Fig. 18. Structure of complex [CuBr(η^1-S–HL)(Ph_3P)$_2$] **241** {adapted from reference [13]}.

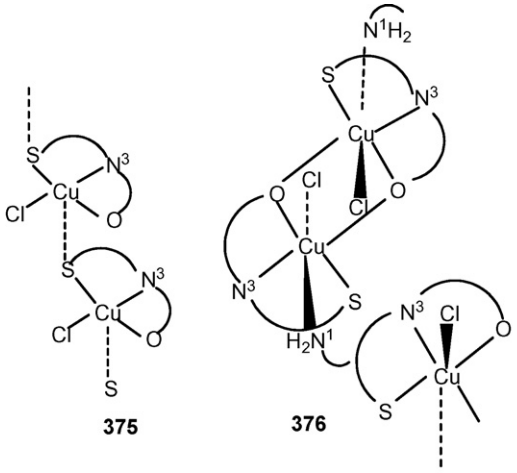

In complex **378**, the dinegative (deprotonation of both carboxylic protons) tridentate (O^1, N^3, S) ligand initially forms species {CuL}; its fourth site is occupied by carboxylic oxygen (O^2) of the second ligand molecule (Cu—O, 1.928(3) Å), while the carbonyl oxygen (O^3) of the third molecule occupies the apical position (Cu—O, 2.460(3) Å). A layered polymeric structure is formed and each Cu has trigonal bipyramidal geometry.

Polymer {[Cu(H_2L)][Fe(CN)$_5$(NO)]}$_n$·2nH_2O **379** has dication balanced by the dianion. The neutral ligand coordinates to Cu center via its O, N, S-donor atoms (Fig. 30). The hydroxyl group of pyridoxal moiety occupies an axial position to provide square pyramidal geometry. The cyanide group acts as a bridging ligand between two heterometallic Cu^{II}–Fe^{III} units, giving rise to a nearly linear sequence Cu–N≡C–Fe in the equatorial plane. The formation of polymer {[Cu(HL)]$_2$[Fe(CN)$_5$(NO)]}$_n$·6nH_2O **380** (Fig. 31) [178] with square pyramidal Cu, is similar (Chart 45). The EPR spectra of complexes **379** and **380** ($g_{||}$ = 2.21; $g_{\perp}$ = 2.05, **379**; $g_{||}$ = 2.19; $g_{\perp}$ = 2.06, **380**) reveal the axial anisotropy (g = 2) around the Cu centers.

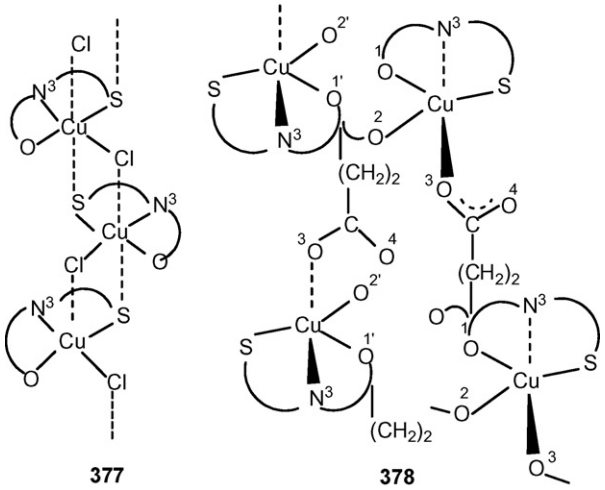

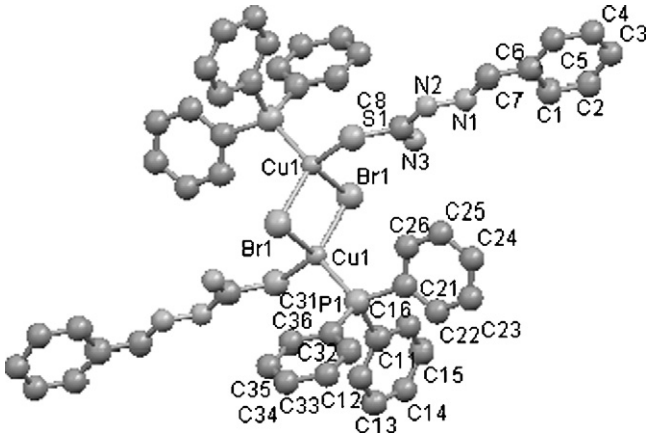

Fig. 19. Structure of complex **257** [CuBr(HL)(Ph_3P)]$_2$ {adapted from reference [13]}.

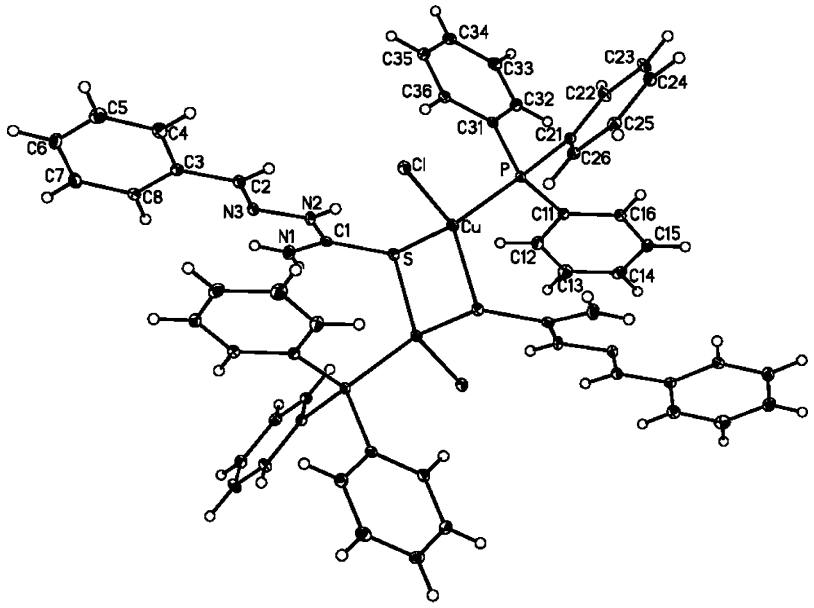

262

Fig. 20. Structure of $[CuCl(HL)(Ph_3P)]_2$ **262**{adapted from reference [13]}.

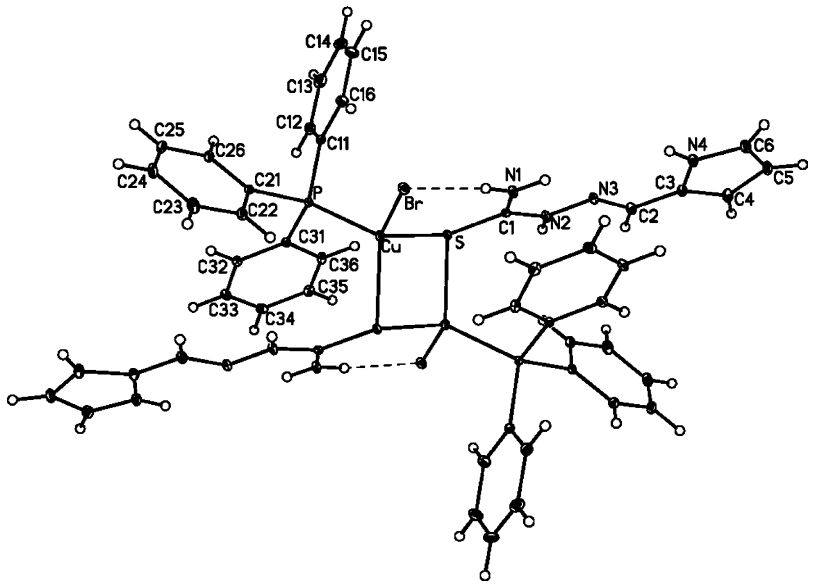

Fig. 21. Structure of complex $[CuBr(Hptsc)(Ph_3P)]_2{\cdot}2H_2O$ **258** {adapted from reference [13]}.

3.4.5.3. Silver(I) and gold(I, III).

3.4.5.3.1. Silver(I). There are a few silver(I)–thiosemicarbazone complexes [308–312]. Thiosemicarbazones with silver(I) halides in presence of PPh_3 have yielded a variety of compounds, (Chart 46), (i) monomers, $[AgX(\eta^1\text{-S–HL})(PPh_3)_2]{\cdot}CH_3CN$ **381**, **382** (Fig. 32, **381**), (ii) halogen-bridged dimers, $[Ag_2(\mu\text{-X})_2(\eta^1\text{-S–HL})_2(PPh_3)_2]$ **383–386** (Fig. 33, **384**) and (iii) sulfur-bridged dimers, $[Ag_2Br_2(\mu\text{-S–HL})_2(PPh_3)_2]{\cdot}2H_2O$ **387** (Fig. 34), $[Ag_2Cl_2(\mu\text{-S–HL})_2(PPh_3)_2]{\cdot}2CH_3CN$ **388** [310]. Silver(I) nitrate forms sulfur-bridged dimers, $[Ag_2(\eta^1\text{-N-}\mu\text{-S–HL})_2(Ph_3P)_2](NO_3)_2$ **389** (Fig. 35), $[Ag_2(\eta^1\text{-S–HL})_2(\mu\text{-S–HL})_2(Ph_3P)_2](NO_3)_2{\cdot}2CHCl_3$ **390** [310] and a triply hetero-bridged $[Ag(\mu\text{-P,P-dppm})_2(\mu\text{-S–HL})Ag(ONO_2)]NO_3$ **391** dimer (Fig. 36) with a short Ag···Ag contact of 2.9939(7) Å [311].

A novel neutral tetrameric silver(I) cluster $[AgL]_4{\cdot}2CHCl_3$ **392** was obtained from the reaction of the thiosemicarbazone with [AgL′] (L′ = 2-pyrrolidine-5-carboxylate) [312]. The ligand acts as uninegative tridentate N, N, S-donor.

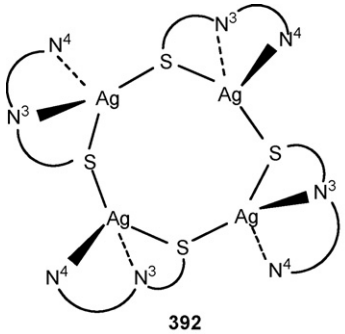

392

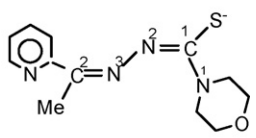

393 [321]

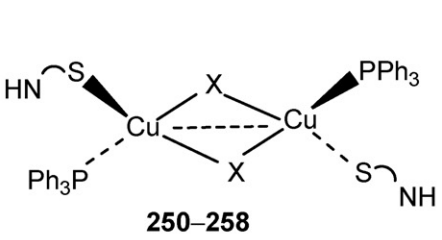

250–258

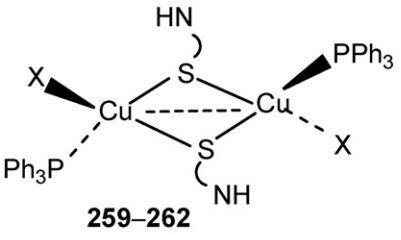

259–262

R^1R^2C=N-NH-C(=S)NH_2

R^1					CH_3	CH_3				
R^2	H	H	H	CH_3	CH_3	H	H	H	H	H
X	I	I	I	Br, Cl	I	Br, I	Br	Br, Cl	Br, Cl	Cl
	249 [12]	**250** [13]	**251** [13]	**252, 253** [14]	**254** [15]	**255, 256** [15]	**257** [13]	**258, 259** [13]	**260, 261** [13,248]	**262** [13]

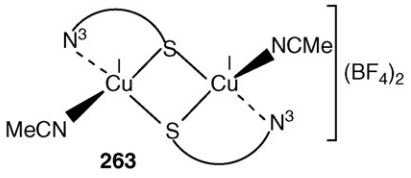

263

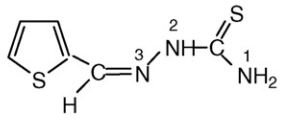

263 [250]

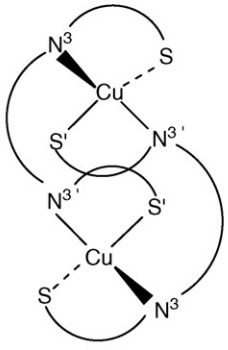

264

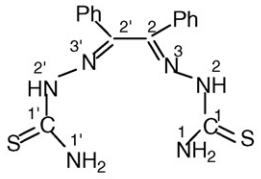

264 [251]

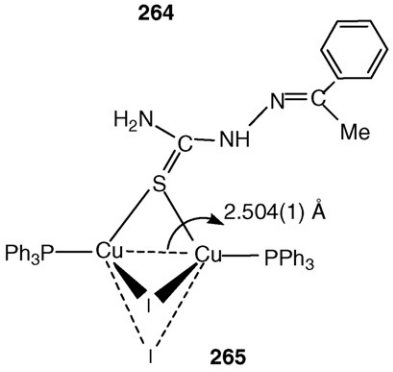

265

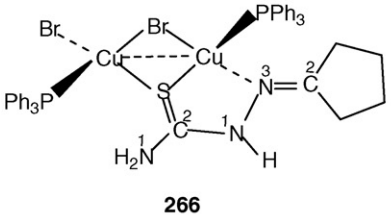

266

Chart 30.

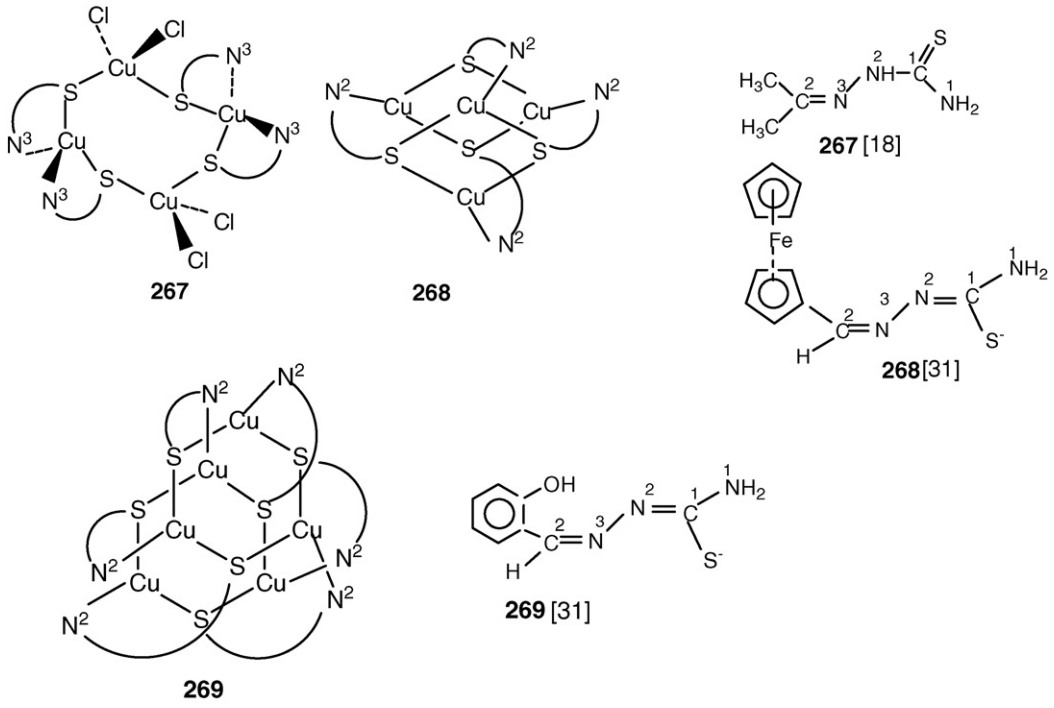

Chart 30. (*Continued*)

Hexanuclear $[Ag_6L_6]$ **393** complex (Fig. 37) (L = anion of salicylaldehyde thiosemicarbazone, H_2L), contains three Ag and three S atoms of the anionic ligands forming a six-membered ring; two such rings are connected by the N^2 atom of ligand, which results in the formation of the hexanuclear complex, and the ligand is in N^2, S-bridging and S-bridging mode [31]. The Ag···Ag bond distances {3.391(5) – 3.720(5) Å} are close to twice the sum of the van der Waals' radius of silver atoms, 3.40 Å [313]. This complex exhibited fluorescent emission at 480 nm in DMSO ($\lambda_{excitation}$ = 380 nm).

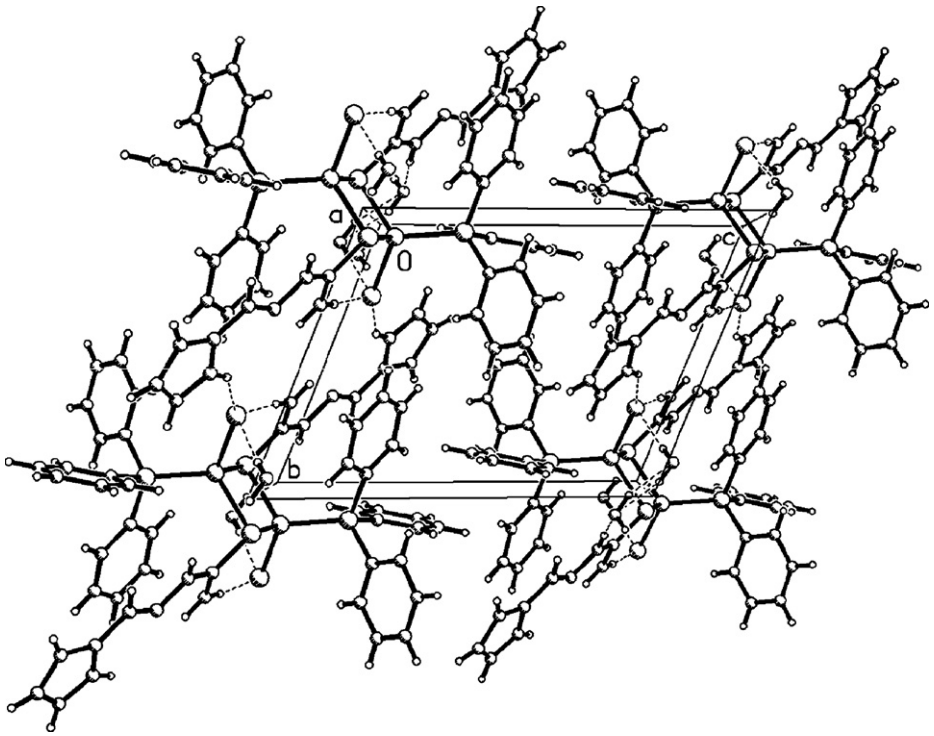

Fig. 22. Packing diagram of complex $[CuBr(Hptsc)(Ph_3P)]_2{\cdot}2H_2O$ **258** shows the presence of H_2O–halogen hydrogen bonding {adapted from reference [13]}.

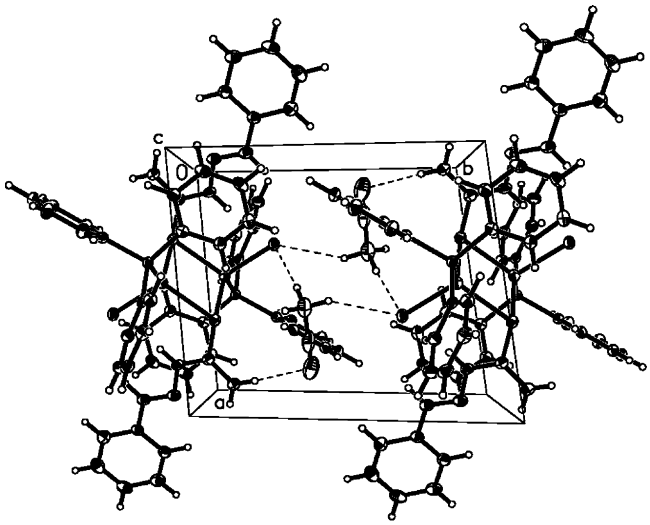

262

Fig. 23. Packing diagrams of complex **262** shows the presence of CH_3CN-halogen hydrogen bonding {adapted from references [13]}.

3.4.5.3.2. Gold(I, III). There is only one reported gold(I) complex [Au(PEt_3)(HL)] **394** (Fig. 38) (HL = vitamin K3 thiosemicarbazonate [115]. The gold(I) center is coordinate linearly to the neutral ligand S atom and PEt_3 with a P–Au–S bond angle of 172.15(5)° [115].

More Au^{III} complexes, namely, [AuCl(L)(Hdamp-C^1)]X (X = Cl, **395**–**397** and PF_6^-, **398;** Hdamp-C^1 = –C_6H_4–CH_2–N^+HMe_2) [116,117], and [Au(L)(Hdamp-C^1)]Cl_2 **399**, **400**, [Au(L)(Hdamp-C^1)]Cl_2 **401** (Fig. 39), **402** [116,117,314], [AuCl(L)][$AuCl_2$] **403** (Fig. 40) and [AuCl(L)]Cl **404–405** [314,315] with square planar geometry have been reported (Chart 47). These were obtained from reaction of [Au(damp-C^1, N)Cl_2] with a thiosemicarbazone.

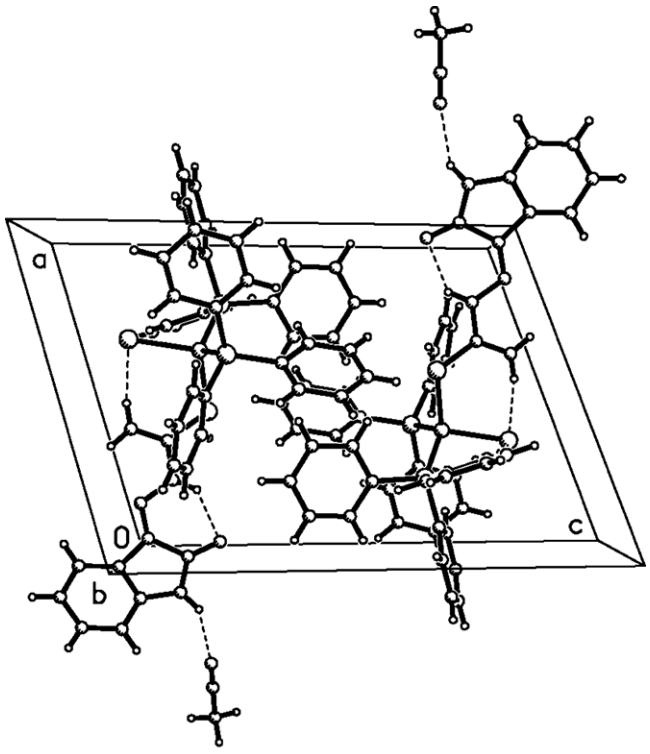

239

Fig. 24. Packing diagarm of **239** {adapted from reference [248]}.

The anionic thiosemicarbazones (deprotonation of N^2H) act as bidentate N^3, S- or tridentate N^4, N^3, S-donor ligands. Complexes **396**, **399** and **400** are methanol solvates, and **397** is water solvate.

3.4.6. Group 12 elements (Zn, Cd, Hg)

A significant number of mono-, di- and a few poly-nuclear complexes of Zn^{II}, Cd^{II}, or Hg^{II} with geometries such as distorted

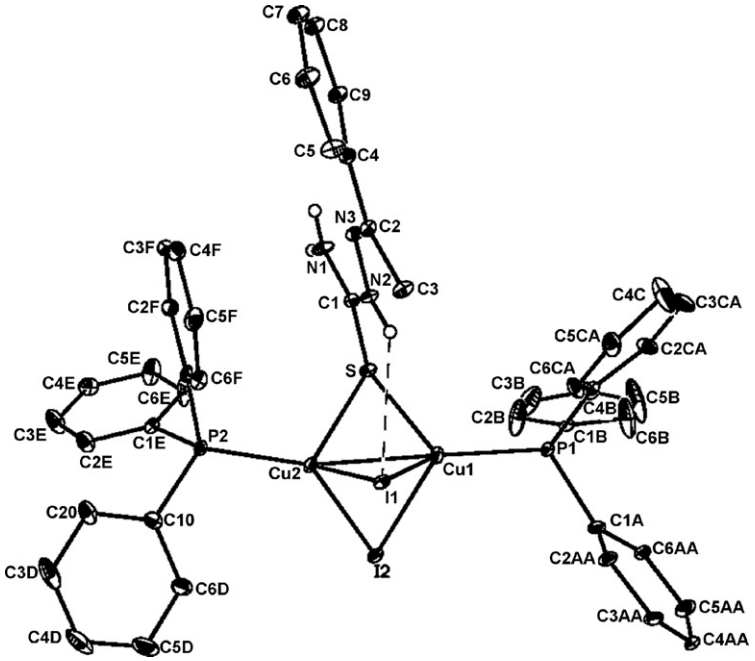

Fig. 25. Structure of complex [Cu_2(μ-I)$_2$(μ-S–HL)(PPh_3)$_2$] **265** {adapted from reference [16]}.

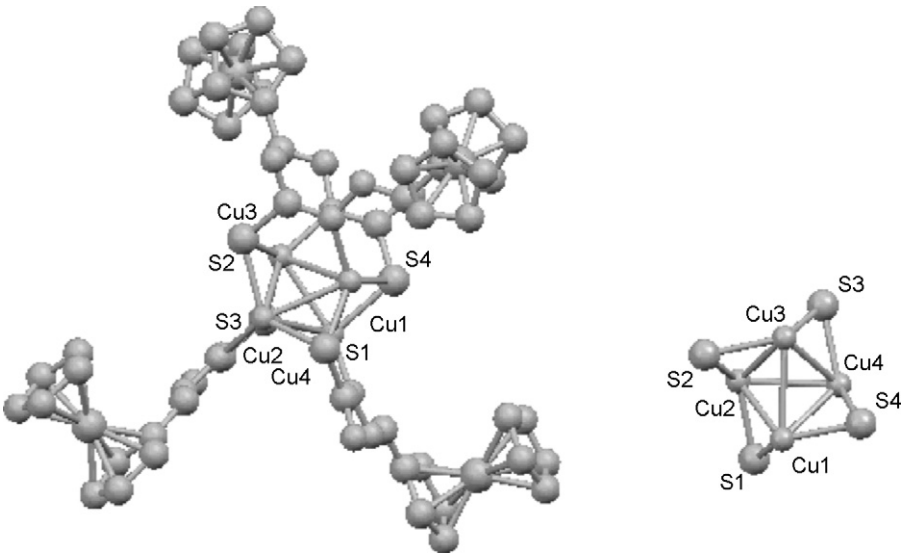

Fig. 26. Structure of complex $[Cu_4L_4]$ **268**{adapted from reference [31]}.

tetrahedral, trigonal bipyramidal, square pyramidal, and octahedral have been reported. Organomercury(II) substrates form trigonal planar and square planar complexes.

3.4.6.1. Zinc(II).

3.4.6.1.1. Mononuclear complexes. Both the neutral and the anionic thiosemicarbazones form tetrahedral Zn^{II} complexes, namely, $[ZnX_2(HL)_2]$ **406–412** [66–71] and $[ZnL_2]$ **413–416** [316–320] (Chart 48). The ligands are η^1-S bonded in **406–412** and are N^3, S-chelating in **413–416**. The distortion from a regular tetrahedral geometry is more in the former than in the latter complexes.

A series of square pyramidal complexes [ZnXY(HL)], **417–426** [321–327,330] having neutral thiosemicarbazones (N^4, N^3, S-, or O, N^3, S-donor atoms) have been reported (Chart 49). In fact, the geometries are distorted and lie in between a square pyramid and a trigonal bipyramid. The axial site is occupied by a halogen or oxygen atoms (from ONO_2 or OSO_3).

Zinc(II) forms a slightly distorted, square pyramidal mixed–ligand complex [ZnL(tmen)] **427** with a tridentate O, N, S thiosemicarbazone and N,N,N,N′-tetramethylethylenediamine (tmen) [327]. One N atom of tmen is in basal plane and the other N atom of tmen is in the apex of the pyramid [327].

Bis-thiosemicarbazones yield a few square-pyramidal zinc(II) complexes, **428–430** (Chart 50) [246,328]. In complex **428**, the neutral ligand is tetradentate with one water molecule as a solvent of crystallization, whereas in complex **430**, the ligand is dianionic tetradentate with the DMF as a solvent of crystallization. Complex **429** has one uninegative tetradentate bis-thiosemicarbazone (deprotonation $-N^2H$).

Chart 51 depicts some octahedral Zn^{II} complexes, $[Zn(HL)_2]\cdot(NO_3)_2$ **431** [330], and $[ZnL_2]$ **432–434** [185,326,329]. The ligand is neutral in **431** and anionic in **432–434**, and ligands bind via N^4, N^3, S- or O, N^3, S-donor atoms. The sulfur atoms occupy *trans* positions, a usual trend observed in Ru^{II} chemistry as well as in other complexes detailed in this review.

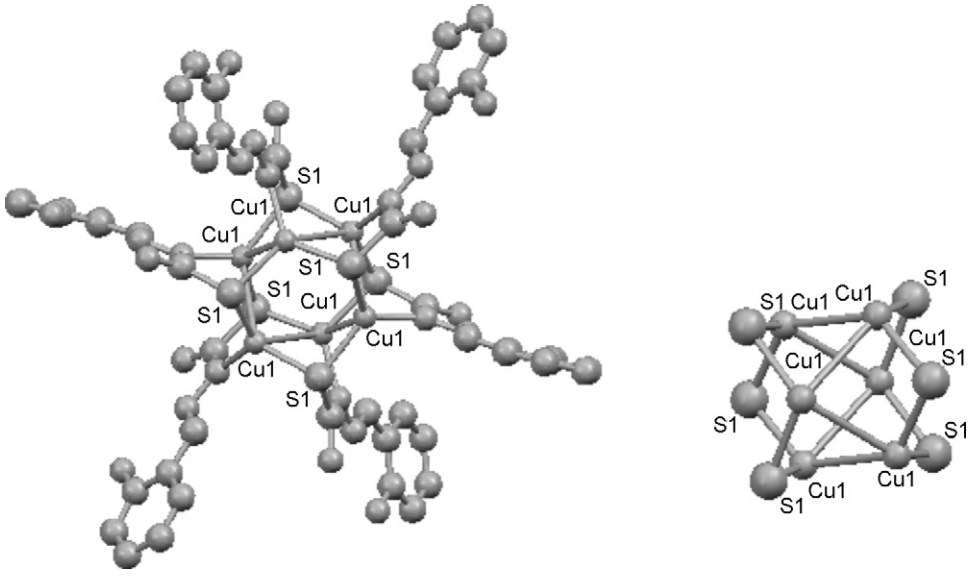

Fig. 27. Structure of complex $[Cu_6L_6]$ **269** {adapted from reference [31]}.

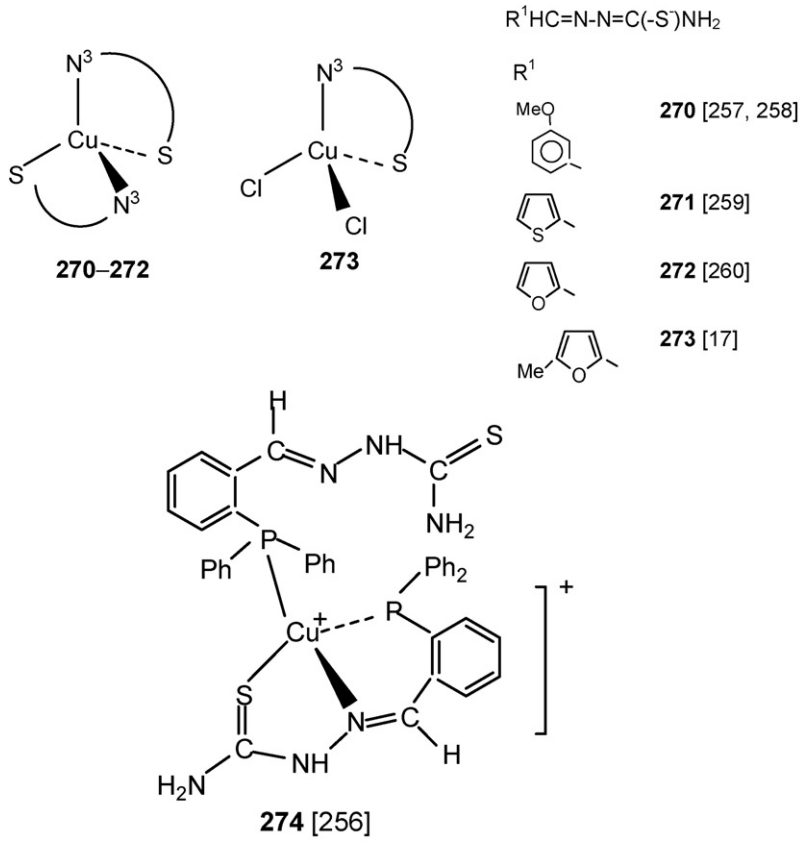

Chart 31.

3.4.6.1.2. Di-nuclear and poly-nuclear complexes. Chart 52 depicts two dimeric square pyramidal Zn^{II} complexes, $[Zn_2L_2(O–DMF)_2]$ **435**, and $[Zn_2L_2(\mu\text{-}O_2CCH_3)(\mu\text{-}OOCCH_3)]$ **436** [330,331]. Thiosemicarbazone ligand is dinegative O, N^3, S-donor in the former, and uninegative N^4, N^3, S-donor in the latter complex. Further, DMF is O-donor in **435**, while one acetate is O_2-bridging and second O-bridging in **436**.

Bis-thiosemicarbazones also form a series of dinuclear Zn^{II} complexes **437–443**, as shown in Chart 53 [325,328,332–336]. In complex, $[Zn_2L(py)_2(\mu\text{-}OH)]–C_5H_5N$ **437** [328], pyridine occupies *trans* axial positions, and OH group is bridging two Zn centers. Each zinc(II) has square pyramidal geometry, and the ligand is hexadentate. Each Zn has trigonal bipyramidal geometry in dinuclear complex $[Zn_2L_2]\cdot DMF\cdot CH_3OH$ **438** [336], but in $[Zn_2L_2]\cdot CH_3CN$ **439** [332], one Zn(II) has square planar and second octahedral geometry. Complex $[Zn_2L_2]$ **440** [325] has sulfur-bridging and the structure is similar to **438**. The ligand is pentadentate in complex $[Zn_2L_2]$ **441** [333], with one hydrazinic nitrogen (N^2) of each bis-thiosemicarbazone also taking part in coordination. Finally, in complexes $[Zn_2L_2]$ **442** and **443**, each ligand is tetradentate; one set of N^3, S-donor atoms coordinates to one metal centre, and second N^3, S-donor set of the same ligand coordinates to second metal centre. Both thiosemicarbazones act as pentadentate dianionic ligands in complex $[Zn_2L_2]$ **444** (Fig. 41) [34], coordinating through pyridyl nitrogen, both iminic nitrogen atoms, and thiocarbonyl sulfur atoms. Rotation about C—C bond allows the pyridyl nitrogen atom to bind to one zinc atom, and its remaining donor atoms to bind a second zinc atom resulting in a helical structure.

Only one polymeric complex with a thiosemicarbazone, namely, $[Zn(L)(OAc)]_n$ **445** [322] is known. In this complex, the ligand is tridentate coordinating via, N^4, N^3, S-donor atoms, and the geometry is square pyramidal with three donor atoms of thiosemicarbazone, and one oxygen atom of acetate anion in the plane, whereas the axial position is occupied by the second acetate oxygen atom. The acetate bridges two metal centers, as well as takes part in the polymerization of the parent complex unit $\{Zn(N^4,N^3,S)(OAc)\}$.

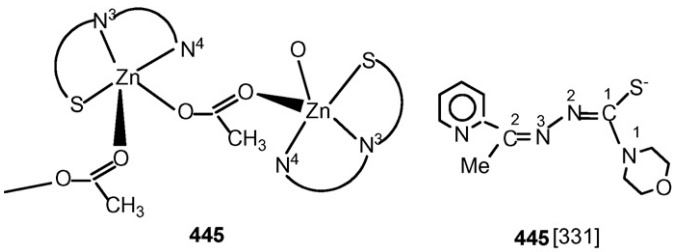

3.4.6.2. Cadmium(II). Chart 54 depicts several mononuclear tetrahedral Cd^{II} complexes of stoichiometry, $[Cd(HL)_2X_2]$ **446–454** [69,337–341]. In all these complexes, two tetrahedral sites are occupied by two neutral thiosemicarbazone ligands, which coordinate via thione sulfur only, and two halogen atoms occupy the other two sites. In complex **446**, one acetonitrile molecule is present as a solvent of crystallization. The ^{113}Cd NMR of **447** showed a single peak at δ 254.6 ppm with chemical shifts within the expected ranges for these complexes in a tetrahedral environment [337].

Most five-coordinate square pyramidal complexes, $[CdLX_2]$ **455–464** [19,118,120,303,342], are formed by the neutral thiosemicarbazones with a pyridyl substituent at C^2 carbon (Chart 55), and each ligand is tridentate. There is one complex [CdLX] **465** [246] with a uninegative tetradentate bis-thiosemicarbazone ligand. Two halogen atoms occupy *cis*-positions in complexes, **455–464**, while in complex **465**, the halogen atom occupies axial position. Most of these complexes are DMSO solvates [19,118,120,342].

Chart 56 depicts Cd^{II} octahedral complexes of formulae, $[CdL_2]$ **466** [344], $[CdL_2]$ **467** [343], $[CdL(py)_3](py)(C_6H_{12})$ **468** [345], and $[Cd(HL)_2Cl_2(DMF)_2]$ **469** [341]. The ligand is uninegative in complexes **466**, **467**, dinegative in complex **468**, and neutral in complex **469**. Complex **468** has one cyclohexane and one pyridine molecule present as solvents of crystallization. Bis-thiosemicarbazone ligand forms a six-coordinate $[Cd(H_2L)(ONO_2)_2]$ **470** [346], and seven-coordinate $[Cd(HL)(NO_3)_2]$ **471** complexes [347]. Another seven-coordinate complex, $[Cd(HL)Cl_2(OH_2)]\cdot H_2O$ **472** is formed by 6-acetyl-2-acetyl pyridine thiosemicarbazone [348] (Chart 57). The ligand is tetradentate involving O, N^4, N^3, S-coordination with Cd^{II} having nearly pentagonal bipyramidal geometry. The ^{113}Cd NMR spectrum of complex **470** exhibits a peak at δ 177.8 ppm in agreement with the cadmium coordination sphere formed by nitrogen, sulfur and oxygen atoms [346]; this signal is downfield relative to that of four-coordinate Cd^{II} complexes.

In dinuclear $[Cd_2L_2(py)_2]$ **473** [345], the dinegative thiosemicarbazone ligand (S, N^3, S-donor atoms) bridges two square pyramidal metal centers via the thiolate group (PhS^-) (Chart 58). Complex $[Cd_3L_4](OAc)_2{-}(DMSO)\cdot 2H_2O$ [349] **474** has a uninegative ligand with deprotonation of the hydroxyl group, and there are three types of coordination environment: namely six-coordinate, four-coordinate and eight-coordinate cadmium centers. Methoxy groups are also involved in coordination. Complex $(Et_3NH)_2[Cd_3L_4]\cdot MeOH$ **475** [345] has dinegative ligands, and contains one octahedral, and two other square pyramidal cadmium atoms. The three cadmium centers are inter-connected by thiolate sulfur (S^1) of the thioamide group. A seven-atom Cd^{II} cluster, $(Et_3NH)_2[Cd_7L_8]\cdot CH_3OH$ **476** [345] containing eight dinegative ligands has also been reported. The ligand has bridging sulfur atoms, and both ring sulfur (labeled as S^2) and thioamide sulfur (labeled as S^1) are involved in the bridging. The central Cd is six coordinate, and all other Cd atoms are trigonal bipyramidal.

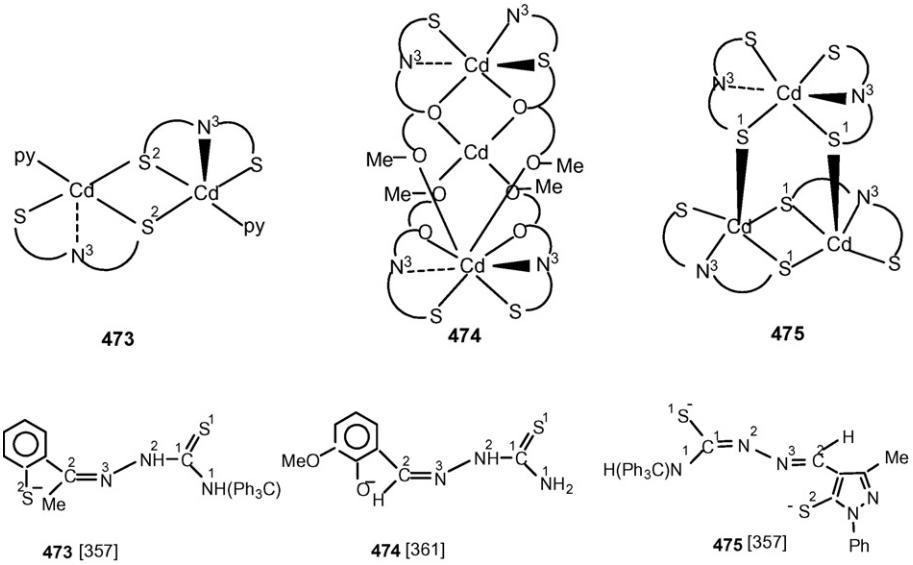

Chart 58

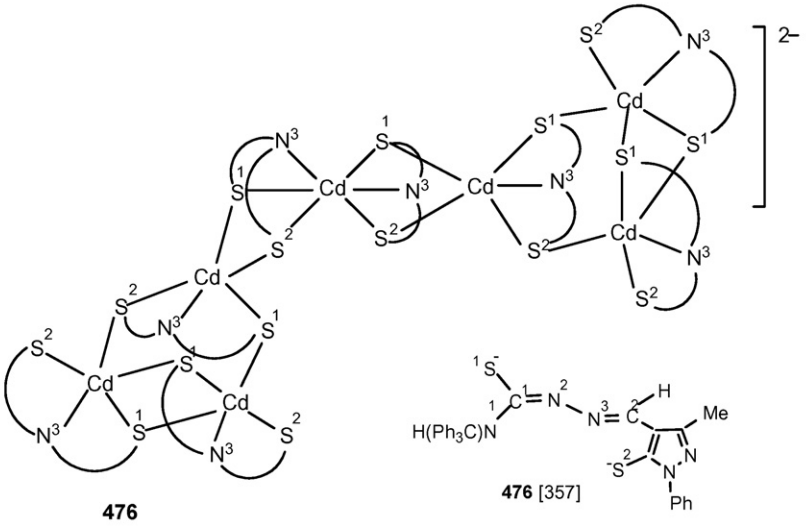

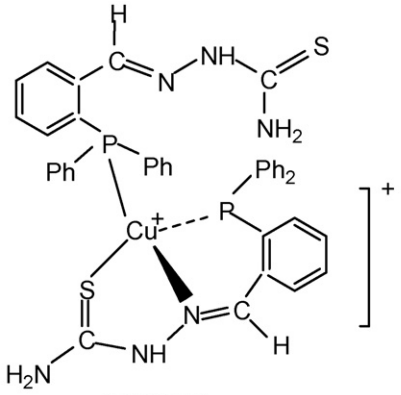

274 [256]

$R^1R^2C{=}N{-}N{=}C(-S^-)NR^3R^4$

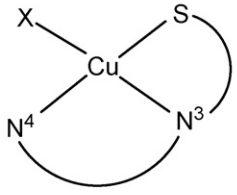

275–283

R^1									
R^2	Ph	Ph	Me	Me	Me	Me	Ph	Me	Ph
NR^3R^4			$(C_6H_{13})_2$	NH_2		NHMe			NHPh
X	Br	SH	Br	Cl	Br	Br	Cl	Br	NCS
	275 [257]	**276** [257]	**277** [258]	**278** [259]	**279** [260]	**280** [261]	**281** [262]	**282** [263]	**283** [264]

Chart 32.

3.4.6.3. Mercury(II). A series of mercury(II) complexes including those with organomercury(II) have been reported. Mercury(II) halides form compounds of stoichiometry, $[Hg(HL)X_2]$ **477**, **478** [118] and $[Hg(HL)X_2]$·DMSO **479**, **480** [119,19] as shown in Chart 59, with neutral ligands. Complexes **477** and **478** are tetrahedral and compounds **479** and **480** have distorted trigonal bipyramidal geometry with tridentate ligands.

Direct reaction of mercury(II) acetate with pyridine-2-carbaldehyde thiosemicarbazone (HL) gave a black insoluble mass, whereas reaction of phenylmercury(II) acetate, or (2-pyridyl)phenyl mercury(II) acetate with HL yielded $[HgL_2]$ **481** (Fig. 42), which is the first octahedral complex with a single uninegative tridentate (N^4, N^3, S) ligand satisfying both the primary and secondary valencies [350].

Organomercury(II) thiosemicarbazonates, [RHgL], **482–487** with distorted T-shaped geometry are shown in Chart 60 [120–123]. The ligands are uninegative in N^3, S-chelating mode (**486**, Fig. 43) with C–Hg–S angles in the range, 162.9–174.2°. The ^{199}Hg NMR spectra of complexes **482** and **484** gave one signal each at δ −687 and δ −672 ppm, respectively, supporting the formation of single component, whereas ^{199}Hg NMR spectrum of complex **483** showed three peaks at δ −773, −942, and −750 ppm due to [HgPhL], $[HgL_2]$ and $[HgPh_2]$ ppm, respectively. Reaction of PhHgCl with acetophenone thiosemicarbazone also formed symmetrized products $HgCl_2(HL)_2$ and Ph_2Hg [351].

2-Pyridylphenylmercury(II) acetate also forms complexes of stoichiometry [2-pyPhHgL] **488**, **489** (Chart 61) [121,357]. Complex **488** has a distorted T-shaped geometry with weak Hg···N^3 interaction [352]. The lack of N^3, S-chelation in this complex is attributed to the strong intramolecular O–H···N(3) hydrogen bonding (R^1 = 2-hydroxyphenyl). However in solution phase the ^{199}Hg NMR spectrum gave two signals {differing in percentage at δ −783 and δ −868 ppm} supporting the formation of two isomers A (minor) and B (major). Interestingly the ^{199}Hg NMR spectrum of **489** showed a major isomer A and minor isomer B [121] and X-ray supported the major isomer A (Fig. 44) [121].

A few known dimeric Hg^{II} complexes, namely, $[Hg_2(\eta^3\text{-}N^4, N^3, S\text{–}L)_2X_2]$ **490** [342], $[Hg_2(\eta^3\text{-}N^3, S\text{–}L)_2X_2]$ **491** [67], and $[Hg_2(\eta^1\text{-}S\text{–}HL)_2X_4]$ **492** [69] are shown in Chart 62. The thiosemicarbazone ligands are uninegative in **490** and **491**, and neutral in **492**. Each Hg center has a distorted square pyramidal geometry (**490**) or distorted tetrahedral geometry (**491** and **492**).

There is only one report of a polymer of Hg^{II} with a thiosemicarbazone, namely, $[Hg(HL)I_2]_n$ **493** [337]. The ligand bonds via the S-donor atom only, and one iodide act as a bridge between two Hg atoms leading to an infinite chain formation.

3.4.7. Group 13 elements (Al, Ga, In, Tl)

Relatively more compounds are reported for indium and thallium elements and less for aluminium and gallium elements. An

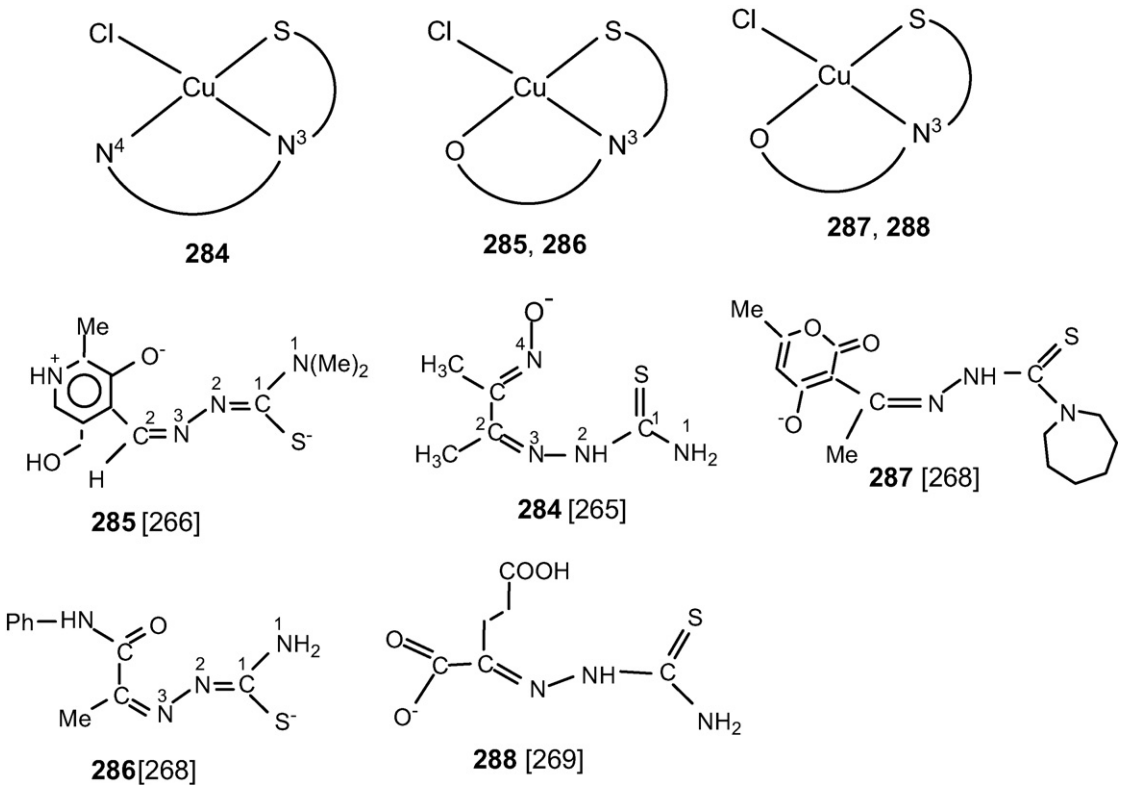

Chart 33.

aluminium(III) complex, [Bu$^i_2$AlL] **494** [124], has square pyramidal geometry with iso-butyl groups occupying axial sites. Compound **495** has dinegative pentadentate ligands (with loss of thiol and pyrrole hydrogen atoms) connecting four Al atoms with two different geometries [353]. The ^{27}Al NMR spectrum consists of two broad resonances at δ 154 and 112 ppm supporting two types of aluminium coordination centers, AlN_2C_2 and AlN_2SC cores, respectively, [354] in N_2C_2 coordination environment; the latter is assigned to the four-coordinate Al(1) atom [355].

Chart 63 depicts complexes of gallium(III) with uninegative thiosemicarbazonates, namely, [Me_2GaL] **496** [125], and [$GaLL_2$][$GaCl_4$] **497** [126]. The ligand is N^3, S-chelating in the tetrahedral **496**, and N^4, N^3, S-tridentate donor in the distorted octahedral cation of **497** with *trans* sulfur atoms.

There is only one report of In^{III} describing mononuclear octahedral complexes, [InClLL′] **498**, [InCl(L)L′]·H_2L^+ **499** (L′ = S, S-donor), [$InCl_2$L(MeOH)] **500** and [InL_2]$^+$ **501** [127] (Chart 64). The anionic ligand coordinates via N^4, N^3, S-donor atoms in these complexes. Similarly, with a uninegative bis-thiosemicarbazone, a seven-coordinate mononuclear complex [In(HL)Cl_2]·DMSO **502** [127], and a seven-coordinate oxo-bridged dinuclear complex, [$In_2(HL)_2(OH)_2O$]·MeOH **503**, have been reported [127] (Chart 65).

Compounds of thallium are reported only with diorganothallium(III), R_2Tl^+ cations (R = Me, Ph), with formulae, [$Ph_2Tl(\eta^2$-N^3, S–L)] **504** [356], [$Me_2Tl(\eta^2$-N^2, S–L)] **505**, **506** [25,128], [$Ph_2Tl(\eta^3$-N^4, N^3, S–L)] **507**, **508** [128], [$Me_2Tl(\eta^3$-N^4, N^3, S–L)] **509** [129], and [$Me_2Tl(\eta^2$- N^2, S–L)(DMSO)] **510** [356] (Charts 66 and 67). Ligands are uninegative in all the cases, and have N^2, S-chelation, or N^3, S-chelation, and if a pyridyl group is present at C^2 carbon, the ligand is tridentate binding via N^4, N^3, S-donor atoms. The geometries are distorted tetrahedral (**504–506**), square pyramidal (**507–509**) or trigonal bipyramidal (**510**). Complexes **507** and **508** showed three independent molecules in their crystal structures; the same could not be observed in their solution state by ^{205}Tl NMR spectrum, probably, the three species do not differ enough to produce significantly distinct ^{205}Tl signals.

The ligand is tetradentate coordinate via O, N^4, N^3, S-donor atoms in octahedral complex, [Ph_2TlL] **511** [357], and pentadentate coordinate via N_3S_2 donor set in [PhTlL]·Me_2CO **512** [35] containing a dinegative bis-thiosemicarbazone. There are three types of dimeric complexes, namely, [$Tl_2L_2Me_4$] **513** [357], [$Tl_2L_2Me_4$] **514** [25] and [$Tl_2L_2(OH_2)_2Me_4$] **515** [23] (Chart 68); the ligands are multifunctional and involve bridging via oxygen atoms or sulfur atoms. Each Tl has square pyramidal geometry (**514** and **515**) or pentagonal bipyramidal geometry (**513**).

3.4.8. Groups 14–15 elements (Sn, Pb, Bi)

3.4.8.1. Tin. Both tin(IV) halides and organotin(IV) substrates form compounds with thiosemicarbazones with coordination numbers ranging from 4 to 7. The uninegative 2-acetyl-salicylaldehyde thiosemicarbazone with Ph_3Sn^+ cation yields [Ph_3Sn(HL)] **516** [358], with distorted tetrahedral tin.

Chart 69 depicts five-coordinate organotin(IV) complexes, [R_2SnLX] **517–521** [130,359–361]. The anionic thiosemicarbazones chelate via N^3, S-donor atoms with square pyramidal geometry for the complexes. The halogen or oxygen {from diphenylthiophosphinato {$Ph_2P(=S)O^-$} occupy the axial sites. Complexes [R_2SnL] have di-anionic tridentate, N^4, N^3, S (**522**) [362], or N^3, S, O-donor ligands (**523–526**) [363,364], while [R_2Sn(HL)] **527** [365] has monoanionic ligand (deprotonation of the hydroxyl group) (Chart 70).

A series of octahedral [R_2SnLX] **528–533** complexes (Fig. 45, **533**) [131,132,366–368] have been reported, in which the anionic thiosemicarabzones bind via N^4, N^3, S-donor atoms (Chart 71). The pyridyl nitrogen and the halide or sulfur {from diphenyldithiophosphate-S, $Ph_2P(S)S^-$} occupy the axial sites, and other donor atoms are in the equatorial plane.

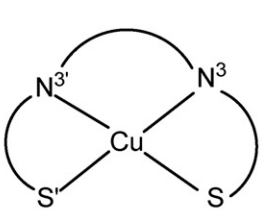

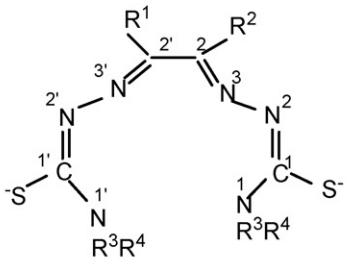

289–305

R^1	Me	Me	Me	Et	H	H	Ph	H
R^2	Me	Me	Et	Et	H	H	Ph	
NR^3R^4	NHMe	NMe_2	NH_2	NH_2	NH_2	NHMe	NH_2	NH_2
	289	**290**	**291**	**292**	**293**	**294**	**295**	**296**
	[270]	[270]	[270]	[270]	[270]	[270]	[271]	[272]

R^1	H	Ph	Ph			Et	Et	Me	Ph
R^2	Ph	Me	Ph			Et	Et	Me	Ph
NR^3R^4	NEt_2				NEt_2			NHMe	NHPh
	297	**298**	**299**	**300**	**301**	**302**	**303**	**304**	**305**
	[273]	[274]	[274]	[275]	[275]	[276]	[276]	[277]	[251]

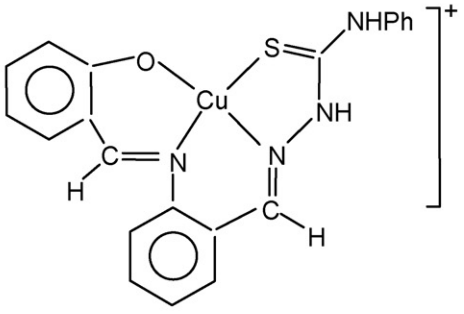

306 [278]

Chart 34.

Tin(IV) chloride also forms octahedral complexes, $[SnLCl_3]$ **534–536** [367,369], **545** [370], $[SnLCl_2R]$ **537–544** [367,371–373,375] and $[SnL_2Cl_2]$ **546** [360] (Charts 72–74). The ligands are uninegative N^4, N^3, S-chelating in **534–545** and N^3, S-chelating in **546**. Organic groups bonded to tin occupy one of the axial sites in **537–539**, and one site of a square plane in **540–544**.

The pyridyl based bis-thiosemicarbazones form a series of seven-coordinate complexes of general formula, $[R_2SnL]$ **547–553** [133,160,334,368,374–376,378] (Chart 75). In complex, $[Ph_2Sn(HL)]Cl$, **549** [133], the ligand is mononegative with one chlorine outside the coordination sphere, while it is neutral in $[Bu^n_2Sn(H_2L)]Cl_2$, **552** [376] and dinegative in $[R_2SnL]$ (**547**, **548**, **550**, **551** and **553**) (Fig. 46). Complexes **547**, **551** and **552** are methanol, acetone or water solvates, respectively.

A dimeric complex, $[Sn_2L_2Cl_2]$ **554** [337] contains square pyramidal tin. The ligand acts as a tridentate dianion coordinating via S, N, O-donor atoms forming a plane and two Cl atoms in the axial positions.

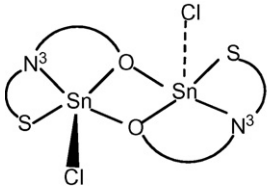

554

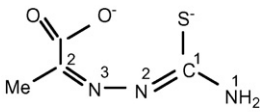

554 [348]

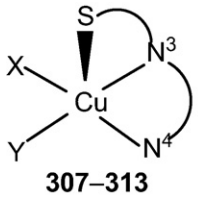

307–313

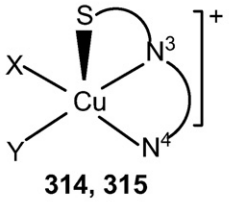

314, 315

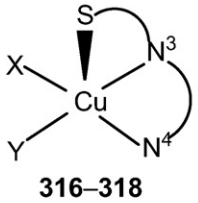

316–318

R^1	R^2	NR^3R^4	X	Y	
	H	NH_2	Br	Br	**307** [280]
	H	NH_2	Cl	Cl	**308** [279]
	H	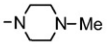	Cl	Cl	**309** [262]
	Ph	N^nPr	Cl	Cl	**310** [262]
	H	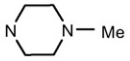	Cl	Cl	**311** [279]
	H	NH_2	OH_2	OSO_3	**312** [284]
	H	NH_2	OH_2	ONO_2	**313** [281]
	H	NH_2	OH_2	ONO_2	**314** [283]
	H	NH_2	OH_2	C_2O_4	**315** [286]
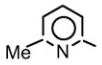	H	NH_2	OH_2	$MeCO_2$	**316** [284]
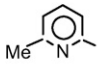	H	NMe_2	OH_2	ONO_2	**317** [285]
	H	NH_2	OH_2	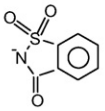	**318** [287]

Chart 35.

3.4.8.2. Lead. Lead forms several complexes with thiosemicarbazones in both of its common Pb^{II} and Pb^{IV} oxidation states. Compounds in the tetravalent state are only with organolead(IV) substrates. Lead(II) forms a tetrahedral complex, [Pb(L)(OAc)] **555** [136], and an octahedral complex, $[PbL_2]$ **556** [339] (Chart 76), with uninegative tridentate N^4, N^3, S-donor ligands in the former, and O, N^3, S-donors in the latter complex.

There is only one report of the pentacoordinate lead complex [Pb(L)] **557** (Fig. 47) [34] with a bis-thiosemicarbazone. It exhibited a distorted pentagonal planar configuration about lead(II) with a doubly deprotonated ligand acting as a pentadentate and coordinating through its pyridyl and N^3 nitrogen atoms along with two sulfur atoms.

Other lead(II) compounds are a seven-coordinate dimer, $[Pb_2(HL)_4]$ **558** [377], and a six-coordinate polymer, $[Pb(L)SCN]_n$ **559** [378] (Chart 77). Dimerization occurs via oxygen atom in the former complex, while polymerization occurs via sulfur atom of thiocyanate in the latter complex.

The organolead(IV) compounds, monomers $[Ph_2PbLCl]$ **560**, **561**, $[Ph_2PbCl_2(HL)_2]$ **562**, dimers $[Ph_4Pb_2(HL)_2Cl_4]$ **563**, $[Ph_4Pb_2(HL)_2Cl_2]Cl_2$ **564**, and a trimer $[Ph_6Pb_3L_2Cl_4]Cl_2$ **565**, are shown in Chart 78 [134]. The geometry around lead is octahedral in **560–563**, and pentagonal bipyramidal in **564**. In trimeric complex **565**, two Pb centers are pentagonal bipyramidal and one is octahedral. The ligands are uninegative in **560**, **561** and neutral in **562–565**. The ^{207}Pb NMR spectrum of complex **561** supported

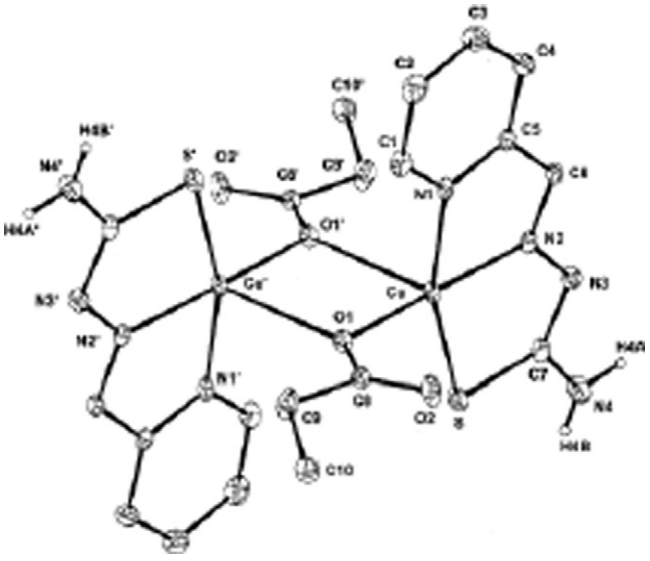

Fig. 28. Structure of complex $[Cu_2(OOCEt)_2L_2]$ **343** {adapted from reference [298]}.

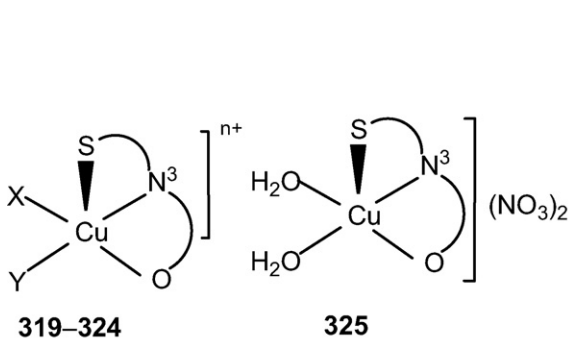

319–324 325

$R^1R^2C{=}N{-}N{=}C(-S^-)NR^3R^4$

R^1	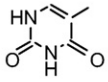	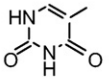	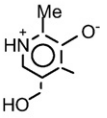
R^2	H	H	H
R^3, R^4	H, Me	Me, Me	H, H
X	Cl	Cl	OH_2
Y	Cl	Cl	Cl
n	0	0	1
	319	**320**	**321**
	[62]	[62]	[63]

R^1	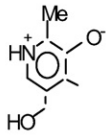	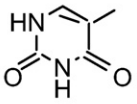	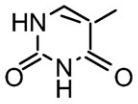	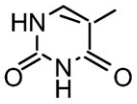
R^2	H	H	H	H
R^3, R^4	H, H	H, H	H, H	H, H
X	OH_2	OH_2	Cl	OH_2
Y	OH_2	OSO_3	Cl	OH_2
N	2	0	0	0
	322 [64]	**323** [65]	**324** [65]	**325** [170]

Chart 36.

its solid state structure in the solution state, while the dimer **563** breaks to monomer with DMSO also participating in coordination.

Bis-thiosemicarbazone ligands also form mononuclear complex $[PbPh_2ClL]\cdot 3H_2O$ **566** (Fig. 48) and a cetrosymmetric sulfur-bridged dinuclear complex $[PbPh_2L]_2\cdot 2H_2O$ **567** (Fig. 49) [135]. In both these complexes, the geometry around lead is distorted pentagonal bipyramidal with phenyl groups occupying axial positions and C–Pb–C angle being 168.27(17)° **566** and 175° **567** (ideal 180°).

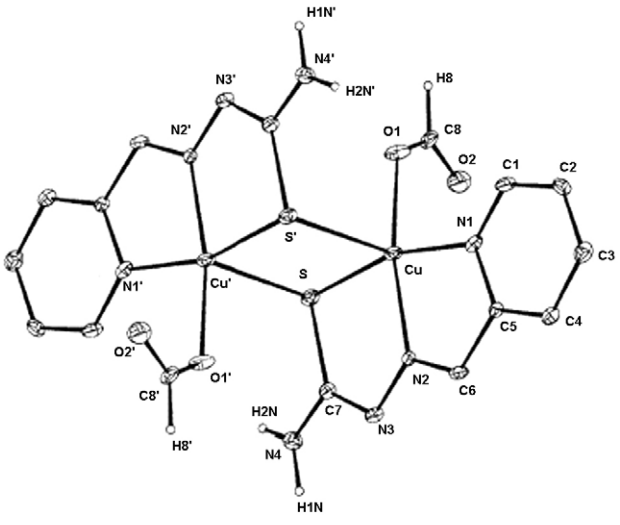

356

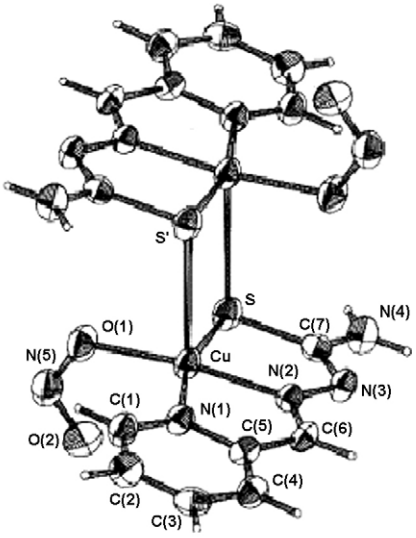

357

Fig. 29. Structures of complexes $[Cu_2L_2(OOCH)_2]$ **356** and $[Cu_2L_2(ONO)_2]$ **357** {adapted from reference [298]}.

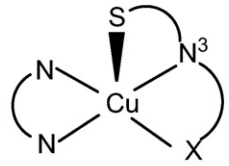

326–332, 334, 335 X =O

309, X = N^4

R^1				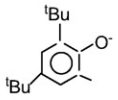
R^2	Me	H	Me	H
R^3, R^4	H, cy	H, H	H, H	H, Ph
N^N				
	326 [289]	**327** [288]	**328** [288]	**329** [288]

R^1			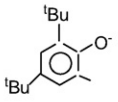			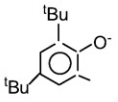
R^2	H	H	H	H	H	H
R^3, R^4	H, H	H, Ph	H, Ph	H, H	H, Ph	H, Ph
N^N						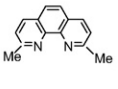
	330 [288]	**331** [288]	**332** [288]	**333** [290]	**334** [291]	**335** [288]

Chart 37.

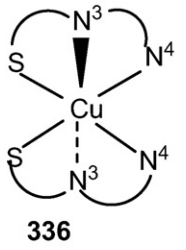

336

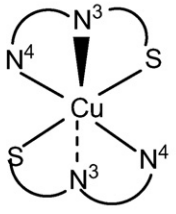

337

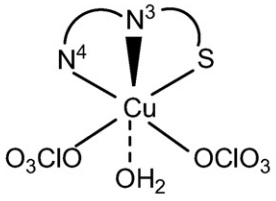

338

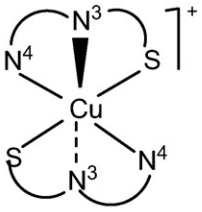

339

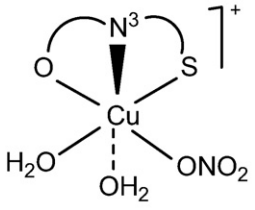

340

R^1	R^2	NR^3R^4	
	H	NMe_2	**336** [285]
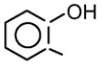	Me		**337** [293]
	H	NH_2	**338** [294]
	Me	NH_2	**339** [294]
	H	NHMe	**340** [62]

Chart 38.

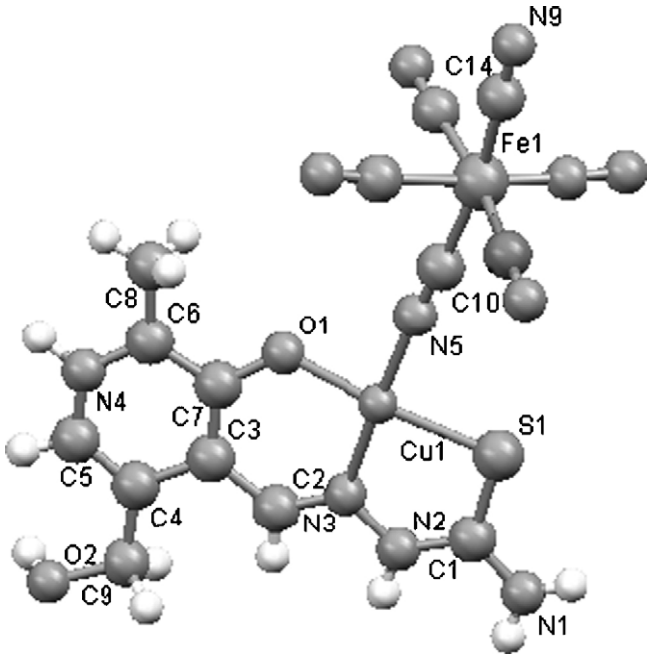

Fig. 30. Structure of complex $\{[Cu(H_2L)][Fe(CN)_5(NO)]\}_n \cdot 2nH_2O$ **379** {adapted from reference [178]}.

3.4.8.3. Bismuth. Among Group 15 elements, only a few complexes, namely, $[BiL_2(ONO_2)]$ **568** [137], $[BiL(N_3)]$ **569** (N_3 = azide) [138], and $[Bi_2L_2(ONO_2)_2]$ **570** [137], are reported (Chart 79) Complex **568**, contains seven-coordinate Bi with distorted pentagonal bipyramid geometry, and it is six coordinate in the monomeric **569** and **570**. In **570**, each bis-thiosemicarbazone ligand is dinegative pentadentate and one position is occupied by ONO_2 group.

3.4.9. f-Block elements

Amongs f-block elements only two U^{VI} complexes, namely, $(Bu_4N)[UO_2(L)(OAc)_2]$ **571** and $(Bu_4N)[UO_2(L)Cl_2]$ **572** are known [379a]. In both complexes, **571** and **572**, the thiosemicarbazone ligand acts as a uninegative, tridentate binding via N^4, N^3, S-donor atoms and uranium metal center has pentagonal bipyramid geometry.

3.4.10. Trends in bond parameters of representative complexes

Table 3 shows important bond parameters of some representative complexes, and a brief commentary of trends is delineated below. The bond parameters considered pertain to the metal–thiosemicarbazone segment of the complexes. Only M–S, M–N^3(azomethine){or M–N^2(hydrazinic nitrogen)}, M–X (X = N^4, O, S or C donor atoms of the substituent R at C^2 carbon atom, and metal–metal distances are shown in the table. Similarly, the bond angles considered are the bite angles, S–M–N^3 (or S–M–N^2) and N^3–M–X.

The M–S distances lie in a close range for many metal complexes (ca. 2.196–2.570 Å), but some have longer bond distances. Similarly, several of M–N^3 (or N^2) distances are in the range, 1.867–2.398 Å, while some complexes have longer distances. Relatively, M–N^3 bonds are stronger than M–N^4 bonds (the latter pertaining to R substituent at C^2 carbon). Further, both N^3, S and N^3, X-chelations (X = N^4, O, S, C) form five-membered rings, and thus the bite angles,

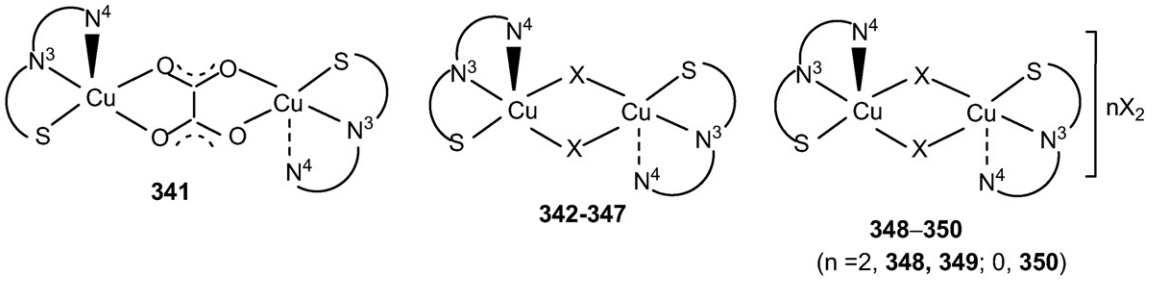

R^1R^2C=N-NH-C(=S)NR^3R^4

R^1										
R^2	Me	H	H	Ph		Ph	NH_2	H	H	H
NR^3R^4	NH_2	NH_2	NH_2		NHPh	NH_2	NH_2	NH_2	NH_2	NH_2
X	-	$MeCO_2$	$EtCO_2$	Cl	Cl	N_3	Cl	H_2PO_3O	CF_3CO_2	O_3SO
	341	**342**	**343**	**344**	**345**	**346**	**347**	**348**	**349**	**350**
	[286]	[295, 297]	[298]	[257]	[264]	[296]	[296]	[292]	[292]	[292]

Chart 39.

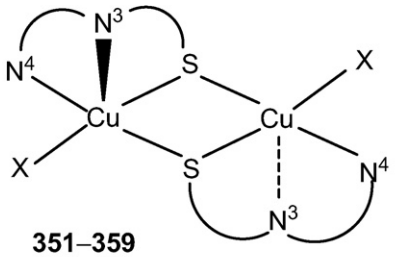

351–359

R^1								
R^2	H	H	H	H	H	H	H	H
R^3, R^4	H, H	H, Me	H, H	H, H	H	H, H	H, H	H, Me
X	I	Br	SCN	Br	Cl	OCHO	ONO	ONO_2
	351	**352**	**353**	**354**	**355**	**356**	**357**	**358**
	[20]	[281]	[281]	[299]	[299]	[298]	[298]	[300]

Chart 40.

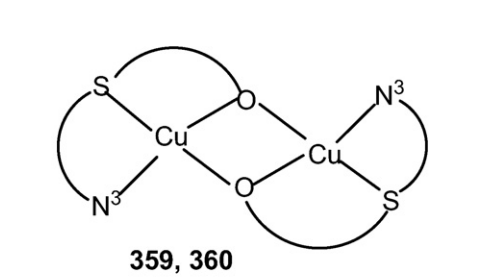

359, 360

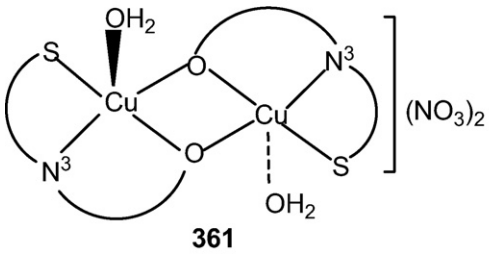

361

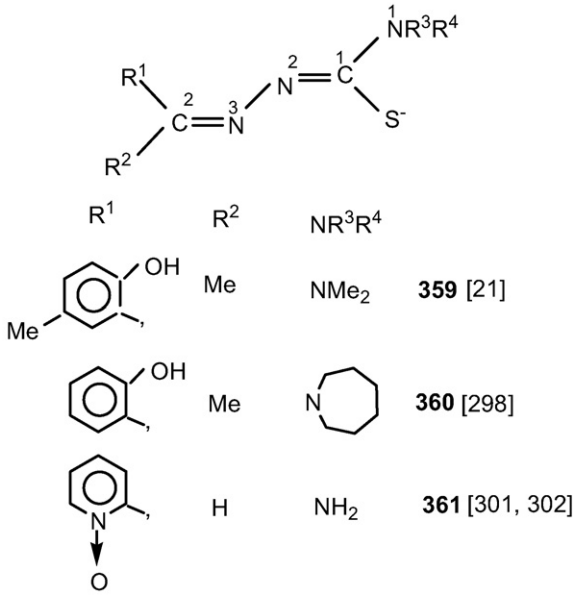

R^1	R^2	NR^3R^4	
	Me	NMe_2	**359** [21]
	Me		**360** [298]
	H	NH_2	**361** [301, 302]

Chart 41.

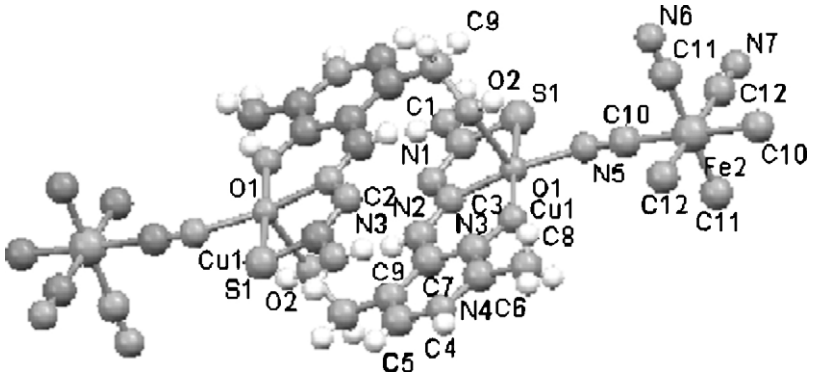

Fig. 31. Structure of complex $\{[Cu(HL)]_2[Fe(CN)_5(NO)]\}_n \cdot 6nH_2O$ **380** {adapted from reference [178]}.

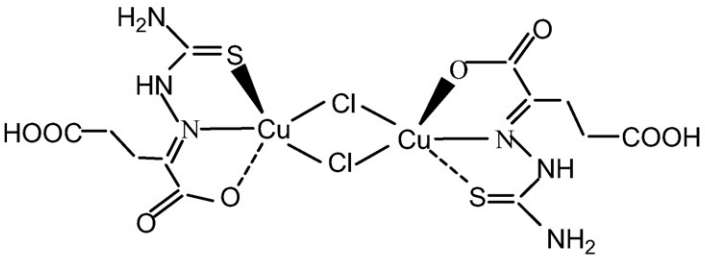

362 [269]

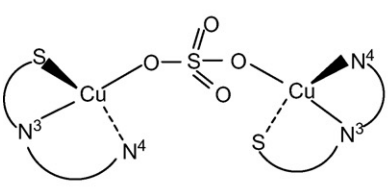

363

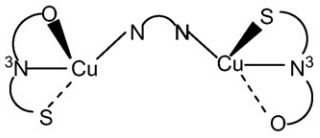

364

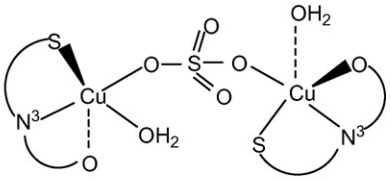

371

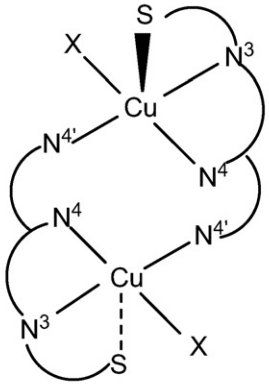

365, 366, 370

R^1	R^2	NR^3R^4	X	
	Me		-	**363** [303]
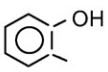	H	NH_2	-	**364** [304]
		NH_2	NCS	**365** [303]
		NH_2	$MeCO_2$	**366** [303]
		NPhMe	Br	**370** [305]

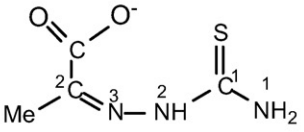

371 [64]

Chart 42.

S–M–N^3 and N^3–M–X fall in a wide range, ca. 66–100° {the origin of C is from R group when it forms M–C bonds after loss of H atom from the ring (i.e. intramolecular metallation)}. On the other hand, N^2, S-chelation forms four-membered rings leading to small N^2–M–S bite angles, ca. 55–66°. It is understood that the bond distances/bond angles are affected by the other co-ligands in the complexes, and also by the type of a thiosemicarbazone used, and a simple rationalization of trends in bond parameters is not possible. With respect to close metal–metal contacts, only distances less than 4 Å are included, and it can be seen that the complexes of coinage metals in univalent state have metal–metal contacts either less than or close to the sum of the van der Waals radius of Cu or Ag as the case may be {Cu···Cu, 2.80; Ag···Ag, 3.40 Å).

4. Applications

4.1. Biological

Thiosemicarbazone and its metal complexes show significant biological activity, suggesting accessibility of coordination site, a fundamental requirement for biological activity by the complexes [379b].

4.1.1. Antifungal and antibacterial properties

Square pyramidal, $[CuL(NO_3)(H_2O)]\cdot H_2O$, **317** [285] complex with 6-methyl-formylpyridine-N^4-dimethyl-thiosemicarbazone showed a lower fungitoxic activity against phytopathogenic fungi,

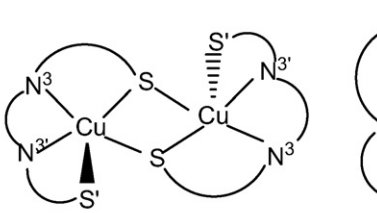

367, **368**

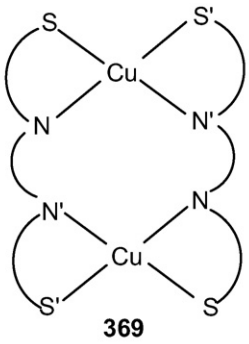

369

R^1	R^2	R^3, R^4	
		Et,Et	**367** [275]
H	H	H, Et	**368** [270]
Me	Me	H, Me	**369** [282]

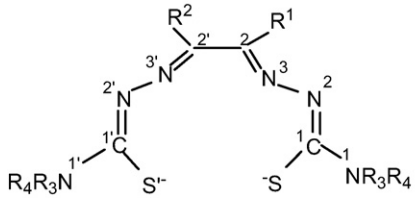

Chart 43.

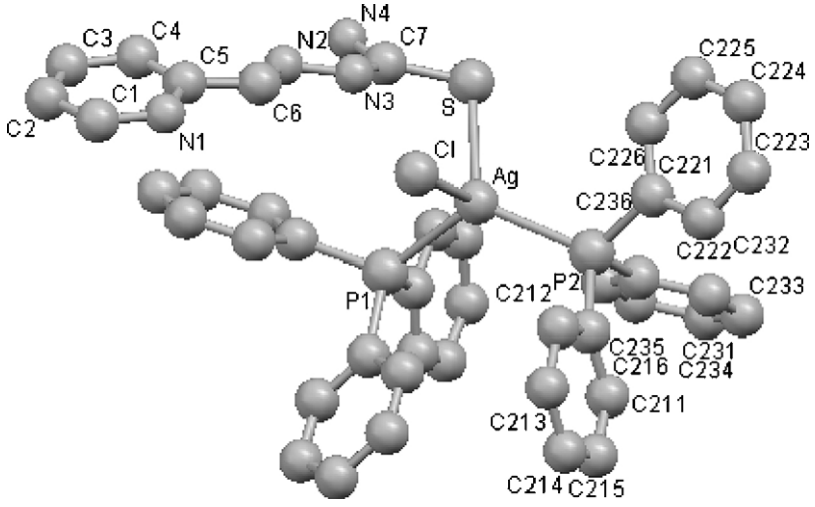

Fig. 32. Structure of $[AgCl(\eta^1\text{-S–HL})(PPh_3)_2]\cdot CH_3CN$ **381** {adapted from reference [310]}.

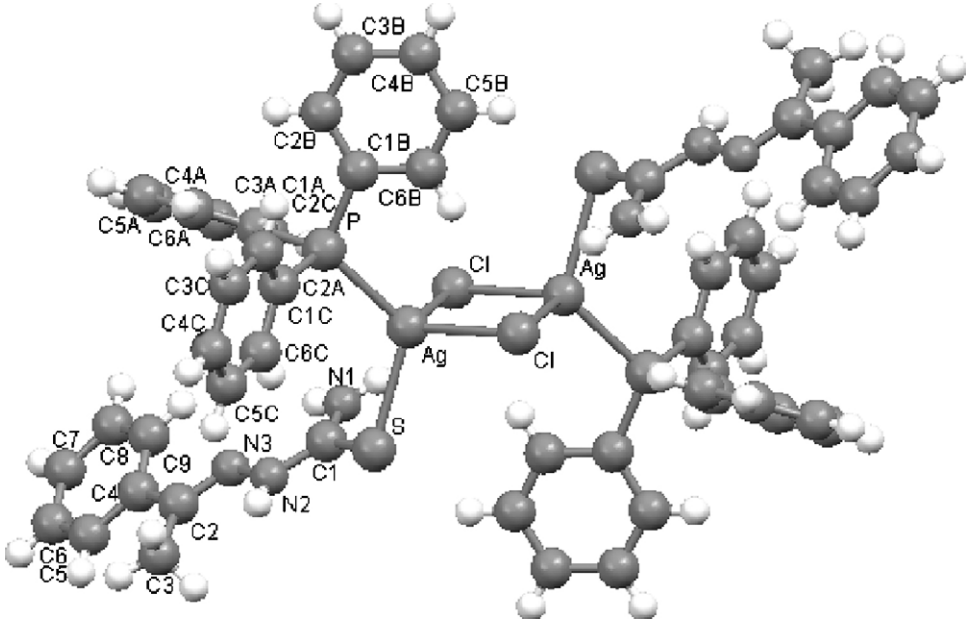

Fig. 33. Structure of $[Ag_2(\mu\text{-Cl})_2(\eta^1\text{-S–HL})_2(PPh_3)_2]$ **384** {adapted from reference [310]}.

A. alternata, *F. phaseoline* and *F. equisetti*, than the free ligand possibly attributed to the lower solubility of complexes in the non-aqueous solvents compared with the free ligand. 2-Benzoylpyridine thiosemicarbazone, and its copper(II) complexes exhibit antifungal activity against various strains of the pathogenic fungi. The activity varied with the nature of the substituent at the amino nitrogen of thiosemicarbazone. 2-Benzoylpyridine-*N*(1)-isopropyl thiosemicarbazone as well as its square pyramidal complex, $[Cu(HL)Cl_2$ **310** [262] were fungitoxic against the human pathogenic fungi, *A. niger* and *P. variotti*. 2-Benzoylpyridine thiosemicarbazone ligand with N(4) phenyl substituent was most active against *S. aureus* while its dimeric complex $[CuLX]_2$ (X = Cl **345**, NCS **283**) [264] was inactive against this strain. They, however, exhibited activity against other strains, *S. paratyphi* and *V. cholerae*, while ligands with bulkier

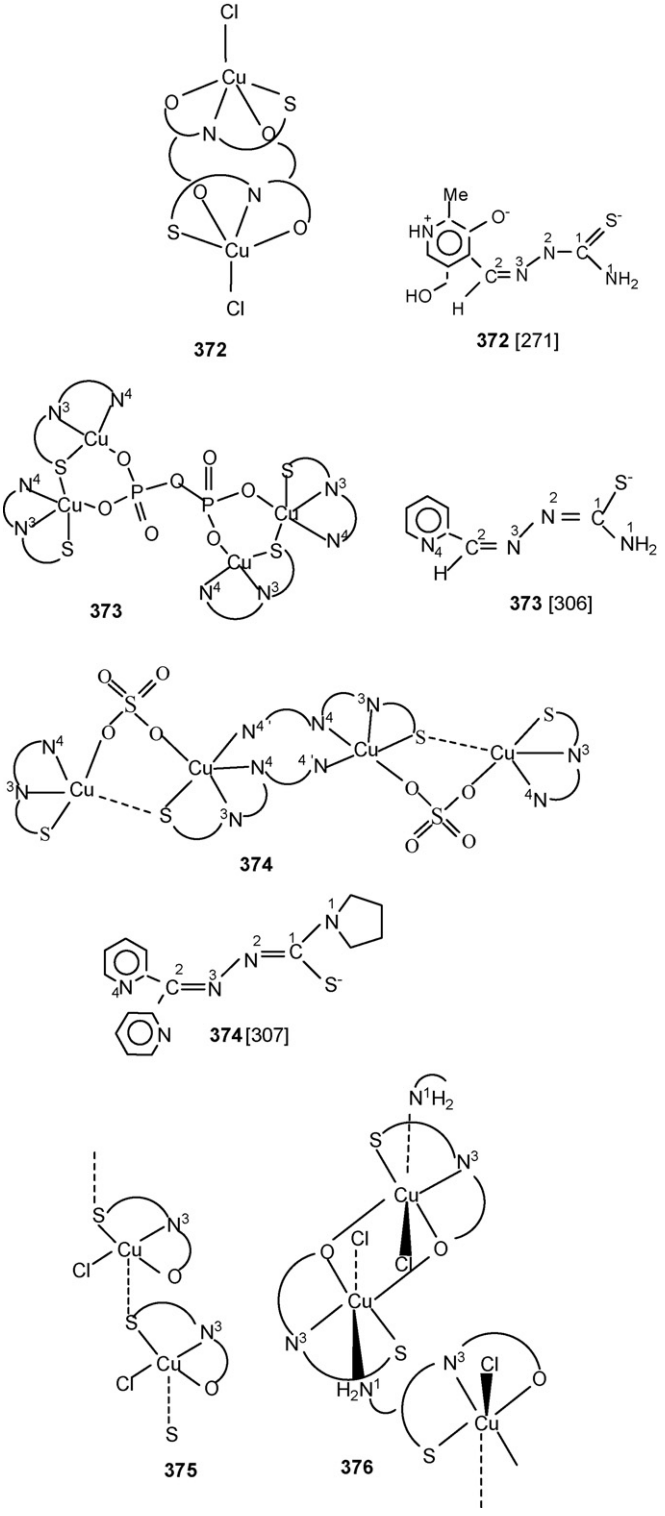

Chart 44.

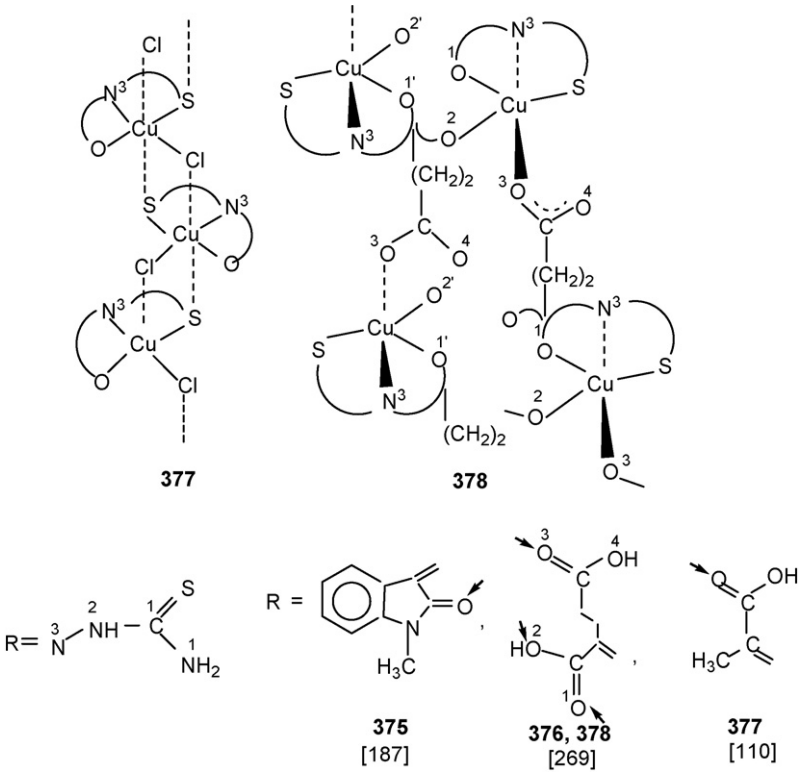

Chart 44. (*Continued*).

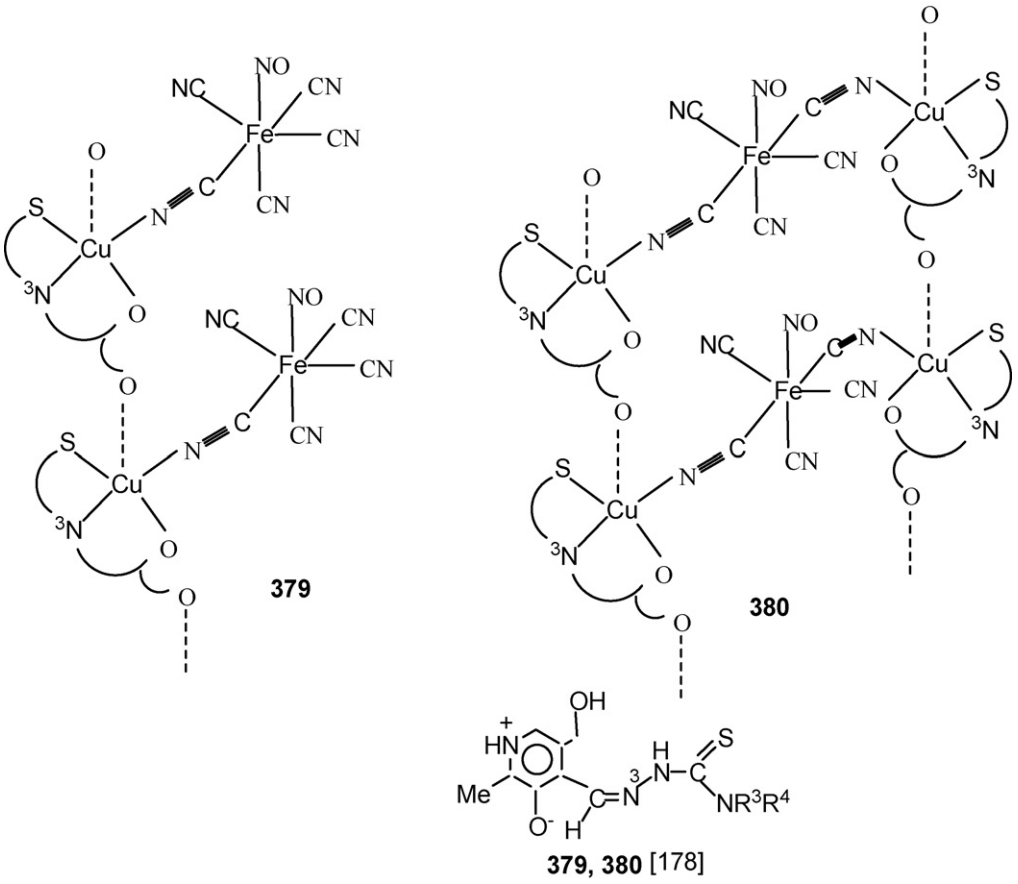

Chart 45.

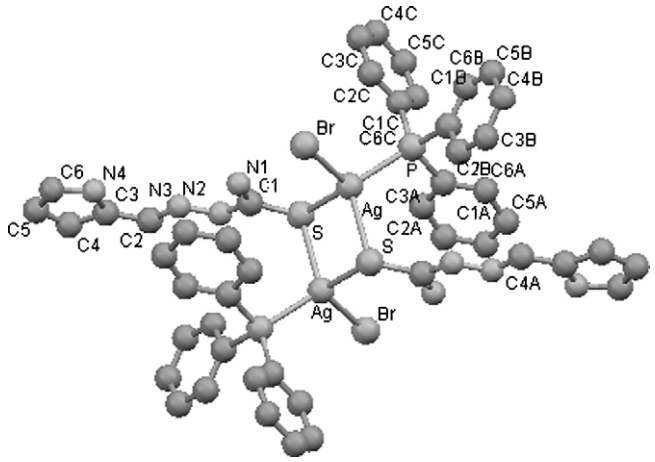

Fig. 34. Structure of $[Ag_2Br_2(\mu\text{-S–HL})_2(PPh_3)_2]\cdot 2H_2O$ **387**{adapted from reference [310]}.

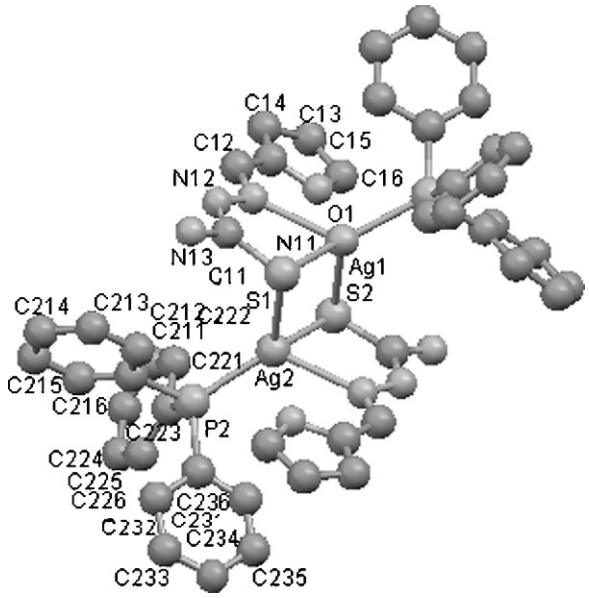

Fig. 35. Structure of $[Ag_2(\eta^1\text{-N-}\mu\text{-S–HL})_2(Ph_3P)_2](NO_3)_2$ **389** {adapted from reference [310]}.

hexamethyleneiminyl group at the amino nitrogen were more active both as free ligand as well as in the form of a copper(II) complex [CuLCl] **281** [262].

Square pyramidal $[Hg(HL)Br_2]$ **415** [139] showed activity at the moderate concentration of 400 μg/ml against *P. variotti* and *A. niger*, while the analogous zinc(II) complex $[Zn(HL)X_2]$ (X = Cl **422** [330], Br **423**) exhibited activity only at higher concentration [325]. The

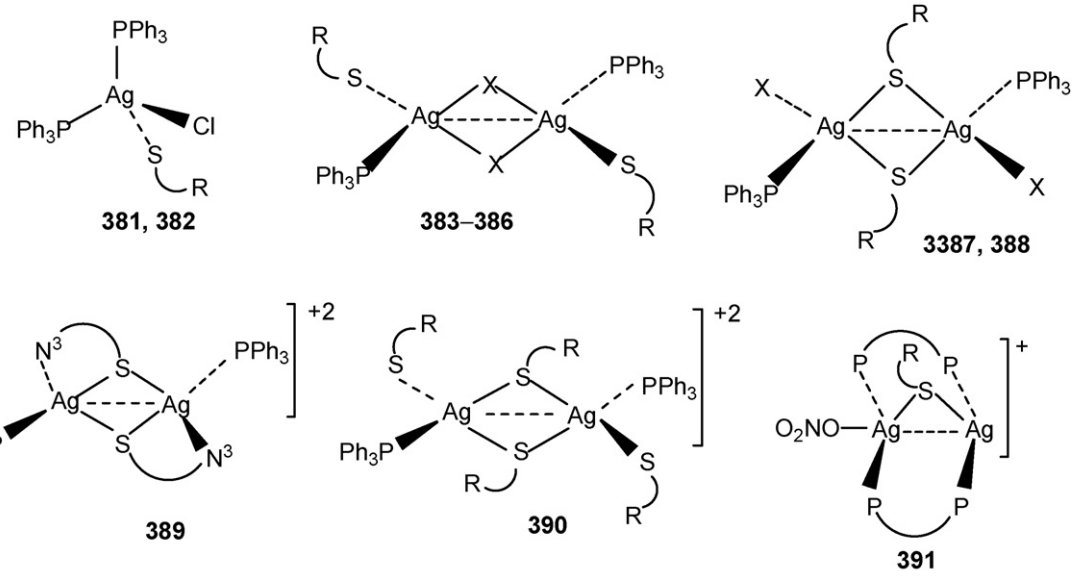

R^1R^2C=N-NH-C(=S)NH_2

R^1		Me			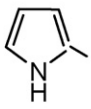	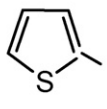			
R^2	H	Me	Me	H	H	H	H	H	Me
X	Cl, Br	Br	Cl, Br	Br	Br	Cl	-	-	ONO_2
	381, 382 [310]	**383** [310]	**384, 385** [310]	**386** [310]	**387** [310]	**388** [310]	**389** [310]	**390** [310]	**391** [310]

Chart 46.

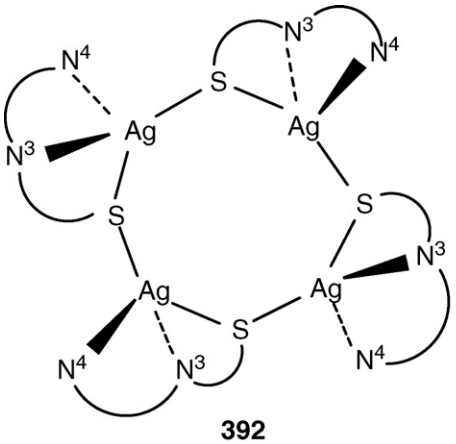

392

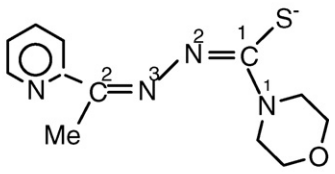

392 [312]

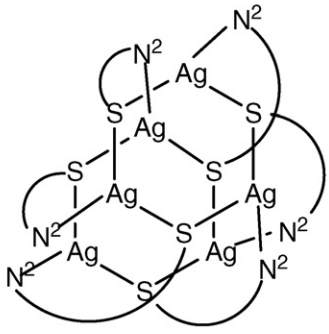

393

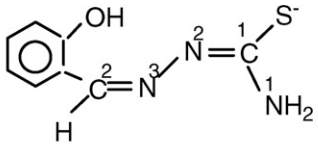

393[31]

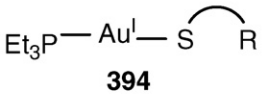

394

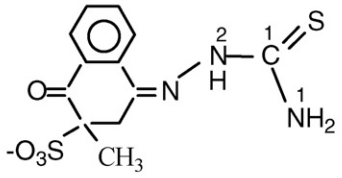

394 [115]

Chart 46. (*Continued*).

dimeric complex [CuL_2] at 1000 μg/ml was less active against *P. variotti* **337** than the free ligand [293]. Most of the thiosemicarbazone complexes displaying anti-bacterial activities have a pyridyl group at the C^2 carbon of the thiosemicarbazone. An enhanced inhibitory effect of complexes in comparison with that of the free ligand may be attributed to the increased lipophilicity of complexes in aqueous solutions, which seems to be responsible for their enhanced biological potency. N^1-substituted 2-acetyl pyridine thiosemicarbazones show remarkable activity upon complexation with various metals. Square pyramidal complexes [$Zn(HL)Cl_2$] **417** and [$Zn(HL)(H_2O)(SO_4)$] **418** display activities against four strains of bacteria (*B. subtilis, S. aureus, E. coli, P. aeruginosa*), two yeast (*C. albicans, S. cerevisae*), and two molds (*A. niger, P. citrinum*) [321]. Square planar complexes [PtLCl] **223** [106] and [PtL_2] **226** [109] exhibit a lethal effect on Gram (+) bacteria only. Monomeric [$BiL_2(NO_3)$] **568**, and dimeric [$BiL(NO_3)]_2$ **569** complexes, showed modest activities against the selective Gram(+) and (−) bacteria (*E. coli*, *B. subtilis* and *S. aureus*) and yeasts (*C. albicans* and *S. cerevisiae*). After complexation, the activity was increased against the bacteria and suppressed against yeasts and molds [137,138].

4.1.2. Anticancer properties

Thiosemicarbazones as well as their complexes are known for their anticancer properties. They act by inducing apoptosis in the cancerous cell lines. Some anti-cancer drugs act by inducing apoptosis by activating the endonucleotidase leading to the DNA fragmentation [269].

4.1.2.1. Cu and Au. The square pyramidal complex [$Cu(H_2L)(OH_2)Cl]Cl$ (H_2L = pyridoxal thiosemicarbazone) **321** induces differentiation of Friend Erthyroleukemia cells (*FLC*) and erythroid cells, and suppresses FLC proliferation [63]. Square pyramidal complexes of 5-formyluracil thiosemicarbazone, [$Cu(H_3L)Cl_2$] **324**, [$Cu(H_3L)H_2O(SO_4)$] **323** [65] and [$Cu(H_3L)(OH_2)_2](NO_3)_2{\cdot}H_2O$ **325** [170] were tested in vitro on the human leukemia cells lines, *K562* and *CEM*. The complex **324** inhibited *CEM* clone-13 and *K562* cell proliferation while **323** inhibited growth of *K562* cells only at the concentration of 40 μg/ml [65]. However, **325** [170] significantly inhibited proliferation of *K562*, *CEM* (35 μg/ml) and *U937* cell lines (30 μg/ml). Pyridoxal N(4)-substituted thiosemicarbazone and its complex,

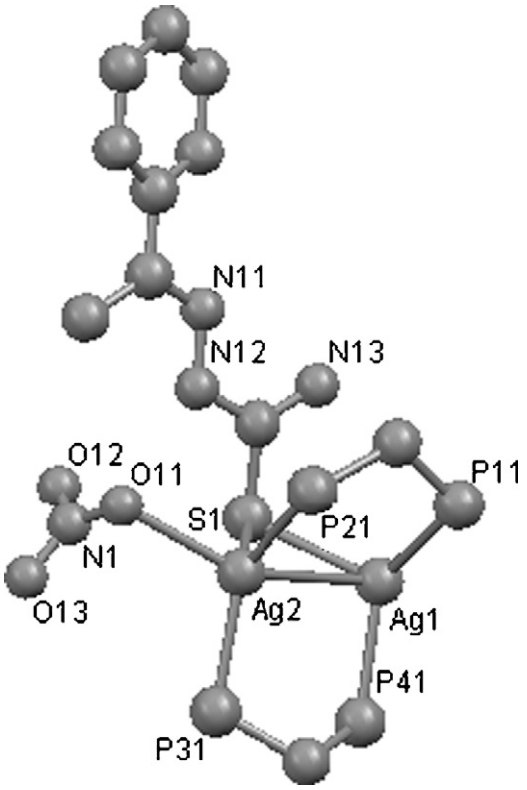

Fig. 36. Structure of $[Ag(\mu\text{-P,P-dppm})_2(\mu\text{-S–HL})Ag(ONO_2)]NO_3$ **391** {adapted from reference [311]}.

$[Cu(HL\text{-}N1,N1Me_2)Cl]_2{\cdot}6H_2O$, **285** [266] showed weak inhibition of proliferation of the adenocarcinoma cell lines, *U937, K562* and *CEM* and also did not induce the apoptosis or limit the telomerase activity. The presence of the substituent on NH_2 group heavily decreased the activity of copper complexes with this kind of thiosemicarbazone. Salicylaldehyde thiosemicarbazone has been observed to possess antibacterial properties, but its copper(II) complex [CuL(phen)] **331** with its N^1-phenyl derivative, exhibited good binding propensity to calf thymus DNA and oxidatively cleave supercoiled PUC19 DNA in the dark under aerobic conditions, and in the light at $\lambda = 312$ and 532 nm [288]. A square planar complex $[CuL_2]$ **271** [254] with thiophene-2-carbaldehyde thiosemicarbazone exhibited cytotoxicity against *Friend Leukemia Cells* and *MelanomaB16F10* cell lines. Polymeric complexes $[CuL]_n$ **377**, $[Cu(H_2L)_n]{\cdot}3nH_2O$ **375** [110,187] (H_3L = α-ketoglutaric acid) were tested on FLC and the human leukemia cell lines, *K562* and *U937*. Both complexes showed proliferation inhibition through the apoptosis on the cell line *U937* only. At high concentration of 50.48 μg/ml, the free ligand showed no effect on cell growth while both complexes were able to do so with IC_{50} value of 35 μg/ml for *U937* and 40 μg/ml for *K562* [269]. Polymeric complexes of pyridoxal thiosemicarbazone, $\{[Cu(HL)]_2[Fe(CN)_5(NO)]\}_n{\cdot}2nH_2O$ **379** and $\{[Cu(HL)]_2[Fe(CN)_5(NO)]\}_n{\cdot}6nH_2O$ **380**, were tested in vitro for their cytotoxicities against the tumour cell lines, U937 and CEM, using peripheral blood mononuclear cells (PBMC) as control. These complexes with 4 + 1 coordination were found to exhibit efficiency in inhibiting the leukaemic cell proliferations of both CEM and U937 cell lines and in inducing the apoptosis. On the contrary, $[Co(HL)_2]_2[Fe(CN)_5(NO)]{\cdot}8H_2O$ **96** with octahedral geometry is ineffective in any biological activity against these cell lines, supporting the fact that accessible coordination is pre-requisite for the biological interactions [178].

A linear gold(I) complex $[Au(PEt_3)(HL)]$ **394** (HL = Vit. K3 thiosemicarbazone), showed similar cytotoxicity as cisplatin against cisplatin sensitive cell line A2780 and 10 times more against cisplatin-resistant cell line A2780cis [115]. Square planar Au^{III} complexes, $[Au(Hdamp\text{-}C^1)Cl(L^1)]PF_6$ **398**, $[Au(Hdamp\text{-}C^1)Cl(L^2)]Cl$ **395**, $[Au(Hdamp\text{-}C^1)\,Cl(H_2L^3)]Cl_2{\cdot}MeOH$ **396**, $[Au(Hdamp\text{-}C^1)\,(L^5)]Cl_2$ **399** [116,117] and, $[Au(Hdamp\text{-}C^1)\,(L^4)]Cl_2{\cdot}2MeOH$ **400** [117] exhibited antiproliferative activity against human *MCF-7* breast cancer cell line. Complexes $[Sn(Me)_2L(S_2PPh_2)]$ **530** and $[Sn(Et)_2L(S_2PPh_2)]$ **531** displayed inhibitory effect on proliferation of the cell lines of *FLC*, *CEM*, *U937*, *K562* and *TOM-1* leukemia cell

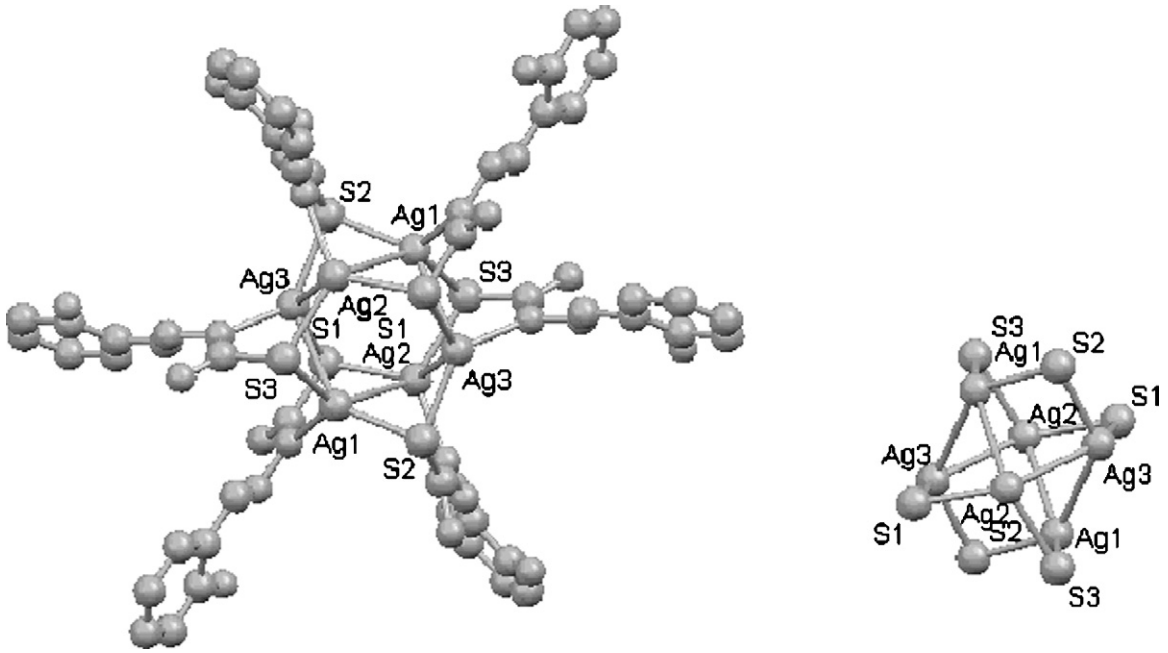

Fig. 37. Structure of complex $[Ag_6L_6]$ **393** {adapted from reference [31]}.

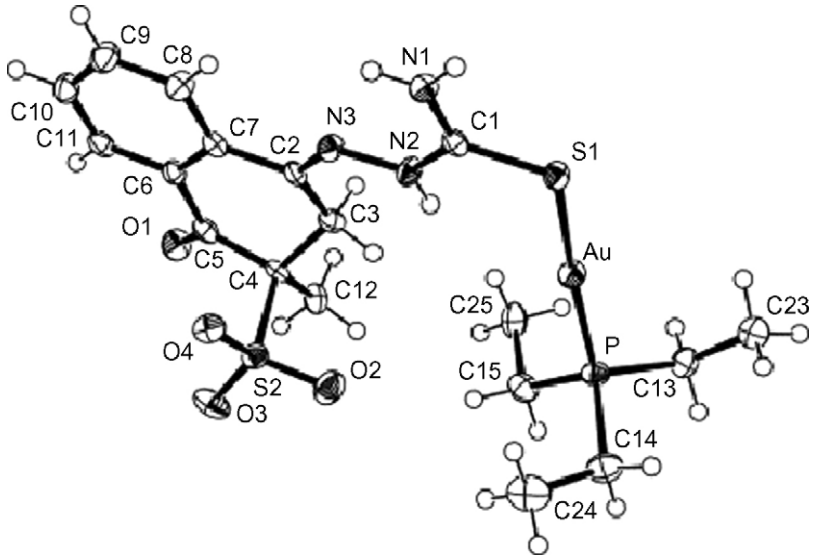

Fig. 38. Structure of complex [Au(PEt_3)(HL)] **394**{adapted from reference [115]}.

lines. These complexes induced significant differentiation of *K562* cell lines but not *FLC* [132].

Labeled copper–thiosemicarbazone complexes have shown an important application as imaging agents. ^{64}Cu or ^{67}Cu labeled complexes of *p*-carboxyalkylphenylglyoxal and *p*-carboxyalkyl-1, 2-diketo-bis-(N^4-methylthiosemicarba zone) bifunctional ligands have been applied for labelling bovine serum albumin protein in 3–40% yields and can be used for tumor imaging [380]. The copper complex of pyruvaldehyde-bis (*N*-4-methylthiosemicarbazone) has acted as a potential imaging agent for heart and brain when labeled with ^{64}Cu or ^{67}Cu and showed no adverse effects on administration in higher doses of 2.16 $\mu g\,kg^{-1}\,day^{-1}$ for two weeks in rabbits [381]. ^{64}Cu-diacetylbis(N^4-ethylthiosemicarbazone) complex showed similar hypoxia selectivity as ^{64}Cu-diacetylbis (N^4-methylthiosemicarbazone) complex [382].

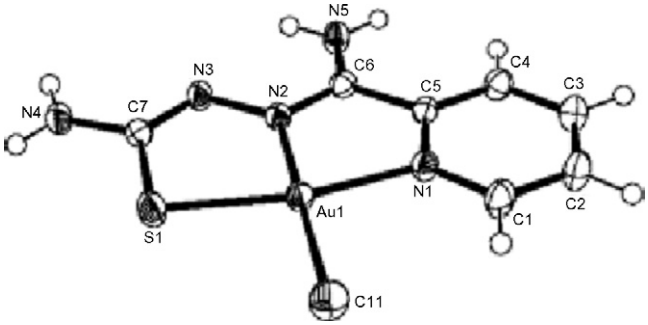

Fig. 40. Structure of complex [AuCl(L)][$AuCl_2$] **403** {adapted from reference [314]}.

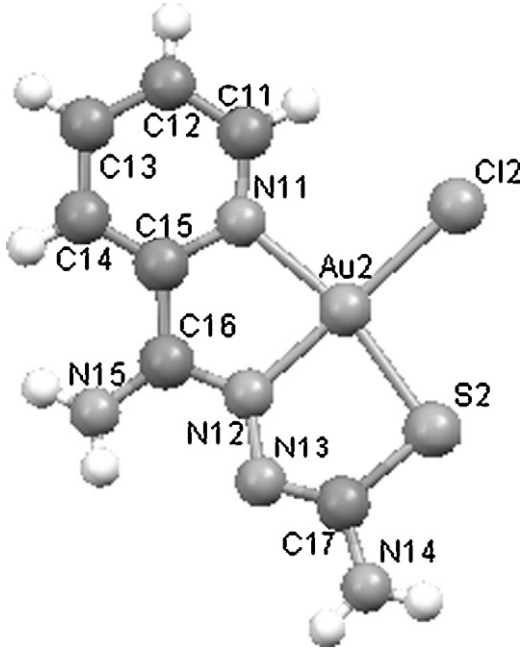

Fig. 39. Structure of complex [Au(L)(Hdamp-C^1)]Cl_2 **401** {adapted from reference [314]}.

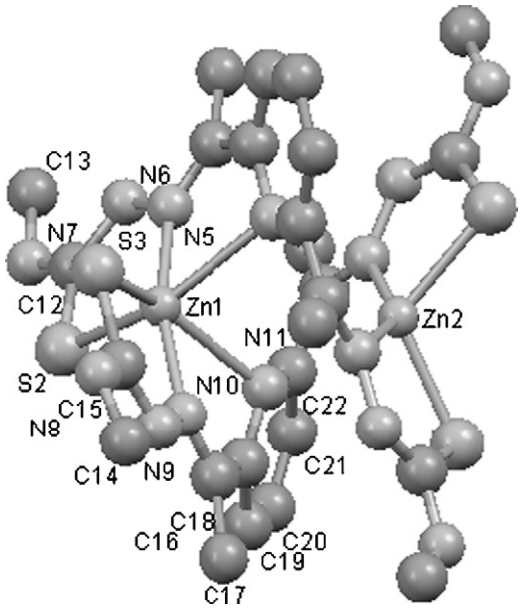

Fig. 41. Structure of complex [Zn_2L_2] **444** {adapted from reference [34]}.

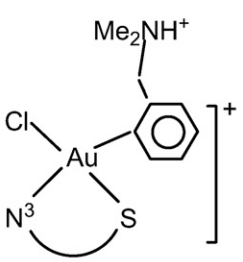

395–398

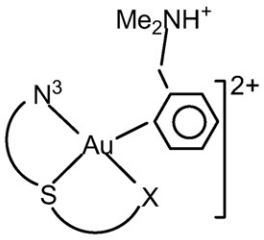

X = P, **399,** X **=** N, **400**

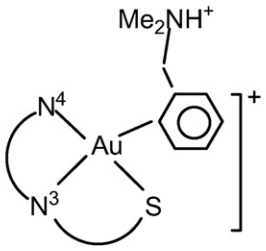

401, **402**

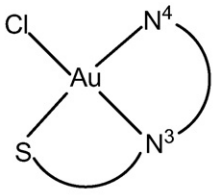

403–405

$R^1R^2C^2{=}N^3{-}N^2H{-}C^1(=S)N^1R^3R^4$

R^1		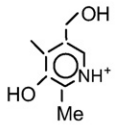	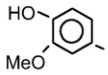		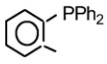					
R^2	H	H	H	H	H	Me	NH_2	Ph	NH_2	NH_2
NR^3R^4	NMe_2	NMe_2	NH_2	NMe_2	NH_2	NHPh	NHMe		NH_2	
X	-	-	-	-	P	N	-	-	-	-
	395	**396**	**397**	**398**	**399**	**400**	**401,**	**403**	**404**	**405**
	[116]	[116]	[117]	[117]	[116]	[117]	**402**	[315]	[314]	[314]
							[314]			

Chart 47.

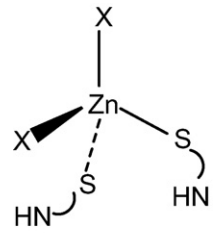

406–412

R^1	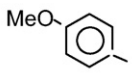	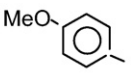				Me	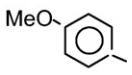
R^2	H	H	Me	H	H	Me	H
R^3, R^4	H, H	H, H	H, Ph	H, H	H, Et	H, Ph	H, H
X	Cl	I	Br	Cl	I	Cl	Br
	406	**407**	**408**	**409**	**410**	**411**	**412**
	[66]	[66]	[67]	[68]	[69]	[70]	[71]

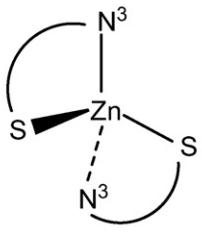

413–416

R^1	Me	Fc	Me	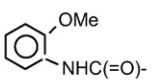
R^2	Me	Me	Me	Me
R^3, R^4		H, H	H, H	H, H
	413	**414**	**415**	**416** [320]
	[316]	[317, 318]	[319]	

Chart 48.

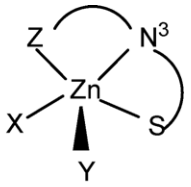

Z = N^4, **417–419, 421, 425, 426**
Z = O, **420, 422–424**

R^1										
R^2	Me	Me	Me	Me	Me	Me	Me	Me	H	Me
R^3, R^4	H, H	H, H		H	H, H	H, Me	H, Et	H, Et	H, H	H, H
X, Y	Cl, Cl	OH_2, SO_4	$2(ONO_2)$	Cl, Cl	Br, Br	Cl, Cl	Br, Br	Cl, Cl	Cl, Cl	Cl, Cl
	417	**418**	**419**	**420**	**421**	**422**	**423**	**424**	**425**	**426**
	[321]	[321]	[322]	[323]	[324]	[330]	[325]	[325]	[326]	[326]

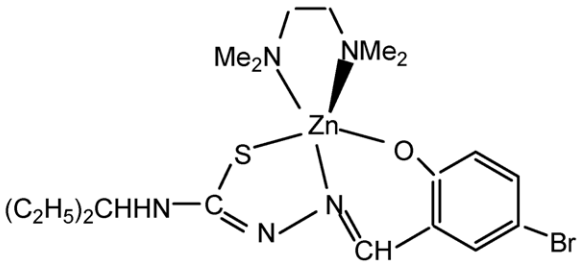

427 [327]

Chart 49.

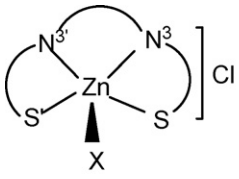

428, 429

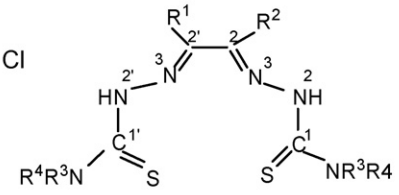

R^1 , R^2	R^3R^4	X	
Cy, Cy	NH_2	Cl	**428** [328]
Ph, H		Cl	**429** [246]
Cy, Cy	NH_2	OH_2	**430**[328] [DMF]

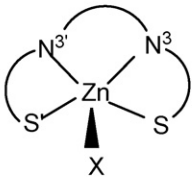

430

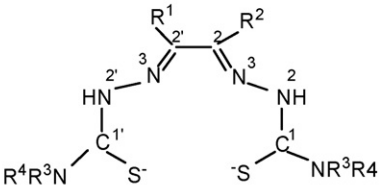

Chart 50.

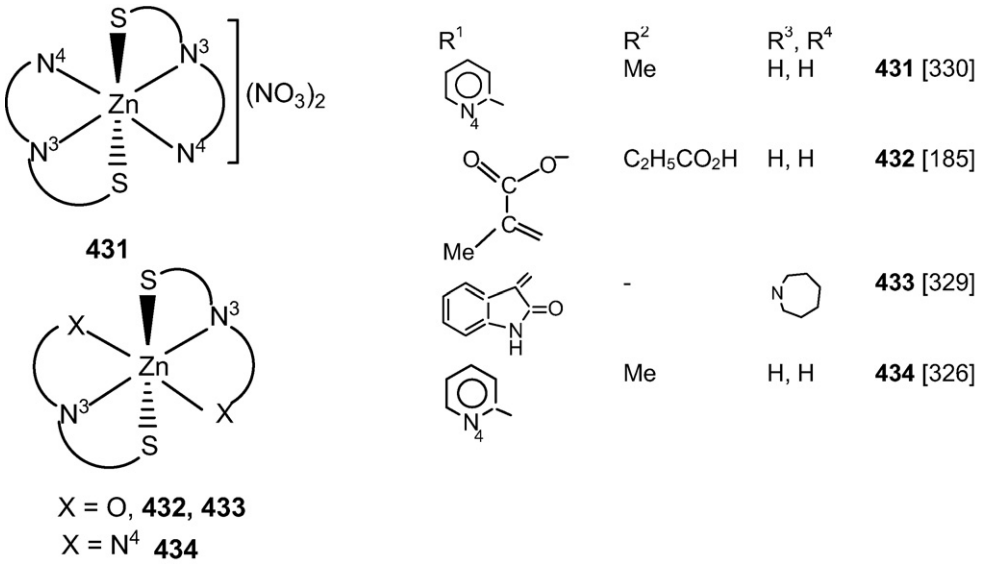

Chart 51.

4.1.2.2. Zn, Ni, Co, Pd, Pt and Sn. The octahedral complex [Co(HL)L]·H_2O **109** with α-ketoglutaric acid thiosemicarbazone was able to induce differentiation in *FLC* cell line [183]. Nickel and cobalt complexes with 5-formyluracil thiosemicarbazone were found to be less active than copper(II) complex with the same ligand, when tested against the human leukemic cell lines *K562* and *CEM* [170]. Complex, [NiL_2] **135** with thiophene-2-carbaldehyde thiosemicarbazone ligand tested against *MelanomaB16F10* and FLC cell lines, was less active than the free ligand [24]. The octahedral [NiL_2] complex **145** with phenanthrenequinone thiosemicarbazone was tested on human breast cancer cell line, T47D rich in the progesterone receptors and has a synergistic effect on the antiproliferative activity of the cell lines [185]. Most of the thiosemicarbazone complexes of Pd and Pt exhibit antitumor activities. The square planar complex [PtLCl] **220** with 2-acetyl pyridine thiosemicarbazone–N–Me showed higher cytotoxicity against the cisplatin resistant and sensitive ovarian cancer cell lines, *A2780* and *A2780/Cp8* with IC_{50} values of 0.08 and 0.14 μM, respectively, greater than the cisplatin [105]. The square planar complex [PdL_2] **209** with 2-acetylpyridine-3-hexamethyleneiminyl thiosemicarbazone also showed potential antitumor activities [60]. Octahedral complexes, [Sn(2-Bz4Ph)Cl_3]·CH_3CH_2OH **535** and [Sn(2-Bz4Ph)$BuCl_2$]·H_2O **539** (H2-Bz4Ph = N(4)-phenyl-2-benzoylpyridine thiosemicarbazone, Bu = butyl group) and H2-Bz4Ph were tested against the *MCF-7*, *TK-10* and *UACC-62* human tumor cell lines. The ligand H2-Bz4Ph and all its com-

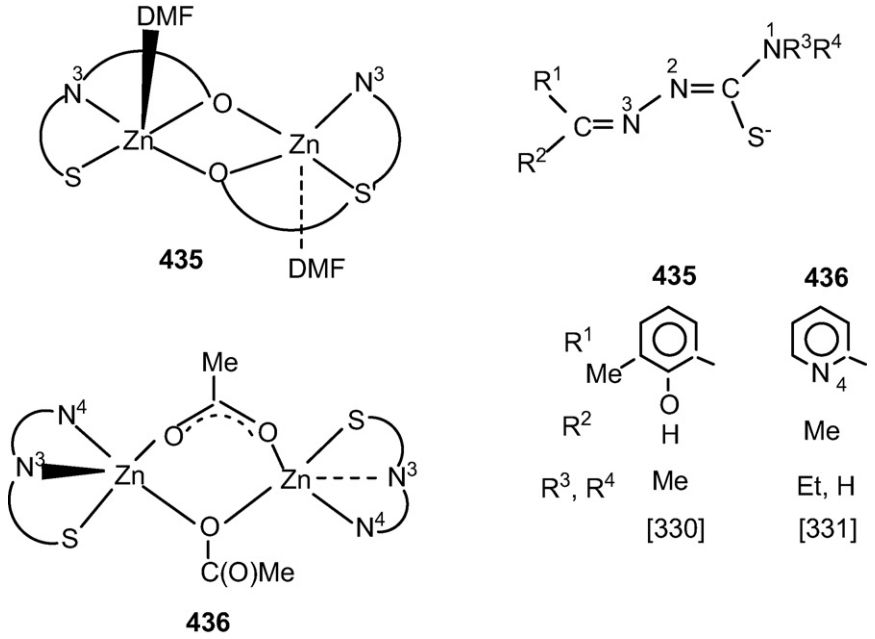

Chart 52.

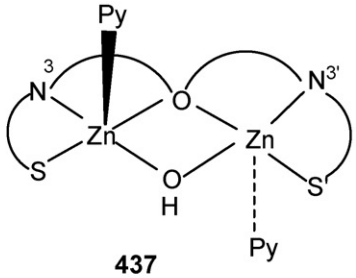

437

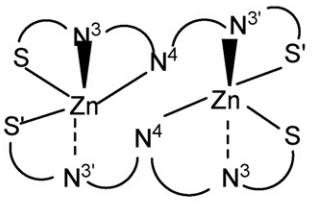

438

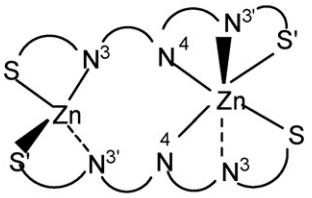

439

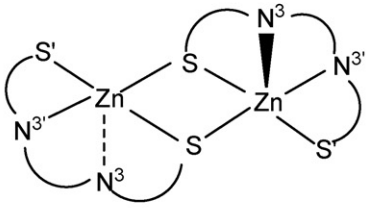

440

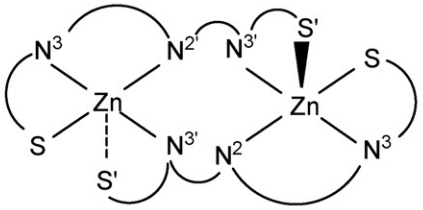

441

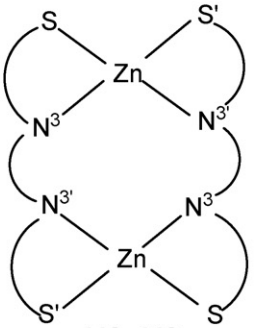

442, 443

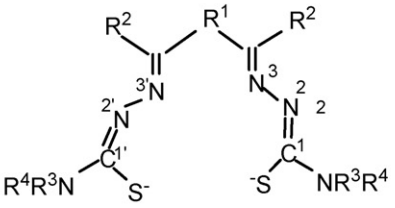

437–439, 442, 444

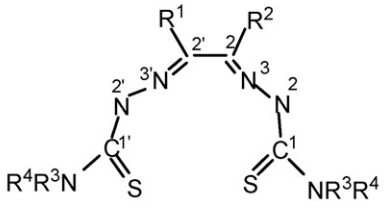

440, 441, 443

R^1	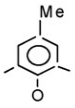			Me	Ph		Fc	
R^2	H	Me	Me	Me		Me	Me	Me
NR^3R^4	NH_2	NH_2	NMe_2	NHMe	NH_2		NH_2	NHMe
	437	**438**	**439**	**440**	**441**	**442**	**443**	**444**
	[328]	[336]	[332]	[325]	[333]	[334]	[335]	[34]

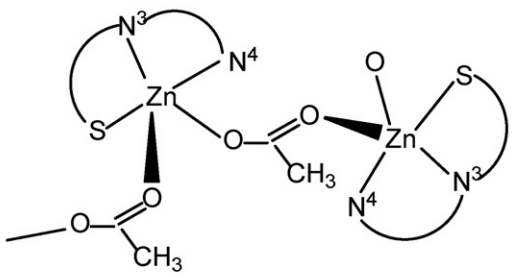

445

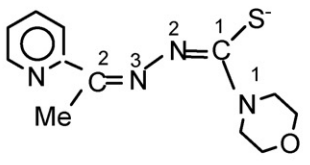

445 [322]

Chart 53.

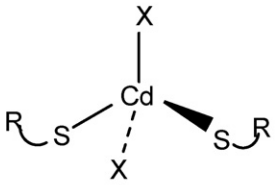

446–454

R^1									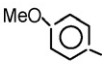
R^2	Me	H	H	Me	H	H	H	H	H
R^3, R^4	H, H	H, H	H, Et	H, Me	H, H	H, H	H, H	H, H	H, H
X	I	Br	Br	I	I	Br	I	I	I
	446	**447**	**448**	**449**	**450**	**451**	**452**	**453**	**454**
	[337]	[337]	[69]	[338]	[338]	[338]	[339]	[340]	[341]

Chart 54.

plexes were able to induce apoptosis in *UACC-62* cell lines [367,373].

4.2. Analytical

Thiosemicarbazones find applications in the determination of the trace metals in the biological and the pharmaceutical samples in the extraction of metals, for the inhibition of corrosion, etc. The mode of action is basically the formation of complexes of the thiosemicarbazones with the metal ions. Generally, the chelates are formed and can be extracted into suitable solvents. A brief summary given herewith demonstrates the versatility of thiosemicarbazones in the analytical field. Chart 80 displays thiosemicarbazones used for the analytical applications.

Trace amounts of Cu^{II} were determined with cyclopentanone thiosemicarbazone [**I**] by using stripping voltammetry (detection limits, 1.57×10^{-9} M) [383]. *N*-Ethyl-3-carbazolecarboxaldehyde thiosemicarbazone [**II**] was used for spectrophotometric determination of Cu^{II} in the environmental and pharmaceutical samples, by forming a green complex (pH 3.0), which can be extracted into *n*-butanol [384]. The Cu^{II} acetophenone-*p*-chlorophenylthiosemicarbazone **III** complex floats quantitatively with the oleic acid surfactant, which can be separated further. Beer's law is obeyed over concentration range of 0.25–6.35 mg L^{-1}, with the detection limit of 0.021 mg L^{-1} [385]. Benzildithiosemicarbazone **IV** has been used for the determination of both Cu^{II} and Pd^{II} by the extractive spectrophotometric method (pH 1–7, Cu^{II}; 2.5, Pd^{II}). This method has been used for the determination of Cu^{II} in the pharmaceutical/environmental samples and for Pd^{II} in the synthetic samples and the hydrogenation catalysis [386]. Phenanthraquinone monophenyl thiosemicarbazone **V** forms intense red 1:2 complex with Cd^{II}, which interacts with the oleic acid surfactant at pH 6.5 and separates quantitatively (i.e. floats) on the surface of the reaction system. This method has been used for detecting traces of Cd in the human hair samples and the natural waters [387]. Carbon paste electrode modified with the benzyl bis(thiosemicarbazone) **VI** is used for mercury speciation in the water samples [388]. Thallium(III) forms

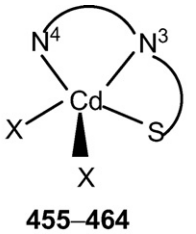

455–464

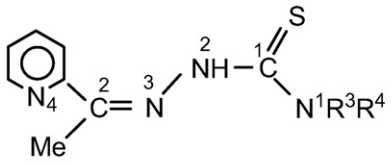

R^3, R^4	H, Et	H, Et	H, Et	H, Me	H, Me	H, Ph	Me	Me	H, Me	H
X	Cl	Br	I	Br	Cl	Br	Cl	I	Cl	Cl
	455	**456**	**457**	**458**	**459**	**460**	**461**[1	**462**	**463**	**464**
	[19]	[19]	[19]	[120]	[120]	[342]	18]	[118]	[118]	[303]

Chart 55.

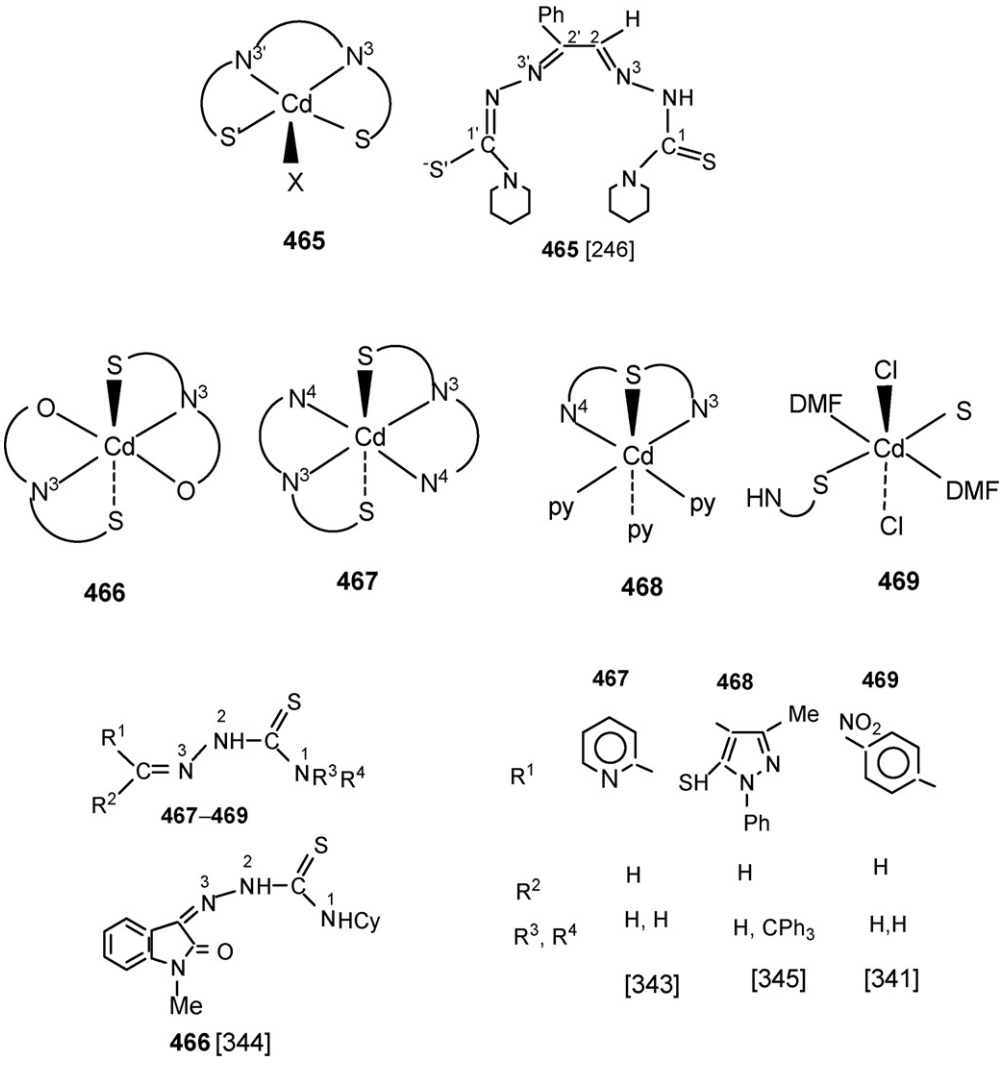

Chart 56.

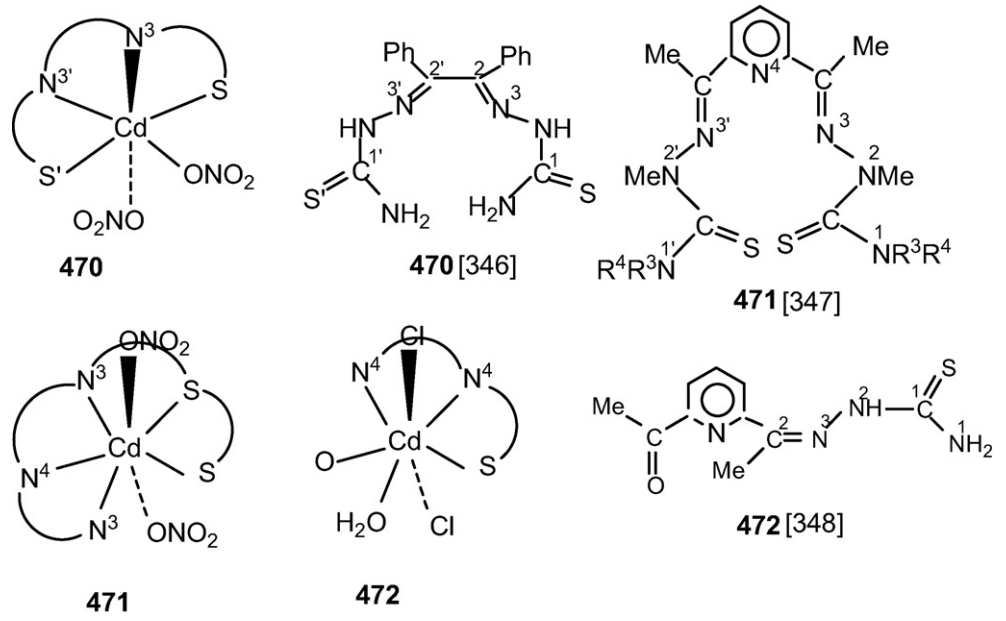

Chart 57.

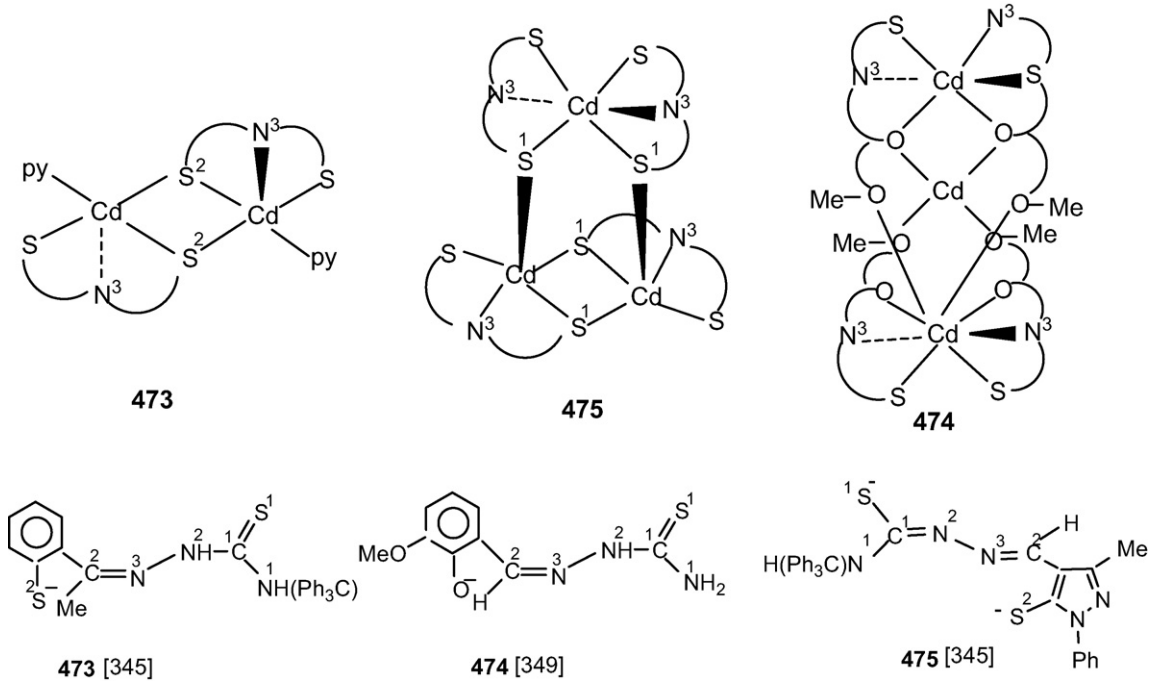

Chart 58.

red complexes with 9,10-phenanthaquinone monoethyl thiosemicarbazone **VII** and diacetylmonoxime(*p*-anisyl)thiosemicarbazone **VIII**, (λ_{max}, 516 and 460 nm), and this method has been used to determine Tl^{I} and Tl^{III} in the synthetic and natural samples after floatation and solid phase extraction studies [389] as well as in minerals, alloys, urine samples, soil and the water samples [390].

Pyridoxal-4-phenyl-3 thiosemicarbazone **IX** acts as a sensitive and selective analytical reagent for the extractive spectrophotometric determination of Co^{II} in biological, oil and pharmaceutical samples [391]. Silver(I) has been extracted in 0.5 M HNO_3 in the presence of the cyanide using 2,4-dihydroxy acetophenone thiosemicarbazone **X** with the quantitative recovery using 12.5 fold excess of the ligand [392]. Isatin-3-(3 thiosemicarbazone) **XI** acts as an effective inhibitor of corrosion in Al alloys, and this property increases with the increase in the temperature [393]. The extraction of Th^{IV} from the aqueous nitric acid medium with 2-hydroxy-1-naphthaldehyde thiosemicarbazone **XII** has been studied in the presence of various donors, like trioctylphosphine oxide (TOPO), calix[3]OH[3]OMe[6]arene, trioctylamine (TOA), dimethylsulfoxide (DMSO) in ethylacetate solvent, and maximum extraction occurs at pH 1.0 [394].

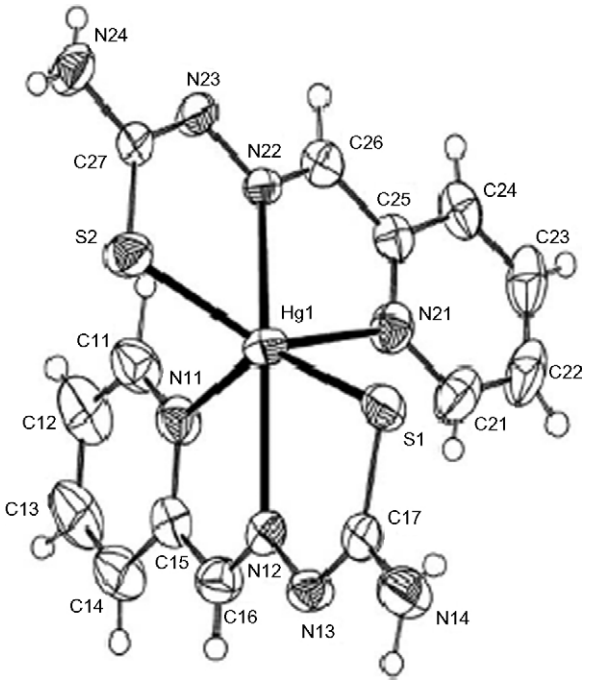

Fig. 42. Structure of [HgL_2] **481** {adapted from reference [350]}.

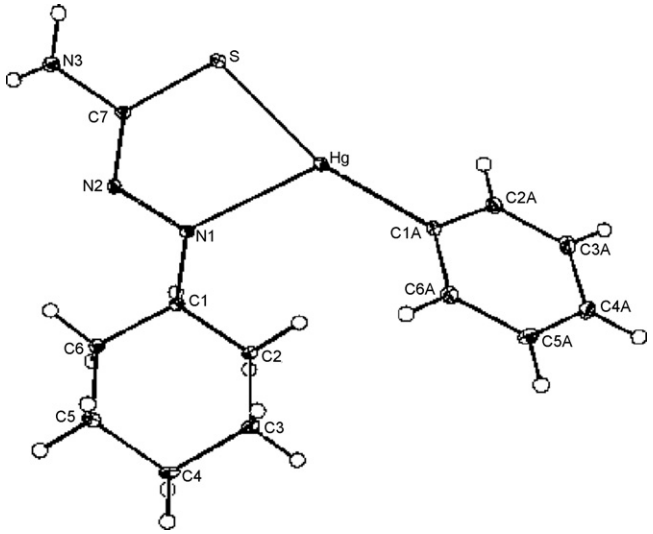

Fig. 43. Structure of complex [PhHgL] **486** {adapted from reference [121]}.

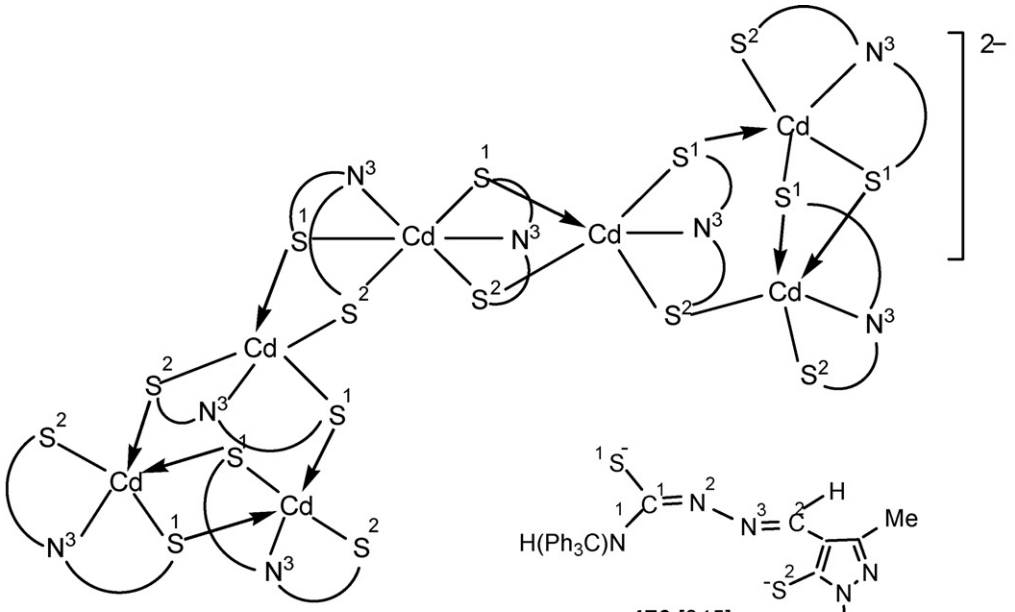

476

476 [345]

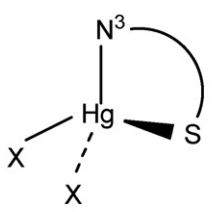

477, 478

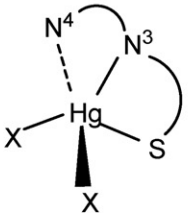

479, 480

$R^1R^2C^2{=}N^3{-}N^2H{-}C^1(=S)N^1R^3R^4$

R^1	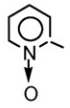	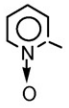	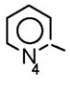	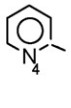
R^2	Me	Me	Me	Me
R^3, R^4	Me, Me	Me, Me	H, Me	H, Et
X	Cl	Br	Cl	Br
	477	**478**	**479**	**480**
	[118]	[118]	[119]	[19]

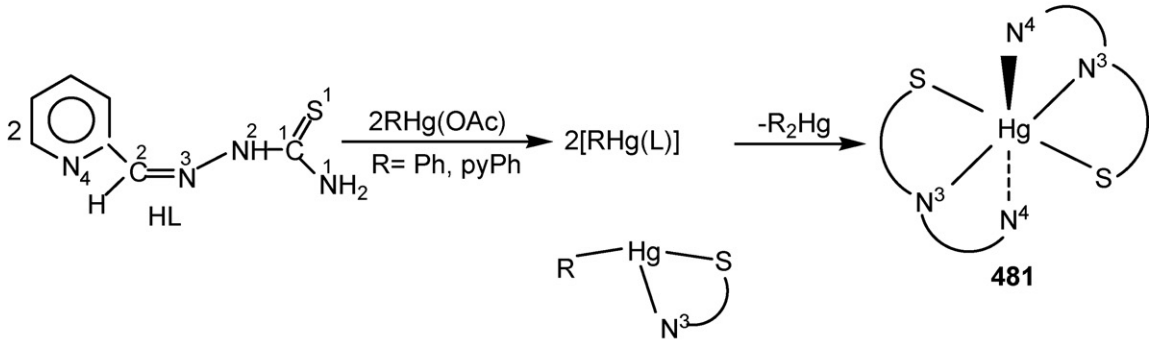

481

Chart 59.

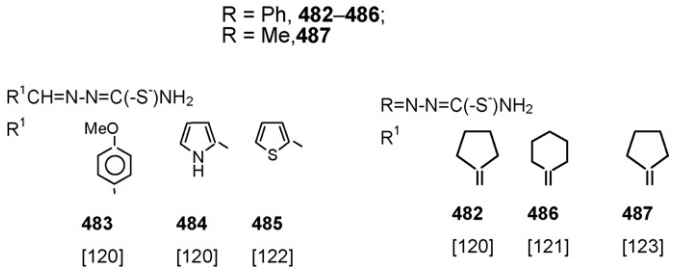

Chart 60.

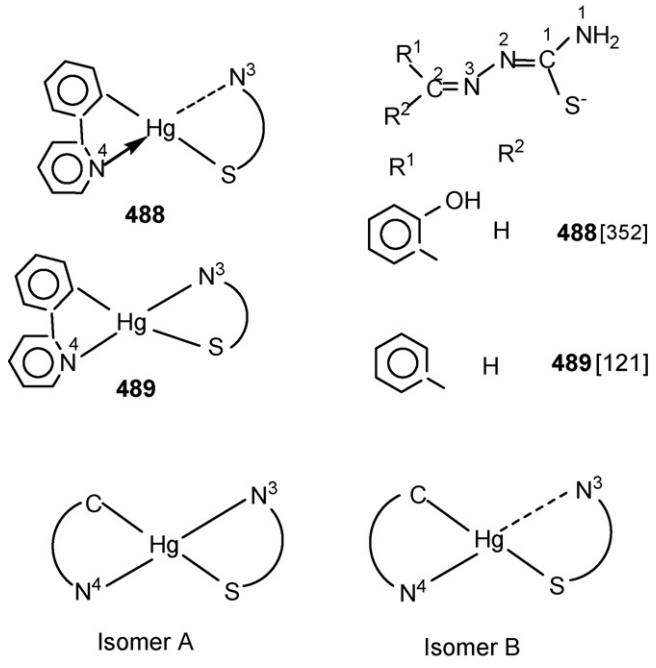

Chart 61.

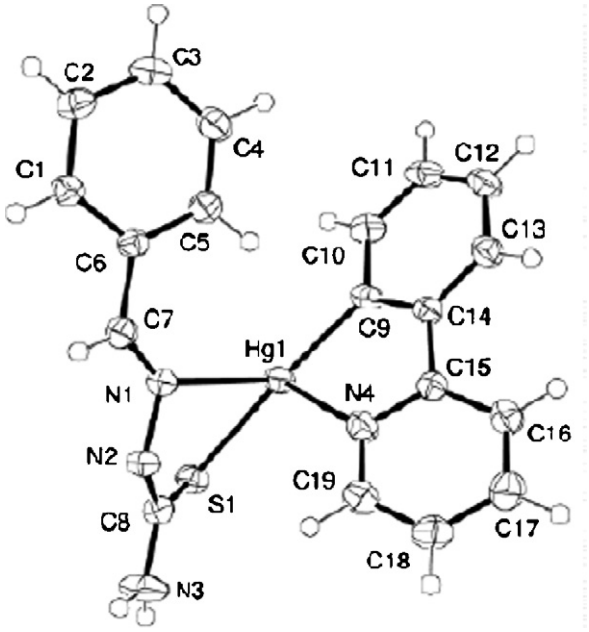

Fig. 44. Structure of complex [2-pyPhHgL] **489** {adapted from reference [121]}.

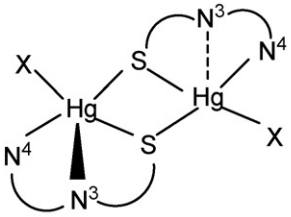

490

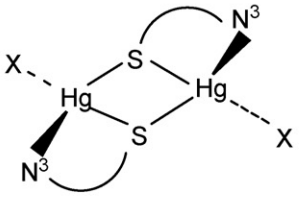

491

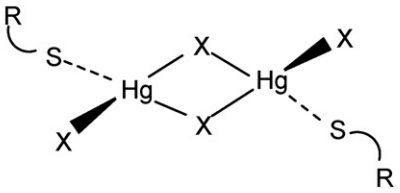

492

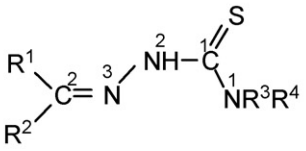

R^1	R^2	R^3, R^4	X	
	Me	H, Ph	I	**490** [342]
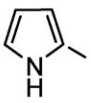	H	H, Ph	Br	**491** [67]
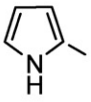	H	H, Et	Cl	**492** [69]

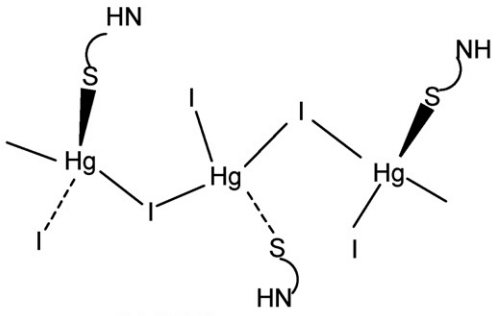

493 [337]

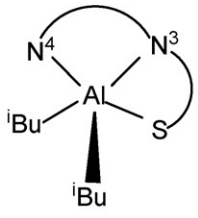

494

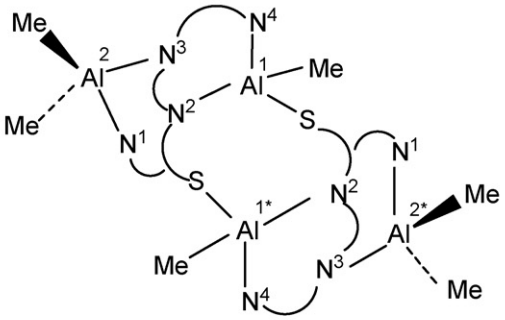

495

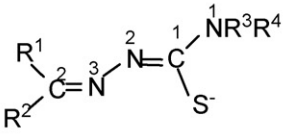

R^1	R^2	R^3	R^4	
	Me	H	Ph	**494** [124]
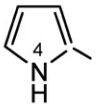	H	H	Pr^i	**495** [353]

Chart 62.

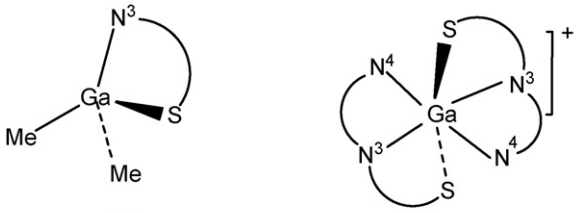

496 **497**

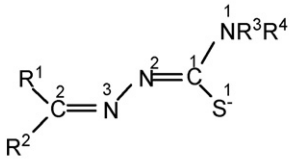

R^1	R^2	R^3, R^4	
	H	H, Me	**496** [125]
	Me	Me, Me	**497** [126]

Chart 63.

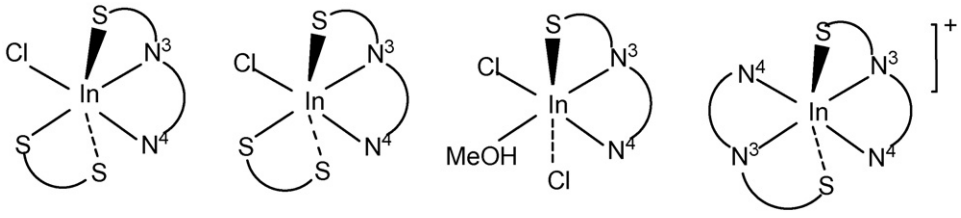

498 [127] **499** [127] **500** [127] **501** [127]

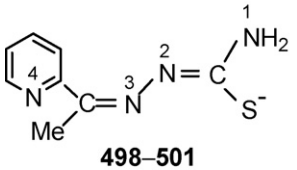

498–501

S, S'=

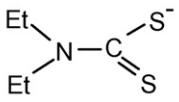

498

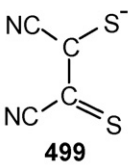

499

Chart 64.

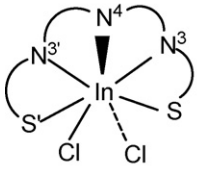

502

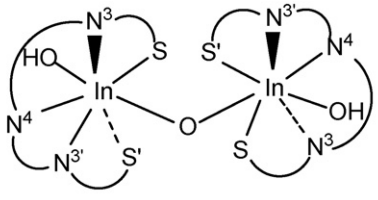

503

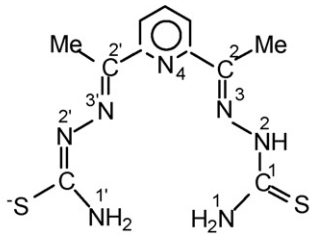

502, 503 [127]

$^1R^2C^2{=}N^3{-}N^2{=}C^1(-S^-)NR^3R^4$ $R{=}N^3{-}N^2{=}C^1(-S^-)NR^3R^4$

Chart 65.

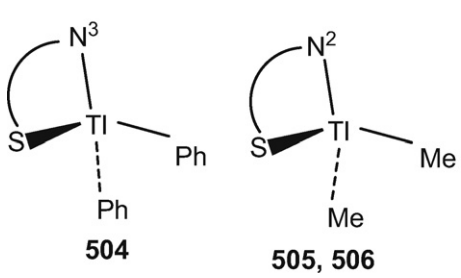

R^1	MeO	Fc	
R^2	H	Me	-
R^3, R^4	H, H	H, Ph	H, H
	504 [356]	**505** [25]	**506** [128]

Chart 66.

$R^1R^2C^2=N^3-N^2=C^1(-S^-)NR^3R^4$

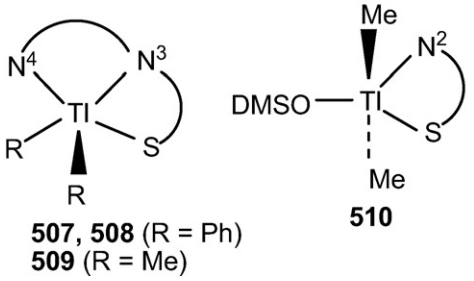

R^1	N_4	N_4	N_4	Fc
R^2	H	Me	H	Me
R^3, R^4	H, H	H, H	H. H	H, Ph
	507	**508**	**509**	**510**
	[128]	[128]	[129]	[356]

Chart 67.

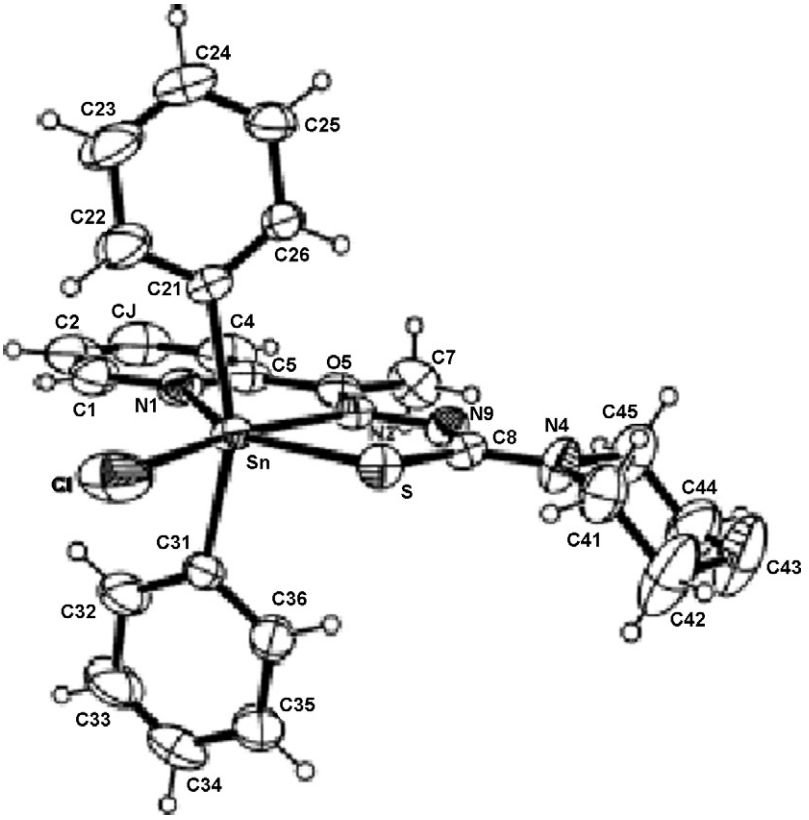

Fig. 45. Structure of complex [Ph_2SnLCl] **533** {adapted from reference [368]}.

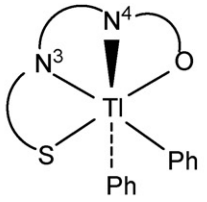

511

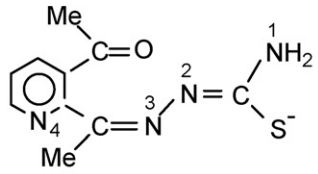

511 [357]

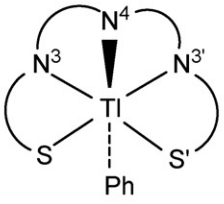

512

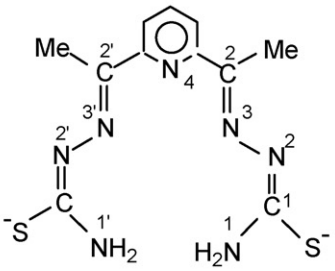

512 [35]

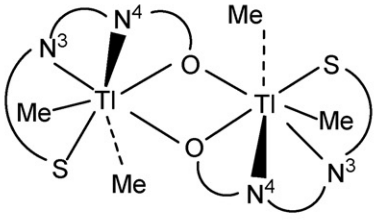

513

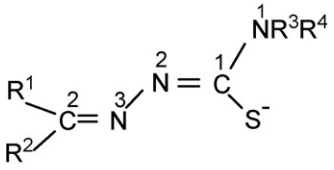

R^1	R^2	R^3, R^4	
Me	Me	H, H	**513** [357]
Fc	Me	Me,H	**514**[25]
H	H	H, H	**515**[23]

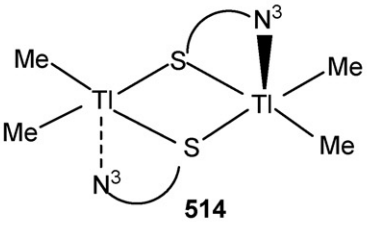

514

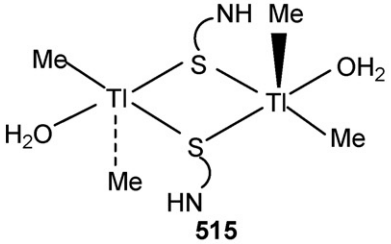

515

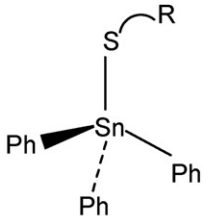

516[358]

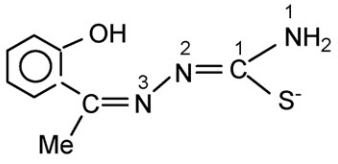

Chart 68.

$R^1R^2C^2{=}N^3{-}N^2{=}C^1(-S^-)NR^3R^4$, $R{=}N^3{-}N^2{=}C^1(-S^-)NR^3R^4$

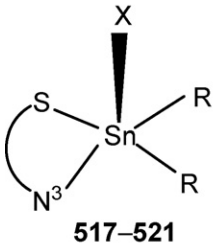

517–521

R^1	Me	Me		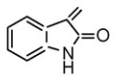	
R^2	Me	Me	H	-	H
R^3, R^4	H, Ph	H, Ph	H. H	H, H	H, H
X	Br	Cl	Cl	Ph_2PSO	Cl
R	Me	Me	Ph	-	Me
	517 [359]	**518** [359]	**519** [360]	**520** [130]	**521** [361]

Chart 69.

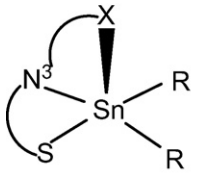

X =N^4, **522**

X =O, **523–527**

R^1						
R^2	H	Me	Me	H	H	H
R^3, R^4	H	H, Ph	H. Ph	H	H	H
R	Me	Me	Bu^n	Bu^n	Me	Ph
	522 [362]	**523** [363]	**524**[363]	**525** [364]	**526** [364]	**527** [365]

Chart 70.

$^1R^2C{=}N{-}N{=}C(-S^-)NR^3R^4$

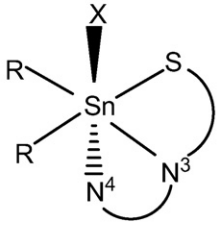

528-533

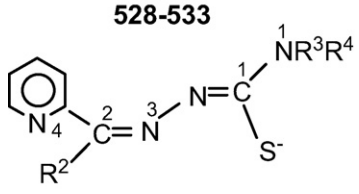

R^2	R^3, R^4	R	X	
Ph	H, Ph	Et	Cl	**528** [366]
Me	H, Ph	Me	Cl	**529** [131]
H	H, H	Me	Ph_2PS_2	**530** [132]
H	H, H	Et	Ph_2PS_2	**531** [132]
Ph	H, Ph	Ph	Cl	**532** [367]
Me		Ph	Cl	**533** [368]

Chart 71.

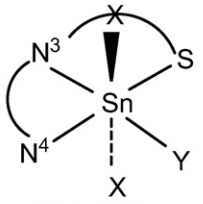

534–536

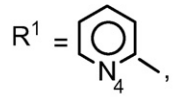

R^2 = Ph

R^3, R^4 =	H, H	Me, H	Ph, H
X =	Cl	Cl	Cl
Y =	Cl	Cl	Cl
	534	**535**	**536**
	[367]	[367]	[369]

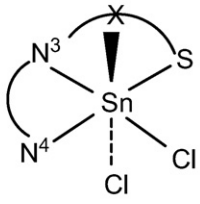

537–539

$R^1PhC^2=N^3-N^2=C^1(-S^-)N^1R^3R^4$

R^1			
R^2	Ph	Ph	Ph
R^3, R^4	H, H	H, Ph	H. Ph
X	Ph	Ph	Bu
	537 [367]	**538** [367]	**539** [373]

Chart 72.

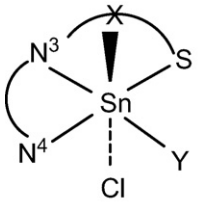

540-544

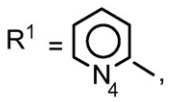

R^2 = Me

NR^3R^4					NHPh
Y =	Me	Ph	Me	Ph	Me
	540	**541**	**542**	**543**	**544**
	[385]	[385]	[372]	[372]	[371]

Chart 73.

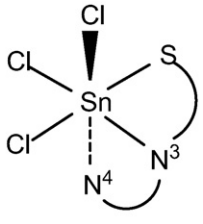

545

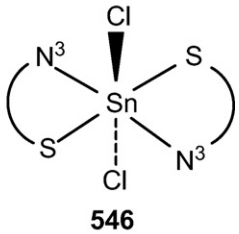

546

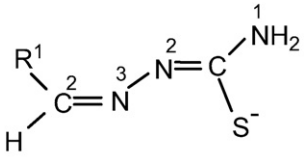

R^1		
	545	**546**
	[370]	[360]

Chart 74.

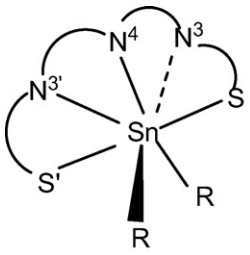

547–553

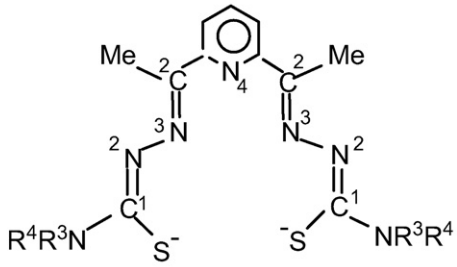

NR^3R^4	NHMe		NH_2	NHPh	NH_2	NH_2	
R	Me	Et	Ph	Et	NCS	Bu^n	Bu^n
	547 [374]	**548** [334]	**549** [133]	**550** [375]	**551**[160]	**552** [376]	**553** [368]

Chart 75.

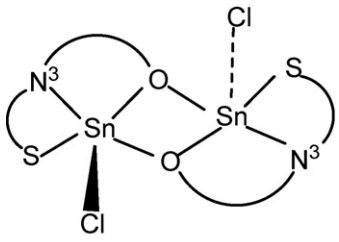

554

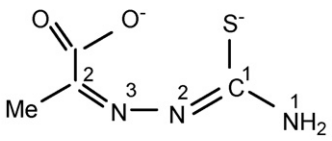

554 [337]

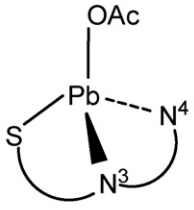

555

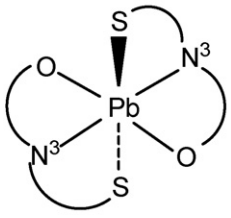

556

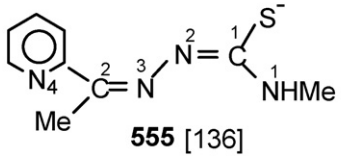

555 [136]

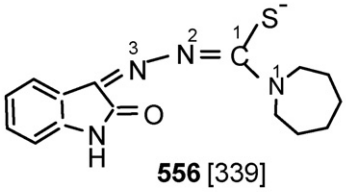

556 [339]

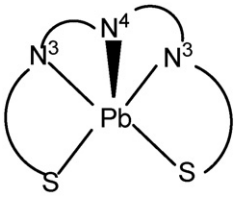

557 [34]

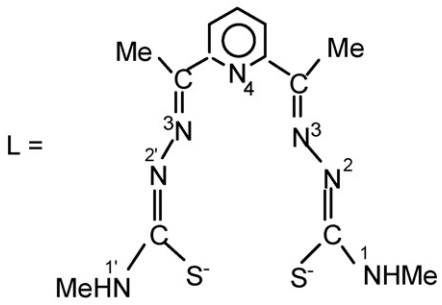

Chart 76.

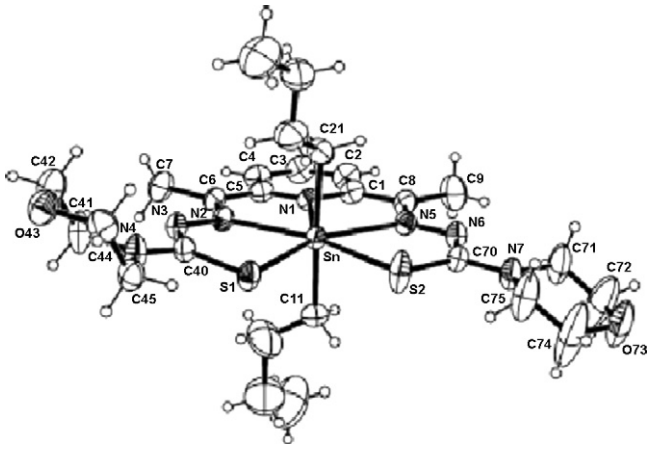

Fig. 46. Structure of complex $[(Bu^n)_2SnL]$ **553** {adapted from reference [368]}.

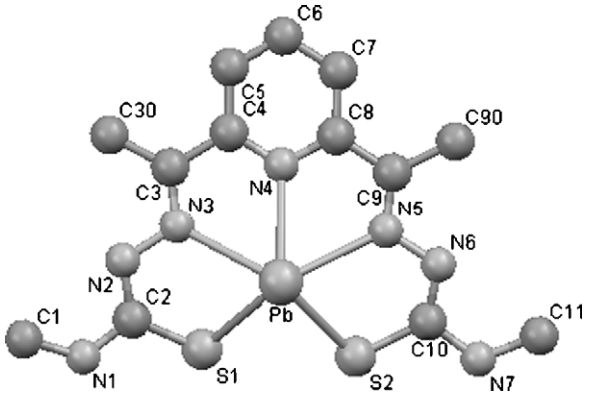

Fig. 47. Structure of complex [Pb(L)] **557** {adapted from reference [34]}.

1-(2-Hydroxy-4-methoxybenzophenone)-4-phenylthiosemicarbazone (HMBPT) **XIII** has been developed as a new reagent for the extraction of V^{IV} using spectrophotometric and flotation method. The 1:1 complex formed has molar absorbtivities of the 0.4×10^4 L mol^{-1} cm^{-1} at 560 nm. This method has been used for the analysis of V^{IV} in the synthetic mixtures, power stations wastes, simulated samples and in the real ores [395]. Osmium(VIII) has been determined by the application of 1,2,3-indanetrione mono-thiosemicarbazone **XIV** spectrophotometrically [396]. Zinc and Cd are extracted from their aqueous solutions employing 1,2-napthoquinone thiosemicarbazone, and the chelate formed are extracted in methyl isobutyl ketone (the sensitivity is 0.3 ng/ml) [397]. Pyridoxal-4-phenyl-3-thiosemicarbazone **IX** has been used as an analytical reagent for the determination of Zn^{II} [394] and Pd^{II} [398] using spectrophotometric methods (the detection limit, 0.04 μg/ml for Zn^{II} and 0.05 μg/ml for Pd^{II}).

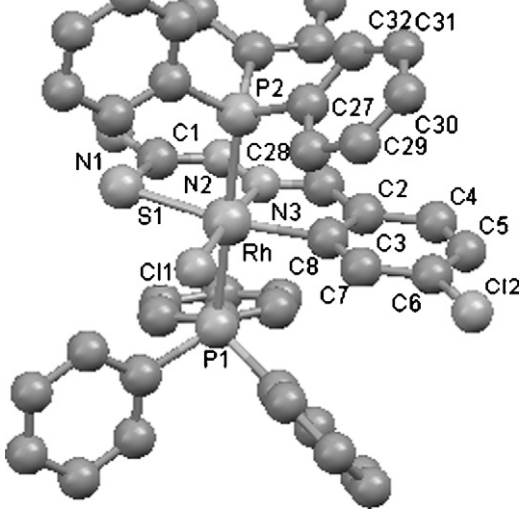

Fig. 48. Structure of complex $[PbPh_2ClL] \cdot 3H_2O$ **566** {adapted from reference [135]}.

Many thiosemicarbazone ligands have been employed for the determination of $Fe^{II/III}$ in the biological and various iron containing samples (e.g. ores, steel, acids, waters, wines and fruit juices). Salicylaldehyde thiosemicarbazone **XV** reacts with $Fe^{II/III}$ to form a

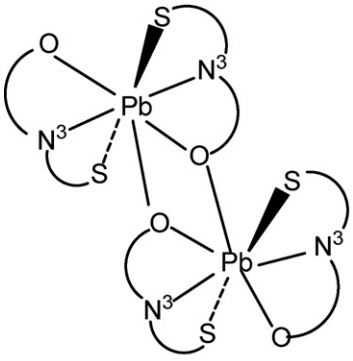

558

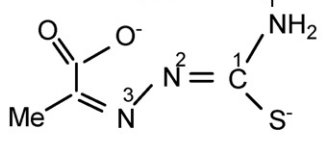

558 [377]

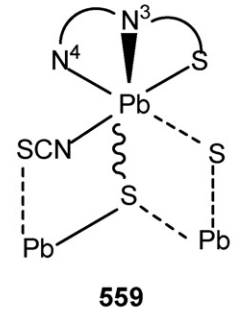

559

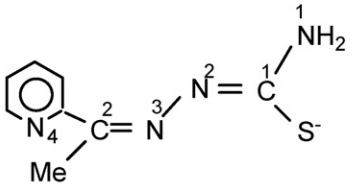

559 [378]

Chart 77.

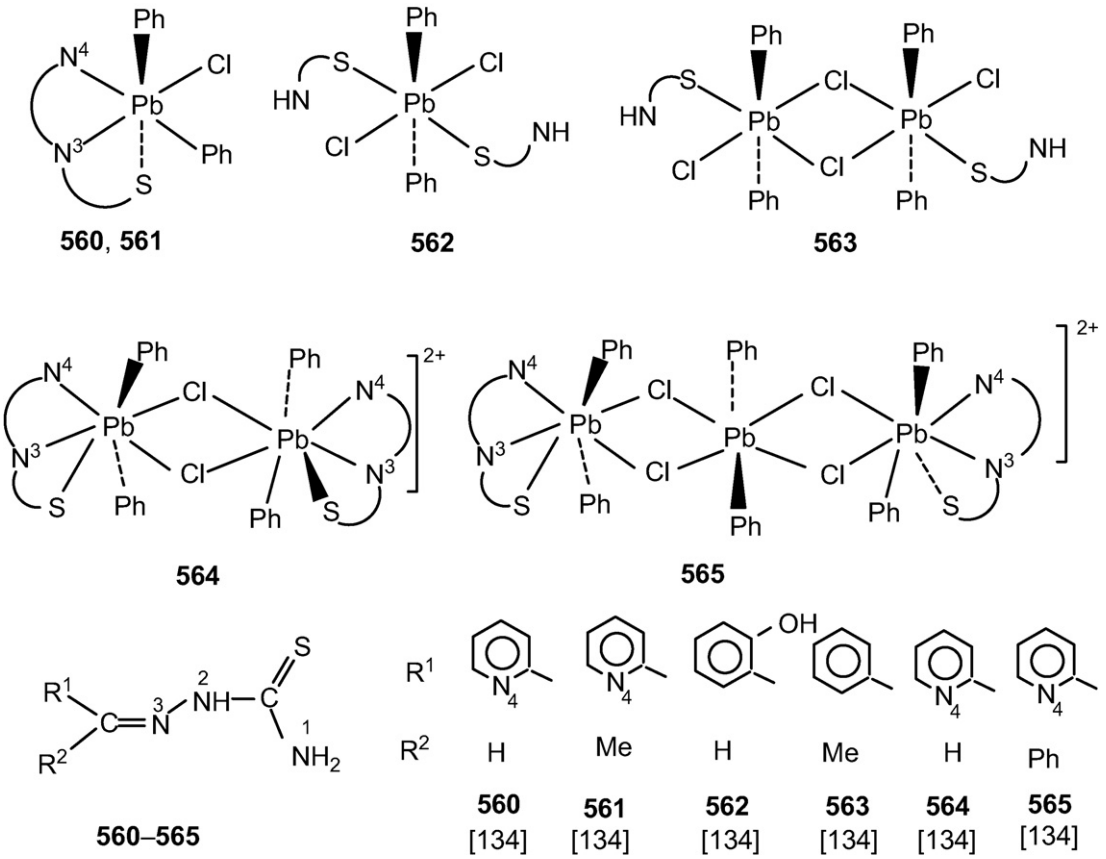

Chart 78.

green complex and this method has been used for determining Fe in their mixtures with Mo^{VI}. Similarly, ligand **XV** can be used for estimating Mo^{VI} in presence of Fe. A major application is in the analysis of steel [399]. Similarly, 2-benzoylpyridine-4-phenyl-3-thiosemicarbazone **XVI** acts as a reagent for the spectrophotometric determination of iron [400]. 5,5-Dimethylcyclohexane-1,2,3-trione 1,2-dioxime 3-thiosemicarbazone **XVII** is employed for determination of Fe(II) by differential pulse polarography. This method was applied for the determination of iron in acids, waters, wines and fruit juices [401]. A very sensitive and selective method for determination of Pt employs thiosemicarbazide as a reagent, using voltammetric method. The detection limit of Pt in this method is 1.5×10^{-13} mol L^{-1} after 50 s of accumulation time. This method was applied for determining Pt in hydroponically cultivated plants after microwave decomposition [402]. Trace levels of Co(II), Ni(II), Fe(II) and Cu(II) could be recovered from the drinking and tap water samples by complexing them with di-2-pyridylketonethiosemicarbazone **VIII** and retaining quantitatively on amberlite XAD4 column. The concentration of metals was determined using atomic spectrometry method after eluting with 1 M

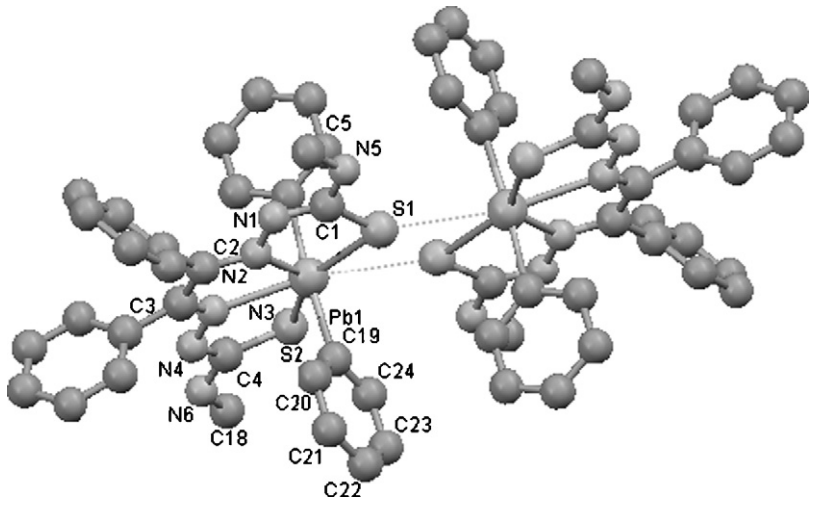

Fig. 49. Structure of complex $[PbPh_2L]_2 \cdot 2H_2O$ **567** {adapted from reference [135]}.

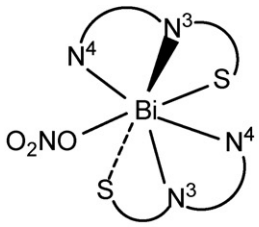

568

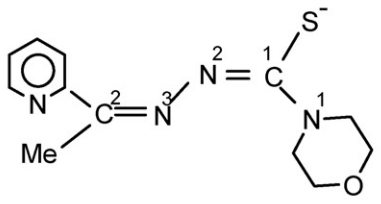

568 [137]

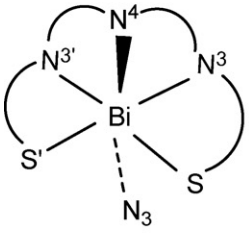

569

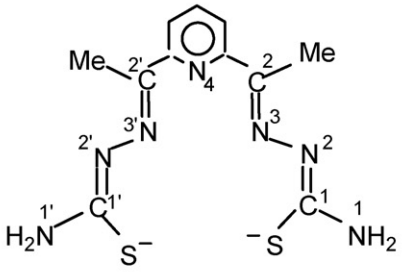

569 [138]

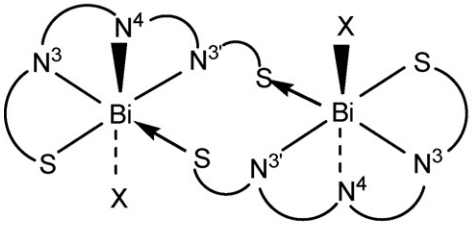

570 (X = ONO_2)

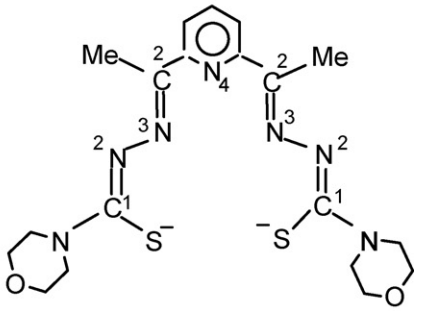

570 [137]

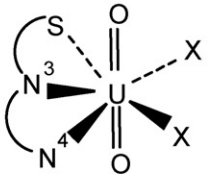

571, 572

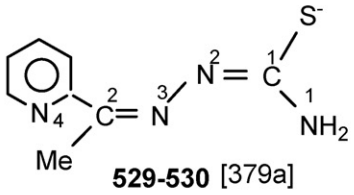

529-530 [379a]

X =OAc, **571**; Cl, **572**

Chart 79.

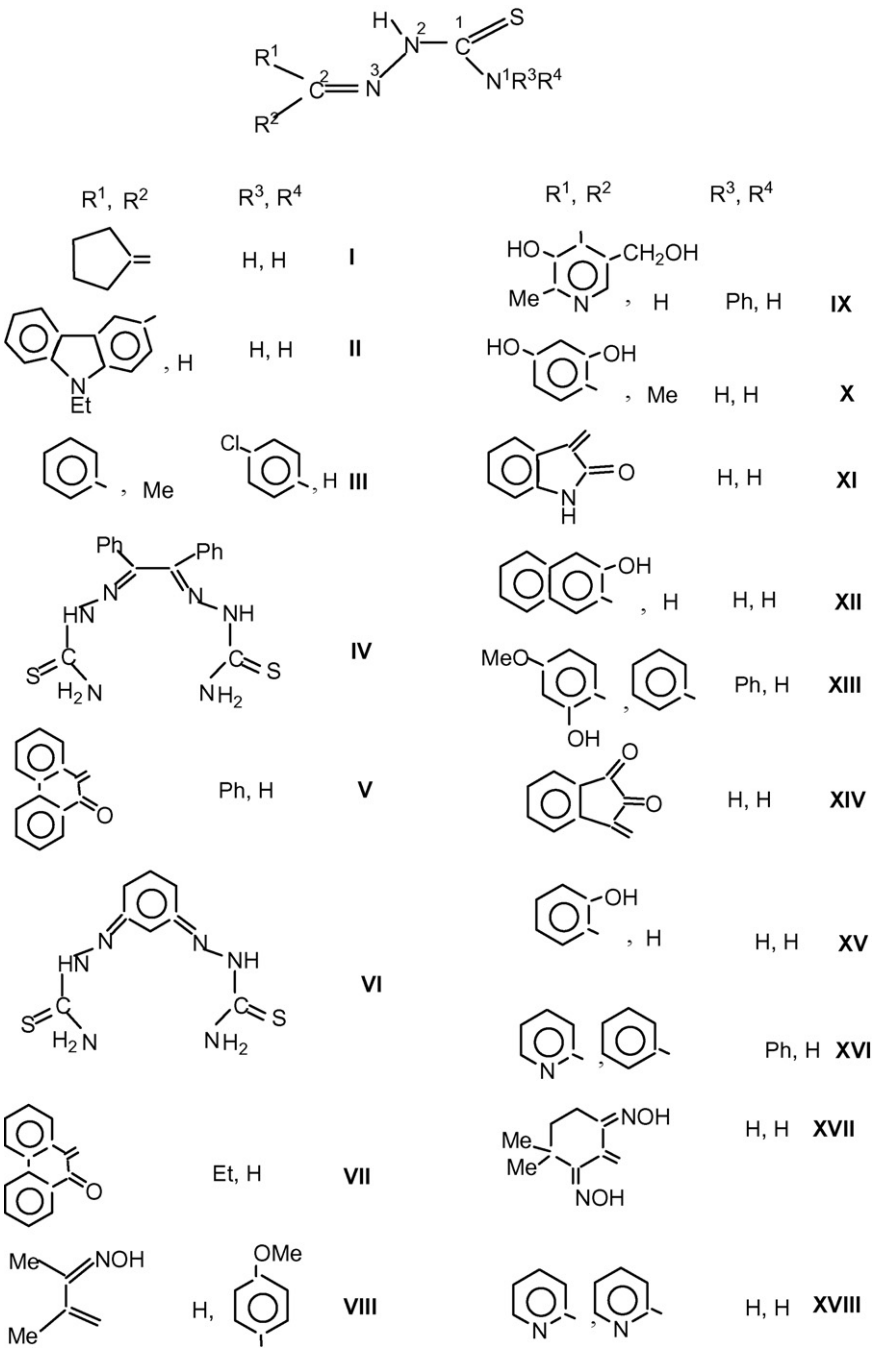

Chart 80.

HNO_3 in acetone [403]. Mercury(II) ion has been detected with a series of thiosemicarbazones [404]. Salicylaldehyde thiosemicarbazone has been used for determining copper(II) in blood using adsorptive stripping voltammetry [405].

5. Conclusions and future outlook

Thiosemicarbazones have emerged as an important class of ligands over a period of time, for a variety of reasons, such as variable donor properties, structural diversity, and biological applications. Coordination chemistry of a number of metals has been investigated, and a wide variety of complexes have been reported. The nuclearity of complexes varies from mononuclear to hexanuclear, though a few polymeric networks are also reported. The denticity of the ligands varies widely, affected by the substituents at C^2 carbon of thiosemicarbazone ($R^1R^2C^2{=}N^3{-}N^2(H){-}C^1(=S)N^1R^3R^4$). The substituents at C^2 carbon have also induced metal–carbon bond formation (ortho-metallation) in thiosemicarbazone complexes with metals such as palladium, platinum, ruthenium etc. This area of coordination chemistry of thiosemicarbazones is likely to be pursued further by modifying the ligands, which are subject to the variation when an aldehyde or ketone and a thiosemicarbazide are changed.

Thiosemicarbazone complexes have shown interesting biological properties such as anticancer, antibacterial, antifungal, and antiviral owing to their property to diffuse through the semi-

permeable membrane of the cell lines. The enhanced effect may be attributed to the increased lipophilicity of the complexes compared to the ligand alone. The presence of coordination sites in the complexes enhances their activity. The inhibitory effect occurs by action of the complexes on the proliferation and differentiation of the cell lines. These complexes can further find their use in the treatment of other incurable diseases such as hepatitis, AIDS etc.

Due to the tendency of thiosemicarbazone ligands to form complexes with metals, analytical applications have also been observed. Basic mode of action is through the formation of colored chelates with common as well as trace metals such as thallium, osmium etc., for their extraction as well as determination in biological as well as pharmacological samples. The low cost of thiosemicarbazones as well as their easy preparative methods could provide a major attraction for the development of analytical reagents for a range of applications in future.

Acknowledgement

The authors thank Prof. Chen Wei Liu of National Dong Hua University Hualien, Taiwan for help in X-ray data collection.

References

[1] B.A. Gingras, R.L. Somorjai, C.H. Bayley, Can. J. Chem. 39 (1961) 973.
[2] P.T. Sah, T.C. Daniels, Rec. Trav. Chim. 69 (1950) 1545.
[3] F.E. Anderson, J.C. Duca, J.W. Scudi, J. Chem. Soc. (1951) 4967 (references therein).
[4] B.A. Gingras, R.W. Hornal, C.H. Bayley, Can. J. Chem. 38 (1960) 712.
[5] M. Akbar Ali, S.E. Livingstone, Coord. Chem. Rev. 13 (1974) 115.
[6] M.J.M. Campbell, Coord. Chem. Rev. 15 (1975) 279.
[7] S. Padhye, G.B. Kauffman, Coord. Chem. Rev. 63 (1985) 127.
[8] D.X. West, S. Padhye, P.B. Sonawane, Struct. Bond. (Berlin, Ger.) 76 (1991) 4.
[9] D.X. West, A.E. Liberta, S. Padhye, R.C. Chilkate, P.B. Sonawane, A.S. Kumbhar, R.G. Yerande, Coord. Chem. Rev. 123 (1993) 49.
[10] J.S. Casas, M.S. Garcia-Tasende, J. Sordo, Coord. Chem. Rev. 209 (2000) 197.
[11] J.S. Casas, M.S. Garcia-Tasende, J. Sordo, Coord. Chem. Rev. 193-195 (1999) 283.
[12] T.S. Lobana, Rekha, R.J. Butcher, Transition Met. Chem. 29 (2004) 291.
[13] T.S. Lobana, Rekha, R.J. Butcher, A. Castineiras, E. Bermejo, P.V. Bharatam, Inorg. Chem. 45 (2006) 1535.
[14] T.S. Lobana, S. Khanna, R.J. Butcher, A.D. Hunter, M. Zeller, Inorg. Chem. 46 (2007) 5826.
[15] T.S. Lobana, S. Khanna, R.J. Butcher, Z. Anorg. Allg. Chem. 633 (2007) 1820.
[16] T.S. Lobana, P. Kumari, R.J. Butcher, Inorg. Chem. Commun. 11 (2008) 11.
[17] E.M. Jouad, A. Riou, M. Allain, M.A. Khan, G.M. Bouet, Polyhedron 20 (2001) 67.
[18] S. Lhuachan, S. Siripaisarnpipat, N. Chaichit, Eur. J. Inorg. Chem. (2003) 263.
[19] E. Bermejo, R. Carballo, A. Castineiras, R. Dominguez, C. Maichle-Mossmer, J. Strahle, D.X. West, Polyhedron 18 (1999) 3695.
[20] P. Gomez-Saiz, J. Garcia-Tojal, M.A. Maestro, J. Mahia, F.J. Arniaz, L. Lezama, T. Rojo, Eur. J. Inorg. Chem. (2003) 2639.
[21] E. Labisbal, K.D. Haslow, A. Sousa-Pedrares, J. Valdes-Martinez, S. Harnandez-Ortega, D.X. West, Polyhedron 22 (2003) 2831.
[22] D. Kovala-Demertzi, A. Domopoulou, M.A. Demertzis, J. Valdes-Martinez, S. Hernandez-Ortega, G. Espinosa-Perez, D.X. West, M.M. Salberg, G.A. Bain, P.D. Bloom, Polyhedron 15 (1996) 2587.
[23] J.S. Casas, E.E. Castellano, M.C. Rodriguez-Arguelles, A. Sanchez, J. Sordo, J. Zukerman-Schpector, Inorg. Chim. Acta 260 (1997) 183.
[24] J. Garcia-Tojal, J.L. Pizarro, A. Garcia-Orad, A.R. Perez-Sanz, M. Ugalde, A.A. Diaz, J.L. Serra, M.I. Arriortua, T. Rojo, J. Inorg. Biochem. 86 (2001) 627.
[25] J.S. Casas, M.V. Castano, M.C. Cifuentes, A. Sanchez, J. Sordo, Polyhedron 21 (2002) 1651.
[26] T.S. Lobana, G. Bawa, A. Castineiras, R.J. Butcher, Inorg. Chem. Comm. 10 (2007) 505.
[27] S. Halder, S.-M. Peng, G.-H. Lee, T. Chatterjee, A. Mukherjee, S. Dutta, U. Sanyal, S. Bhattacharya, New J. Chem. 32 (2008) 105.
[28] D. Kovala-Demertzi, N. Kourkoumelis, M.A. Demertzis, J.R. Miller, C.S. Frampton, J.K. Swearingen, D.X. West, Eur. J. Inorg. Chem. (2000) 727.
[29] Z. Lu, C. White, A.L. Rheingold, R.H. Crabtree, Inorg. Chem. 32 (1993) 3991.
[30] T.S. Lobana, G. Bawa, Ray J. Butcher, B.-J. Liaw, C.W. Liu, Polyhedron 25 (2006) 2897.
[31] L.J. Ashfield, A.R. Cowley, J.R. Dilworth, P.S. Donnelly, Inorg. Chem. 43 (2004) 4121.
[32] I. Pal, F. Basuli, T.C.W. Mak, S. Bhattacharya, Angew. Chem. Int. Ed. 40 (2001) 2923.
[33] M. Gil, E. Bermejo, A. Castineiras, H. Beraldo, D.X. West, Z. Anorg. Allg. Chem. 626 (2000) 2353.
[34] R. Pedrido, M.R. Bermejo, M.J. Romero, M. Vazquez, A.M. Gonzalez-Noya, M. Maneiro, M.J. Rodriquez, M.I. Fernandez, J. Chem. Soc. Dalton Trans. (2005) 572.
[35] J.S. Casas, E.E. Castellano, J. Ellena, M.S. Garcia-Tasende, A. Sanchez, J. Sordo, E.M. Vazquez-Lopez, M.J. Vidarte, Z. Anorg. Allg. Chem. 629 (2003) 261.
[36] V. Ruangpornvisuti, Structural Chemistry 18 (2007) 977.
[37] V. Ruangpornvisuti, K. Supakornchailert, C. Tungchitpienchai, B. Wanno, Struct. Chem. 17 (2006) 27.
[38] D. Mishra, S. Naskar, M.G.B. Drew, S.K. Chattopadhyay, Inorg. Chim. Acta 359 (2006) 585.
[39] D. Mishra, S. Naskar, M.G.B. Drew, S.K. Chattopadhyay, Polyhedron 24 (2005) 1861.
[40] C. Paiola, R. Cammi, J. Mol. Struct: Theochem. 623 (2003) 105.
[41] B. Fábián, V. Kudar, A. Csámpai, J. Organomet. Chem. 692 (2007) 5621.
[42] A.M.B. Bastos, A.F. de Carvalho-Alcantara, H. Beraldo, Tetrahedron 61 (2005) 7045.
[43] A. Pérez-Rebolledo, I.C. Mendes, N.L. Speziali, P. Bertani, J.M. Resende, A.F. de Carvalho Alcântara, H. Beraldo, Polyhedron 26 (2007) 1449.
[44] R.I. Maurer, P.J. Blower, J.R. Dilworth, C.A. Reynolds, Y. Zheng, G.E.D. Mullen, J. Med. Chem. 45 (2002) 1420.
[45] D.L. Klayman, J.E. Bartosevich, T.S. Griffin, C.J. Mason, J.P. Scovill, J. Med. Chem. 22 (1979) 855.
[46] D.L. Klayman, A.J. Lin, Org. Prep. Proced. Int. 16 (1984) 79.
[47] J.P. Scovill, Phosphorus, Sulfur, Silicon 60 (1991) 15.
[48] J.J. Blanksma, Rs. Trav. Chim. 29 (1910) 408.
[49] L. Katz, W.E. Hamlin, Contribution from Sehenely Lab Inc. (1951) 2801.
[50] J.K. Lim, C.J. Matheas, M.A. Green, J. Med. Chem. 40 (1997) 132.
[51] B.A. Wilson, R. Venkatraman, C. Whitaker, Q. Tillison, Int. J. Environ. Res. PublicHealth 2 (2005) 170.
[52] R. Venkatraman, K. Devis, A. Shelby, J.D. Zubkowskii, E.J. Valente, J. Chem. Cyrstallogr. 29 (1999) 4.
[53] N.A. Keiko, T.N. Mamashvili, Pharm. Chem. J. 39 (2005) 82.
[54] A. Usman, I.A. Razak, S. Chantrapromma, H.-K. Fun, A. Sreekanth, S. Sivakumar, M.R.P. Kurup, Acta Crystallogr. Sect. C: Cryst. Struct. Commun. 58 (2002) m461.
[55] R.P. John, A. Sreekanth, M.R.P. Kurup, H.-K. Fun, Polyhedron 24 (2005) 601.
[56] L. Liu, W. Shi, X.-Y. Chen, Y.-L. Chen, P. Cheng, Synth. React. Inorg., Metal-Org. Nano Met. Chem. 36 (2006) 549.
[57] D. Kovala-Demertzi, V. Gangadharmath, M.A. Demertzis, Y. Sanakis, Inorg. Chem. Commun. 8 (2005) 619.
[58] G. Chen, S.-J. Ou, Z.-P. Bai, G. Han, C.-Y. Duan, Chin. J. Inorg. Chem. 19 (2003) 501.
[59] J.M. Vila, T. Pereira, A. Amoedo, M. Grana, J. Martinez, M. Lopez-Torres, A. Fernanadez, J. Orgnomet. Chem. 623 (2001) 176.
[60] D. Kovala-Demertzi, M.A. Demertzis, J.R. Miller, C.S. Frampton, J.P. Jasinski, D.X. West, J. Inorg. Biochem. 92 (2002) 137.
[61] A. Castineiras, M. Gil, E. Bermejo, D.X. West, Z. Naturforach. B. Chem. Sci. 55 (2000) 863.
[62] M. Baldini, M.B. Ferrari, F. Bisceglie, G. Pelosi, S. Pinelli, P. Tarasconi, Inorg. Chem. 42 (2003) 2049.
[63] M.B. Ferrari, G.G. Fava, P. Tarasconi, R. Albertini, S. Pinelli, R. Starcich, J. Inorg. Biochem. 53 (1994) 13.
[64] M.B. Ferrari, G.G. Fava, C. Pelizzi, G. Pelosi, P. Tarasconi, Inorg. Chim. Acta 269 (1998) 297.
[65] M.B. Ferrari, G.G. Fava, E. Leporati, G. Pelosi, R. Rossi, P. Tarasconi, R. Albertini, A. Bonati, P. Lunghi, S. Pinelli, J. Inorg. Biochem. 70 (1998) 145.
[66] Y.-P. Tian, W.-T. Yu, C.-Y. Zhao, M.-H. Jiang, Z.-G. Cai, H.K. Fun, Polyhedron 21 (2002) 1217.
[67] R. Carballo, A. Castineiras, T. Perez, Z. Naturforsch. B: Chem. Sci. 56 (2001) 881.
[68] P. Souza, L. Sanz, V. Fernandez, A. Arqueru, E. Gutierrez, A. Monge, Z. Naturforsch B: Chem. Sci. 46 (1991) 767.
[69] E. Bermejo, A. Castineiras, T. Perez, R. Carballo, W. Hillar, Z. Anorg. Allg. Chem. 627 (2001) 2377.
[70] V.K. Bel'skii, A.I. Prisyazhnyuk, E.V. Kolchinskii, T.V. Koksharova, J. Struct. Chem. 27 (1986) 148.
[71] C.-Y. Duan, Z.-H. Liu, Y.-C. Shi, X.-Z. You, J. Coord. Chem. 47 (1999) 433.
[72] D. Wang, M. Ebel, C. Schulzke, C. Gruning, S.K.S. Hazari, D. Rehder, Eur. J. Inorg. Chem. (2001) 935.
[73] M. Milanesio, D. Viterbo, R.P. Hernandez, J.D. Rodriguez, J. Ramirez-Ortiz, J. Valdes-Martinez, Inorg. Chim. Acta 306 (2000) 125.
[74] M. Soriano-Garcia, J. Valdes-Martinez, R.A. Toscano, J. Gomez-Lara, Acta Crystallogr. Sect C: Cryst. Struct. Commun. 41 (1985) 500.
[75] P. Sonawane, R. Chikate, A. Kumbhar, S. Padhye, R.J. Doedens, Polyhedron 13 (1994) 395.
[76] M.D. Timken, S.R. Wilson, D.N. Henderickson, Inorg. Chem. 24 (1985) 3450.
[77] G. Argay, A. Kalman, V.M. Leovac, V.I. Cesljevic, B. Ribar, J. Coord. Chem. 37 (1996) 165.
[78] L. Stelzig, S. Kotte, B. Krebs, J. Chem. Soc. Dalton Trans. (1998) 2921.
[79] A.B. Llyukhin, V.L. Abramenko, V.S. Sergienko, Koord. Khim. (Russ.) (Coord. Chem.) 20 (1994) 653.
[80] J. Valdes-Martinez, A. Enriquez, A. Cabrera, G. Espinosa-Perez, Polyhedron 15 (1996) 897.
[81] J. Valdes-Martinez, A. Sierra-Romera, C. Alvarez-Toledano, R.A. Toscano, H. Garcia-Tapia, J. Organomet. Chem. 352 (1988) 321.
[82] G. Pereiras-Gabian, E.M. Vazquez-Lopez, H. Braband, U. Abram, Inorg. Chem. 44 (2005) 834.

[83] R. Carballo, J.S. Casas, E. Garcia-Martinez, G. Pereiras-Gabian, A. Sanchez, J. Sordo, E.M. Vazquez-Lopez, J.C. Garcia-Monteagudo, U. Abram, J. Organomet. Chem. 656 (2002) 1.
[84] R. Carballo, J.S. Casas, E. Garcia-Martinez, G. Pereiras-Gabian, A. Sanchez, J. Sordo, E.M. Vazquez-Lopez, Inorg. Chem. 42 (2003) 6395.
[85] A.R. Cowley, J.R. Dilworth, P.S. Donnelly, J. Wollard-Shore, J. Chem. Soc. Dalton Trans. (2003) 748.
[86] F. Basuli, M. Ruf, C.G. Pierpont, S. Bhattacharya, Inorg. Chem. 37 (1998) 6113.
[87] F. Basuli, S.-M. Peng, S. Bhattacharya, Inorg. Chem. 36 (1997) 5645.
[88] M. Maji, S. Ghosh, S.K. Chattopadhyay, T.C. Mak, Inorg. Chem. 36 (1997) 2938.
[89] P. Sengupta, R. Dinda, S. Ghosh, W.S. Sheldrick, Polyhedron 22 (2003) 447.
[90] M. Maji, M. Chatterjee, S. Ghosh, S.K. Chattopadhyay, B.M. Wu, T.C.W. Mak, J. Chem. Soc. Dalton Trans. (1999) 135.
[91] F. Basuli, S.M. Peng, S. Bhattacharya, Inorg. Chem. 39 (2000) 1120.
[92] S. Dutta, F. Basuli, S.-M. Peng, G.-H. Lee, S. Bhattacharya, New. J. Chem. 25 (2002) 1607.
[93] P. Pelagatti, A. Venturini, A. Leporati, M. Carcelli, M. Costa, A. Bacchi, G. Pelizzi, C. Pellizi, J. Chem. Soc. Dalton Trans. (1998) 2715.
[94] K.V. Katti, P.R. Singh, C.L. Barnes, J. Chem. Soc., Dalton Trans. (1993) 2153.
[95] D. Kovala-Demertzi, A. Domopolou, M. Demertzis, C.P. Raptopoulou, A. Terzis, Polyhedron 13 (1994) 1917.
[96] D. Kovala-Demertzi, P.N. Yadav, M.A. Demertzis, J.P. Jasiski, F.J. Andreadaki, I.D. Kostas, Tetrahedron Lett. 45 (2004) 2923.
[97] K.I. Goldberg, J. Valdes-Martinez, G. Espinosa-Perez, L.J. Ackerman, D.X. West, Polyhedron 18 (1999) 1177.
[98] D. Kovala-Demertzi, M.A. Demertzis, P.N. Yadav, A. Castineiras, D.X. West, Transition Met. Chem. 24 (1999) 642.
[99] E. Bermejo, R. Carballo, A. Castineiras, R. Dominguez, A.E. Liberta, C. Maichle-Moessmer, M.M. Salberg, D.X. West, Eur. J. Inorg. Chem (1999) 965.
[100] D. Kovala-Demertzi, M.A. Demertzis, A. Castineiras, D.X. West, Polyhedron 17 (1998) 3739.
[101] D. Kovala-Demertzi, J.R. Miller, N. Kourkoumelis, S.K. Hadjikakou, M.A. Demertzis, Polyhedron 18 (1999) 1005.
[102] J.M. Vila, M.T. Pereira, J.M. Ortigueira, M. Grana, D. Lata, A. Suarez, J.J. Fernandez, A. Fernandez, M. Lopez-Torres, H. Adams, J. Chem. Soc. Dalton Trans. (1999) 4193.
[103] A. Amoedo, M. Grana, J. Martinez, T. Pereira, M. Lopez-Torres, A. Fernandez, J.J. Fernandez, J.M. Vila, Eur. J. Inorg. Chem. (2002) 613.
[104] F.-L. Zi, Y.-Z. Zhou, X.-M. Lu, S.-C. Liu, X.-L. Jin, Chin. J. Struct. Chem. 22 (2003) 200.
[105] D. Kovala-Demertzi, P.N. Yadav, M.A. Demertzis, M. Coluccia, J. Inorg. Biochem. 78 (2000) 347.
[106] D. Kovala-Demertzi, M.A. Demertzis, J.R. Miller, C. Papadopoulou, C. Dodorou, G. Filousis, J. Inorg. Biochem. 86 (2001) 555.
[107] D. Vazquez-Garcia, A. Fernanadez, J.J. Fernanadez, M. Lopez-Torres, A. Suarez, J.M. Ortigueira, J.M. Vila, H. Adams, J. Organomet. Chem. 595 (2000) 199.
[108] D. You, S.O. Kang, J. Ko, M. Choi, Bull. Korean Chem. Soc. 18 (1997) 305.
[109] D. Kovala-Demertzi, M.A. Demertzis, E. Filiou, A.A. Pantazaki, P.N. Yadav, J.R. Miller, Y. Zheng, D.A. Kyriakidis, Biometals 16 (2003) 411.
[110] M.B. Ferrari, G.G. Fava, P. Tarasconi, C. Pelizzi, J. Chem. Soc. Dalton Trans. (1989) 361.
[111] M.B. Ferrari, G.G. Fava, M. Lanfranchi, C. Pelizzi, P. Tarasconi, Inorg. Chim. Acta. 181 (1991) 253.
[112] H.-G. Zheng, D.-X. Zeng, X.-Q. Xin, W.T. Wong, Polyhedron 16 (1997) 3499.
[113] M.B. Ferrari, A. Bonardi, G.G. Fava, C. Pelizzi, P. Tarasconi, Inorg. Chim. Acta. 223 (1994) 77.
[114] T.S. Lobana, Rekha, B.S. Sidhu, A. Castineiras, E. Bermejo, T. Nishioka, J. Coord. Chem. 58 (2005) 803.
[115] J.S. Casas, E.E. Catellano, M.D. Couce, J. Ellena, A. Sanchez, J. Sordo, C. Taboada, J. Inorg. Biochem. 100 (2006) 1858.
[116] U. Abram, K. Ortner, R. Gust, K. Sommer, J. Chem. Soc. Dalton Trans. (2000) 735.
[117] K. Ortner, U. Abram, Inorg. Chem. Commun. 1 (1998) 251.
[118] E. Bermejo, R. Carballo, A. Castineiras, R. Dominguez, A.E. Liberta, C. Marchle-Moessmer, D.X. West, Z. Natureforsch B: Chem. Sci. 54 (1999) 777.
[119] E. Bermejo, R. Carballo, A. Castineiras, R. Dominguez, A.E. Liberta, C. Maichle-Mossmer, M.M. Salberg, D.X. West, Eur. J. Inorg. Chem. (1999) 965.
[120] T.S. Lobana, A. Sanchez, J.S. Casas, A. Castineiras, J. Sordo, M.S. Garcia-Tasende, E.M. Vazquez-Lopez, J. Chem. Soc. Dalton Trans. (1997) 4289.
[121] T.S. Lobana, Rekha, R.J. Butcher, T.W. Failes, P. Turner, J. Coord. Chem. 58 (2005) 1369.
[122] T.S. Lobana, A. Sanchez, J.S. Casas, A. Castineiras, J. Sordo, M.S. Garcia-Tasende, Main Group Met. Chem. 24 (2001) 61.
[123] J. Zukerman-Scphector, M.C. Rodriguez-Arguelles, M.I. Svarez, A. Sanchez, J.S. Casas, J. Sordo, J. Coord. Chem. 24 (1991) 177.
[124] Y. Kang, S.-O. Kang, J.-J. Ko, J.-I. Sohn, Bull. Korean Chem. Soc. 20 (1999) 65.
[125] Y. Kang, N. Yang, S.-O. Kang, J. Ko, C.-H. Lee, Y.-H. Lee, Organometallics 16 (1997) 5522.
[126] V.B. Arion, M. Jakupec, M. Galanski, P. Unfried, B.K. Keppler, J. Inorg. Biochem. 91 (2002) 298.
[127] S. Abram, C. Maichle-Mossmer, U. Abram, Polyhedron 17 (1998) 131.
[128] T.S. Lobana, J.S. Casas, A. Castineiras, M.S. Garcia-Tasende, A. Sanchez, J. Sordo, Inorg. Chim. Acta 347 (2003) 23.
[129] J.S. Casas, M.V. Castano, M.C. Rodriguez-Arguelles, A. Sanchez, J. Sordo, J. Chem. Soc. Dalton Trans. (1993) 1253.
[130] J.S. Casas, A. Castineiras, M.C. Rodriguez-Arguelles, A. Sanchez, J. Sordo, A. Vazquez-Lopez, J. Chem. Soc. Dalton Trans. (2000) 4056.
[131] R.H.P. Francisco, M.T.P. Garmbardella, G.F. de Sousa, J. Chem. Cryst. 34 (2004) 39.
[132] J.S. Casas, A. Castineiras, M.C. Rodriguez-Arguelles, A. Sanchez, J. Sordo, A. Vazquez-Lopez, S. Pinelli, P. Lunghi, P. Ciancienaini, A. Bonall, P. Dall'Aglio, R. Albertini, J. Inorg. Biochem. 76 (1999) 277.
[133] P.C. Moreno, R.H.P. Francisco, M.T. do Gambardella, G.F. de Sousa, A. Abras, Acta Crystallogr. Sect C: Cryst. Struct. Commun. 53 (1997) 1411.
[134] J.S. Casas, E.E. Castellano, J. Ellena, M.S. Garcia-Tasende, A. Sanchez, J. Sordo, J.J. Vidarte, Inorg. Chem. 42 (2003) 2584.
[135] D.G. Calatayud, E. Lpoez-Torres, M.A. Mendiola, Inorg. Chem. 46 (2007) 10434.
[136] A. Castineiras, R. Dominguez, L. Bresolin, A.J. Bortoluzzi, R.A. Burrow, M. Horner, Z. Natureforsch B: Chem. Sci. 53 (1998) 81.
[137] K. Nomiya, K. Sekino, M. Ishikawa, A. Honda, M. Yokoyama, N.C. Kasuga, H. Yokoyama, S. Nakano, K. Onodera, J. Inorg. Biochem. 98 (2004) 601.
[138] L.P. Bettaglia, A.B. Corradi, C. Pelizzi, G. Pelosi, P. Tarasconi, J. Chem. Soc. Dalton Trans. (1990) 3857.
[139] T.S. Lobana, S. Khanna, Ray J. Butcher, A.D. Hunter, M. Zeller, Polyhedron 25 (2006) 2755.
[140] N.C. Saha, R.J. Butcher, S. Chaudhari, N. Saha, Polyhedron 22 (2003) 375.
[141] B.K. Koo, Y.J. Jang, U. Lee, Bull. Korean Chem. Soc. 24 (2003) 1014.
[142] A. Sreekanth, S. Sivakumar, M.R.P. Kurup, J. Mol. Struct. 655 (2003) 47.
[143] Y.-Z. Zhou, M. Zhang, F.-L. Zi, X.-M. Lu, S.-C. Liu, X.-L. Jin, Chin. J. Struct. Chem. 20 (2001) 249.
[144] M.S. Shongwe, H.N.R. Al-Kharousi, H. Adams, M.J. Morris, E. Bill, Inorg. Chem. 45 (2006) 1103.
[145] M. Cindric, V. Vrdoljak, M. Strukan, B. Kamanar, Polyhedron 24 (2005) 369.
[146] V. Vrdoljak, M. Cindric, D. Milic, D. Matkovic-Calogovic, P. Novak, B. Kamenar, Polyhedron 24 (2005) 1717.
[147] S.C. Bhatia, P. Batra, Acta Cienc. Indica, Ser. Chem. 15 (1989) 83.
[148] M.B. Ferrari, G.G. Fava, C. Pelizzi, P. Tarasconi, G. Tosi, J. Chem. Soc. Dalton Trans. (1987) 227.
[149] A.H. Othman, K.-L. Lee, H.-K. Fun, B.-C. Yip, Acta Crystallogr., Sect. C: Cryst. Struct. Commun. 52 (1996) m602.
[150] I. Garcia Santos, U. Abram, R. Alberto, E. Vazquez-Lopez, A. Sanchez, Inorg. Chem. 43 (2004) 1834.
[151] N.C. Saha, A. Saha, R.J. Butcher, S. Chaudhari, N. Saha, Inorg. Chim. Acta 339 (2002) 348.
[152] J. Garcia-Tojal, J.L. Pizzaro, L. Lezama, M.I. Arriortus, T. Rojo, Inorg. Chim. Acta 278 (1998) 150.
[153] N.A. Ryabova, V.I. Ponomarev, V.V. Zelentsov, L.O. Atovmyan, Kristallografiya (Russ.) (Crystallogr. Rep.) 27 (1982) 279.
[154] N.A. Ryabova, V.I. Ponomarev, L.O. Atovmyan, V.V. Zelentsov, V.I. Shipilov, Koord. Khim. (Russ) (Coord. Chem.) 4 (1978) 119.
[155] W.-S. Wu, Y.-L. Feng, Z. Kristallogr. New Cryst. Struct. 218 (2003) 529.
[156] L.I. Petuchov, A.V. Ablov, G.F. Volodina, T.I. Malinovskii, Proc. Nat. Acad. Sci. USSR 241 (1978) 115.
[157] J. Garcia Tojal, B. Donnadieu, J.-P. Costes, J.L. Serra, L. Lezama, T. Rojo, Inorg. Chim. Acta 333 (2002) 132.
[158] G. Dessy, V. Fares, Cryst. Struct. Commun. 10 (1981) 1025.
[159] W.-S. Hong, C.-Y. Wu, C.-S. Lee, W.-S. Hwang, M.Y. Chiang, J. Organomet. Chem. 689 (2004) 277.
[160] J.-M. Yang, W.-B. Ma, B.-H. Chen, G.-S. Huang, Y.-X. Ma, Acta Crystallogr., Sect. E: Struct. Rep. Online 60 (2004) m852.
[161] T.S. Lobana, G. Bawa, A. Castineiras, R.J. Butcher, M. Zeller, Organometallics 27 (2008) 175.
[162] T.S. Lobana, G. Bawa, R.J. Butcher, Inorg. Chem. 47 (2008) 1488.
[163] M. Bonamico, G. Dessy, V. Fares, L. Scaramuzza, Cryst. Struct. Commun. 4 (1975) 629.
[164] G. Dessy, V. Fares, L. Scaramuzza, Cryst. Struct. Commun. 7 (1978) 737.
[165] G. Dessy, V. Fares, L. Scaramuzza, A.A.B. Tomlinson, G. De Munno, J. Chem. Soc. Dalton Trans. (1978) 1549.
[166] S.B. Novakovic, G.A. Bogdanovic, V.M. Leovac, Polyhedron 25 (2006) 1096.
[167] S.K. Chattopadhyay, T. Banerjee, P. Roychoudury, T.C.W. Mak, S. Ghosh, Transition Met. Chem. 22 (1997) 216.
[168] D.K. Sau, N. Saha, R.J. Butcher, S. Chaudhuri, Transition Met. Chem. 28 (2003) 229.
[169] K.N. Akatova, T.N. Tarkhova, N.V. Belov, Kristallografiya (Russ.)(Crystallogr. Rep.) 18 (1973) 263.
[170] M.B. Ferrari, F. Bisceglie, G. Pelosi, P. Tarasconi, R. Albertini, A. Bonati, P. Lunghi, S. Pinelli, J. Inorg. Biochem. 83 (2001) 169.
[171] N.C. Saha, A. Seal, R.J. Butcher, N. Saha, J. Indian Chem. Soc. 78 (2001) 601.
[172] N.C. Saha, R.J. Butcher, S. Chaudhuri, N. Saha, Polyhedron 21 (2002) 779.
[173] D.K. Sau, R.J. Butcher, S. Chaudhuri, N. Saha, Polyhedron 23 (2004) 5.
[174] A. Casteneiras, D.X. West, H. Gebremedhin, J. Romack, Inorg. Chim. Acta 216 (1994) 229.
[175] D.X. West, M.A. Lockwood, A. Castineiras, Transition. Met. Chem. 22 (1997) 447.
[176] N.C. Saha, R.J. Butcher, S. Chaudhari, N. Saha, Polyhedron 22 (2003) 383.
[177] H.-S. Wang, L. Huang, Z.-F. Chen, X.-W. Wang, J. Zhou, S.-M. Shi, H. Liang, K.-B. Yu, Acta Crystallogr. Sect. E Struct. Rep. online 60 (2004) m354.
[178] M.B. Ferrari, F. Bisceglie, C. Casoli, S. Durot, I. Morgenstern-Badarau, G. Pelosi, E. Pilotti, S. Pinelli, P. Tarasconi, J. Med. Chem. 48 (2005) 1671.

[179] M.B. Ferrari, G.G. Fava, G. Pelosi, M.C. Rodriguez- Arguelles, P. Tarasconi, J. Chem. Soc. Dalton Trans. (1995) 3035.
[180] C. Maichle, A. Castineiras, R. Carballo, H. Gebremedhin, M.A. Lockwood, C.E. Ooms, T.J. Romack, D.X. West, Transition Met. Chem. 20 (1995) 228.
[181] V.I. Gerasimov, V.N. Byushkin, N.I. Belichuk, N.V. Belov, Krystallografiya (Russ.) (Crystallogr. Rep) 24 (1979) 60.
[182] P.B. Sonawane, A. Kumbhar, S. Padhye, R.J. Butcher, Transition. Met. Chem. 19 (1994) 277.
[183] M.B. Ferrari, G.G. Fava, G. Pelosi, P. Tarasconi, Polyhedron 19 (2000) 1895.
[184] R.P. John, A. Sreekanth, M.R.P. Kurup, S.M. Mobin, Polyhedron 21 (2002) 2515.
[185] M.B. Ferrari, C. Pelizzi, G. Pelosi, M.C. Rodriguez-Arguelles, Polyhedron 21 (2002) 2593.
[186] A. Murugkar, R. Bendre, A. Kumbhar, S. Padhye, R. Pritchard, C.A. McAuffle, Indian J. Chem. Sec. 38 (1999) 977.
[187] R. Acharya, S. Dutta, F. Basuli, S.-M. Peng, G.-H. Lee, L.R. Falvello, S. Bhattacharya, Inorg. Chem. 45 (2006) 1252.
[188] D.X. West, J.S. Ives, J. Krejci, M.M. Salberg, T.L. Zumbahlen, G.A. Bain, A.E. Liberta, J. Valdes-Martinez, S. Hernandez-Ortiz, R.A. Toscano, Polyhedron 14 (1995) 2189.
[189] P. Souza, P. Navarro, A.I. Matesanz, J.M. Moreno, J. Coord. Chem. 48 (1999) 79.
[190] A. Murugkar, R. Bendre, S. Padhye, T. Groy, Indian J. Chem. Sect A 38 (1999) 981.
[191] Z.-H. Liu, Y.-J. Liu, C.-Y. Duan, X.-Z. You, Acta Crystallogr. Sect C,: Cryst. Struct. Commun. 58 (1999) 1804.
[192] D.X. West, J.P. Scovill, J.V. Silverton, A. Bavoso, Transition Met. Chem. 11 (1986) 123.
[193] N.C. Kasuga, A. Ohashi, C. Koumo, J. Uesugi, M. Oda, K. Nomiya, Chem. Lett. (1997) 609.
[194] J.K. Swearingen, W. Kaminsky, D.X. West, Transition Met. Chem. 27 (2002) 724.
[195] J.K. Swearingen, D.X. West, Transition Met. Chem. 26 (2001) 252.
[196] D.X. West, G.A. Bain, R.J. Butcher, J.P. Jasinski, Y. Li, R.Y. Pozdniakiv, J. Valdes-Martinez, R.A. Toscano, S. Hernandez-Ortega, Polyhedron 15 (1996) 665.
[197] D.X. West, M.A. Lockwood, A.E. Liberta, X. Chin, R.D. Willett, Transition Met. Chem. 18 (1993) 221.
[198] L.E. Nikolaeva, T.N. Tarkhova, N.V. Belov, Kristallografiya (Russ.) (Crystallogr. Rep.) 19 (1974) 746.
[199] A. Berkessel, G. Hermann, O.-T. Rauch, M. Buchner, A. Jacobi, G. Huttner, Chem. Ber. 129 (1996) 1421.
[200] E. Gyepes, T. Glowiak, Proc. Conf. Coord. Chem. 11 (1987) 87.
[201] M. Soriano-Garcia, R.A. Toscano, J. Valdes-Martinez, J.M. Fernanadez, Acta Crystallogr., Sect. C: Cryst. Struct. Commun. 41 (1985) 498.
[202] J. Valdes-Martinez, S. Hernandez-Ortega, V.B. Jimenez, Acta Crystallogr. Sect. E: Struct. Rep. Online 58 (2002) m710.
[203] J. Valdes-Martinez, S. Hernandez-Ortega, V.B. Jimenez, Acta Crystall. Sect. E: Struct. Rep. Online 60 (2004) 42.
[204] V.M. Leovac, B. Ribar, G. Argay, A. Kalman, I. Brceski, J. Coord. Chem. 39 (1996) 11.
[205] N.T. Akinchan, U. Abram, Acta Crystallogr. Sect. C: Cryst. Struct. Commun. 56 (2000) 549.
[206] M.B. Ferrari, S. Capacchi, G. Reffo, G. Pelosi, P. Tarasconi, R. Albertini, S. Pinelli, P. Lunghi, J. Inorg. Biochem. 81 (2000) 89.
[207] E.M. Jouad, G. Larcher, M. Allain, A. Riou, G.M. Bouet, M.A. Khan, X.D. Thanh, J. Inorg. Biochem. 86 (2001) 565.
[208] R. Alonso, E. Bermejo, R. Carballo, A. Castineiras, T. Perez, Z. Natureforsch. B: Chem. Sci. 56 (2001) 219.
[209] R. Alonso, E. Bermejo, A. Castineiras, T. Perez, R. Carballo, Z. Anorg. Allg. Chem. 623 (1997) 818.
[210] V.G. Puranik, S.S. Tavale, T.N.G. Row, P. Umapathy, A.P. Budhkar, Acta Crystallogr., Sect. C: Cryst. Struct. Commun. 43 (1987) 2303.
[211] M.B. Ferrari, F. Bisceglie, G. Pelosi, M. Sassi, P. Tarasconi, M. Cornia, S. Capacchi, R. Albertini, S. Pinelli, J. Inorg. Biochem. 90 (2002) 113.
[212] L. Ze-Hua, D. Chun-ying, L. Ji-hui, L. Yong-jiang, M. Yu-Hua, Y. Xiao-Zeng, New J. Chem. 24 (2000) 1057.
[213] F. Chen-Jie, D. Chun-Ying, H. Cheng, H. Gang, M. Quing-jin, New J. Chem. 24 (2000) 697.
[214] Y. Harek, L. Larabi, L. Boukli, F. Kadri, N. Benali-Cherif, M. Mostafa, Transition Met. Chem. 30 (2005) 121.
[215] Z. Afrasiabi, E. Sinn, S. Padhye, S. Dutta, S. Padhye, C. Newton, C.E. Anson, A.K. Powell, J. Inorg. Biochem. 95 (2003) 306.
[216] G.R. Clark, G.J. Palenik, Cryst. Struct. Commun. 9 (1980) 449.
[217] N.C. Kasuga, K. Sekino, C. Kouma, N. Shimada, M. Ishikawa, K. Nomiya, J. Inorg. Biochem. 84 (2001) 55.
[218] M. Mathew, G.J. Palenik, J. Am. Chem. Soc. 91 (1969) 6310.
[219] L. Liu, W. Shi, X.-Y. Chen, Y.-L. Chen, P. Cheng, Synth. React. Inorg. Met.-Org. Nano Met. Chem. 36 (2006) 549.
[220] A.K. Barik, S. Paul, S.K. Kar, R.J. Butcher, J.C. Bryan, Polyhedron 18 (1999) 571.
[221] S.K. Chattopadhyay, D. Chattopadhyay, T. Banerjee, R. Kuroda, S. Ghosh, Polyhedron 16 (1997) 1925.
[222] D.K. Sau, N. Saha, R.J. Butcher, S. Chaudhuri, Transition Met. Chem. 29 (2004) 75.
[223] N.C. Saha, R.J. Butcher, S. Chaudhari, N. Saha, Polyhedron 24 (2005) 1015.
[224] Y. Qing, D.J. Hua, Z.L. Gang, Z.X. Qing, B.H. Dong, L. Hong, J. Mol. Struct. 794 (2006) 71.
[225] M. Zimmer, G. Schulte, X.-L. Luo, R.H. Crabtree, Angew. Chem., Int. Ed. 30 (1991) 193.
[226] M. Mathew, G.J. Palenik, G.R. Clark, Inorg. Chem. 12 (1973) 446.
[227] V.V. Pavlishchuk, S.V. Kolotilov, A.W. Addison, R.J. Butcher, E. Sinn, J. Chem. Soc. Dalton Trans. (2000) 335.
[228] N.A. Bailey, S.E. Hull, C.J. Jones, J.A. McCleverty, J. Chem. Soc., D (1970) 124.
[229] A.K. Nandi, S. Chaudhuri, S.K. Mazumdar, S. Ghosh, Inorg. Chim. Acta 92 (1984) 235.
[230] D.X. West, J.S. Ives, G.A. Bain, A.E. Liberta, J. Valdes Martinez, K.H. Ebert, S. Hernandez-Ortega, Polyhedron 16 (1997) 1895.
[231] A. Castineiras, E. Bermejo, D.X. West, A.K. El Sawaf, J.K. Swearingen, Polyhedron 17 (1998) 2751.
[232] L.J. Ackerman, P.E. Fanwick, M.A. Green, E. John, W.E. Running, J.K. Swearingen, J.W. Webb, D.X. West, Polyhedron 18 (1999) 2759.
[233] E. Bermejo, A. Castineiras, L.J. Ackerman, M.D. Owens, D.X. West, Z. Anorg. Allg. Chem. 627 (2001) 1966.
[234] W. Kaminsky, J.P. Jasinski, R. Woudenberg, K.I. Goldberg, D.X. West, J. Mol. Struct. 608 (2002) 135.
[235] A.P. Rebolledo, M. Vieites, D. Gambino, O.E. Piro, E.E. Castellano, C.L. Zani, E.M. Souza-Fagundes, L.R. Teixeira, A.A. Batista, H. Beraldo, J. Inorg. Biochem. 99 (2005) 698.
[236] J. Martinez, L.A. Adrio, J.M. Antelo, M. Teresa-Pereira, J.J. Fernandez, J.M. Vila, Polyhedron 25 (2006) 2848.
[237] C.G. Suresh, A. Deshpande, S.S. Tavale, P. Umapathy, J. Crystallogr. Spectrosc. Res. 21 (1991) 485.
[238] P.N. Yadav, M.A. Demertzis, D. Kovala-Demertzi, S. Skoulika, D.X. West, Inorg. Chim. Acta 30 (2003) 349.
[239] Z.-H. Liu, C.-Y. Duan, J. Hu, X.-Z. You, Inorg. Chem. 38 (1999) 1719.
[240] L. Papathanasis, M.A. Demertzis, P.N. Yadav, D. Kovala-Demertzi, C. Prentjas, A. Castineiras, S. Skoulika, D.X. West, Inorg. Chim. Acta. 357 (2004) 4113.
[241] J. Martinez, M.T. Pereira, I. Buceta, G. Alberdi, A. Amoedo, J.J. Fernanadez, M. Lopez-Torres, J.M. Vila, Organometallics 22 (2003) 5581.
[242] P. Souza, A.I. Matesanz, C. Pastor, Inorg. Chem. Comm. 5 (2002) 344.
[243] D. Kovala-Demertzi, N. Kourkoumelis, D.X. West, J. Valdes-Martinez, S. Hernandez-Ortega, Eur. J. Inorg. Chem. (1998) 861.
[244] P.N. Yadav, M.A. Demertzis, D. Kovala-Demertzi, A. Castineiras, D.X. West, Inorg. Chim. Acta 332 (2002) 204.
[245] F. Hueso-Urena, N.A. Illan-Cabeza, M.N. Moreno-Carretero, A.L. Penas-Chamorro, R. Faure, Inorg. Chem. Comm. 2 (1999) 323.
[246] A. Castineiras, E. Bermejo, D.X. West, L.J. Ackerman, J. Valdes-Martinez, S. Hernandz-Ortega, Polyhedron 18 (1999) 1463.
[247] A. Castineiras, M. Gil, E. Bermejo, D.X. West, Polyhedron 20 (2001) 449.
[248] T.S. Lobana, Rekha, A.P.S. Pannu, G. Hundal, R.J. Butcher, A. Castineiras, Polyhedron 26 (2007) 2621.
[249] R. Venkatraman, L. Sitole, M.R. Wilson, F.R. Fronczek, Acta. Cryst. E62 (2006) m2992.
[250] R.D. Pike, A.B. Wiles, T.A. Tronic, Acta. Cryst. E62 (2006) m347.
[251] L. Aslop, A.R. Cowley, J.R. Dilworth, Inorg. Chim. Acta. 358 (2005) 2770.
[252] C.-Y. Duan, X.-Z. You, T.C.W. Mak, Acta Crystallogr. Sect. C: Struct. Commun. 54 (1998) 31.
[253] S.-Y. Zhang, Y.-P. Tian, Y.-H. Zhang, F.-X. Xie, C.-Y. Duan, Chin. Chem. Lett. 9 (1998) 599.
[254] J. Garcia-Tojal, A. Garcia-Orad, J.L. Serra, J.L. Pizarro, L. Lezama, M.I. Arriortua, T. Rojo, J. Inorg. Biochem. 75 (1999) 45.
[255] E.M. Jouad, M. Allain, M.A. Khan, G.M. Bouet, Polyhedron 24 (2005) 327.
[256] G. Argay, A. Kalman, L. Parkanyi, V.M. Leovac, I.D. Broeski, P.N. Radivojsa, J. Coord. Chem. 51 (2000) 9.
[257] A. Sreekanth, M.R.P. Kurup, Polyhedron 22 (2003) 3321.
[258] D.X. West, I.S. Billeh, G.A. Bain, J. Valdes-Martinez, K.H. Ebert, S. Hernandez-Ortega, Transition Met. Chem. 21 (1996) 573.
[259] M.A. Ali, K.K. Dey, M. Nazimuddin, F.E. Smith, R.J. Butcher, J.P. Jasinski, J.M. Jasinski, Polyhedron 15 (1996) 3331.
[260] R.J. Butcher, D.X. West, Transition Met. Chem. 18 (1993) 449.
[261] D.X. West, H. Gebremedhin, R.J. Butcher, J.P. Jasinski, Transition Met. Chem. 20 (1995) 84.
[262] D.X. West, J.S. Ives, J. Krejci, M.M. Salberg, T.L. Zumbahlen, G.A. Bain, A.E. Liberta, J. Valdes-Martinez, S. Hernadez-Ortiz, R.A. Toscano, Polyhedron 14 (1995) 2189.
[263] D.X. West, H. Gebremedhin, R.J. Butcher, J.P. Jasinski, A.E. Liberta, Polyhedron 12 (1993) 2489.
[264] M. Joseph, M. Kuriakose, M.R.P. Kurup, E. Suresh, A. Kishore, S.G. Bhat, Polyhedron 25 (2006) 61.
[265] T.I. Malinovskii, V.K. Rotaru, E.W. Suntzov, G.A. Kiosse, A.V. Ablov, Eur. Cryst. Meet. (1973).
[266] M.B. Ferrari, F. Bisceglie, G. Pelosi, P. Tarasconi, A. Albertini, P.P. Dall'Aglio, S. Pinelli, A. Bergamo, G. Sava, J. Inorg. Biochem. 98 (2004) 301.
[267] V.Kh. Kratzov, V.N. Binshkin, M.D. Mazus, N.I. Belichuk, L.A. Nezhel'skaya, A.V. Ablov, T.I. Malinovskii, Coord. Chem. 4 (1978) 1747.
[268] F.A.El. Asmy, W. Kaminsky, D.X. West, Trans. Met. Chem. 28 (2003) 954.
[269] M.B. Ferrari, F. Bisceglie, G.G. Fava, G. Pelosi, P. Tarasconi, R. Albertini, S. Pinelli, J. Inorg. Biochem. 89 (2002) 36.
[270] P.J. Blower, T.C. Castle, A.R. Cowley, J.R. Dilworth, P.S. Donnelly, E. Labisbal, F.E. Sowrey, S.J. Teat, M.J. Went, J. Chem. Soc. Dalton Trans. (2003) 4416.
[271] G.W. Bushnell, A.Y.M. Tsang, Can. J. Chem. 57 (1979) 603.
[272] M.R. Taylor, J.P. Glusker, E.J. Gabe, J.A. Minkin, Bioinorg. Chem. 3 (1974) 189.

[273] A. Castineiras, E. Bermejo, D.X. West, A.K. Ej-Sawaf, J.K. Swearingen, Polyhedron 17 (1998) 2751.
[274] J.P. Jasinski, H.E. Exel, A. Castineiras, E. Bermejo, H. Beraldo, D.X. West, J. Chem. Cryst. 33 (2003) 11.
[275] E. Bermejo, A. Castineiras, M. Gil, E. Labisbal, A. Sousa, H. Beraldo, D.X. West, Z. Anorg. Allg. Chem. 627 (2001) 827.
[276] J.P. Jasinski, J.R. Bianchani, J. Cueva, F.A. El-Saied, A.A. El-Asmy, D.X. West, Z. Anorg. Allg. Chem. 629 (2003) 202.
[277] A.R. Cowley, J.R. Dilworth, P.S. Donnelly, E. Labisbal, A. Sousa, J. Am. Chem. Soc. 124 (2002) 5270.
[278] V.A. Neverov, V.N. Byushkin, Coord. Chem. 9 (1983) 1695.
[279] D.X. West, J.K. Swearingen, T.J. Romack, I.S. Billeh, J.P. Jasinski, Y. Li, R.J. Staples, J. Mol. Struct. 570 (2001) 129.
[280] J. Garcia-Tojal, J. Garcia-Jaca, R. Cortes, T. Rojo, M.K. Urtiage, M.I. Arriortua, Inorg. Chim. Acta. 249 (1996) 25.
[281] J. Garcia-Tojal, L. Lezama, J.L. Pizarro, M. Insausti, M.I. Arriortua, T. Rojo, Polyhedron 18 (1999) 3703.
[282] A.V. Ablov, V.K. Rotaru, G.A. Kiosse, T.I. Malinovskii, M.V. Shopron, N.V. Gerbeleu, Proc. Nat. Acad. Sci. USSR 208 (1973) 353.
[283] E. Bermejo, A. Catineiras, L.J. Ackerman, M.D. Owens, D.X. West, Z. Anorg. Allg. Chem. 627 (2001) 1966.
[284] M.A. Ali, N.E.H. Ibrahim, R.J. Butcher, J.P. Jasinski, J.M. Jasinski, J.C. Bryan, Polyhedron 17 (1998) 1803.
[285] M.A. Ali, A.H. Mirza, A.M.S. Hossain, M. Nazimuddin, Polyhedron 20 (2001) 1045.
[286] P. Gomez-Saiz, J. Garcia-Tojal, M. Maestro, J. Mahia, L. Lezama, T. Rojo, Eur. J. Inorg. Chem. (2003) 2123.
[287] E.W. Ainscough, E.N. Baker, A.M. Brodie, R.J. Cresswell, J.D. Ranford, J.M. Waters, Inorg. Chim. Acta 172 (1990) 185.
[288] A.D. Naik, P.A.N. Reddy, M. Nethaji, A.R. Chakravarty, Inorg. Chim. Acta 349 (2003) 149.
[289] P. Ambalavanan, K. Palani, M.N. Ponnuswany, Cryst. Res. Technol. 37 (2002) 1249.
[290] E.W. Ainscough, A.M. Brodie, J.D. Ranford, J.M. Waters, J. Chem. Soc. Dalton Trans. (1991) 1737.
[291] A.M. Thomas, A.D. Naik, M. Nethaji, A.R. Chakravarty, Inorg. Chim. Acta 357 (2004) 2315.
[292] E.W. Ainscough, A.M. Brodie, J.D. Ranford, J.M. Waters, J. Chem. Soc. Dalton Trans. (1991) 2125.
[293] D.X. West, Y. Yang, T.L. Klein, K.I. Goldberg, A.E. Liberta, J. Valdes-Martinez, R.A. Toscano, Polyhedron 14 (1995) 1681.
[294] P. Souza, A.I. Matesanz, F. Fernandez, J. Chem. Soc. Dalton Trans. (1996) 3011.
[295] A.G. Bingham, H. Bogge, A. Muller, E.W. Ainscough, A.M. Brodie, J. Chem. Soc. Dalton Trans. (1987) 493.
[296] M. del Carmen Aguirre, J. Borras, A. Castineiras, J.M. Garcia-Monteagudo, I. Garcia-Santos, J. Niclos, D.X. West, Eur. J. Inorg. Chem. (2006) 1231.
[297] C.F. Bell, C.R. Theocharis, Acta Crystallogr. Sect. C: Crystal. Struct. Commun. 43 (1987) 26.
[298] P. Gomez-Saiz, J. Garcia-Tojal, A. Mandia, B. Donnadieu, L. Lezama, J.L. Pizarro, M.I. Arriortua, T. Rojo, Eur. J. Inorg. Chem. (2003) 518.
[299] J. Garcia-Tojal, M.K. Urtiaga, R. Cortes, L. Lezama, M.I. Arriortua, T. Rojo, J. Chem. Soc. Dalton Trans. (1994) 2233.
[300] P. Gomez-Saiz, J. Garcia-Tojal, M.A. Maestro, F.J. Arnaiz, T. Rojo, Inorg. Chem. 41 (2002) 1345.
[301] L. Qin, W.-G. Xeng, Z. Yan, Y.-Z. Feng, Z. Chang, Z.-Z. Yuan, Acta Chim. Sci. 47 (1998) 1065.
[302] R.E. Marsh, Acta Crystallogr. Sect. B: Struct. Sci. 53 (1997) 317.
[303] C.-Y. Duan, X.-Z. You, T.C.W. Mak, Acta Crystallogr. Sect. C: Cryst. Struct. Commun. 54 (1998) 1397.
[304] S.V. Kolotilov, O. Cador, S. Golthen, O. Shvets, V.G. Ilyin, V.V. Pavlishchuk, Inorg. Chim. Acta 366 (2007) 1883.
[305] V. Philip, V. Suni, M.R.P. Kurup, M. Nethaji, Polyhedron 24 (2005) 1133.
[306] E.W. Ainscough, A.M. Brodie, J.D. Ranford, J.M. Waters, K.S. Murray, Inorg. Chim. Acta 197 (1992) 107.
[307] V. Philip, V. Suni, M.R.P. Kurup, M. Nethaji, Polyhedron 25 (2006) 1931.
[308] K.K. Aravindakshan, C.G.R. Nair, Ind. J. Chem. 20A (1981) 684.
[309] T.S. Lobana, G. Bhargava, V. Sharma, M. Kumar, Ind. J. Chem. 42A (2003) 309.
[310] T.S. Lobana, S. Khanna, R. Sharma, G. Hundal, R. Sultana, M. Chaudhary, R.J. Butcher, A. Castineiras, Cryst. Growth Des. 8 (2008) 1203.
[311] T.S. Lobana, S. Khanna, A. Castineiras, Inorg. Chem. Commun. 10 (2007) 1307.
[312] K. Onodera, N.C. Kasuga, T. Takashima, A. Hara, A. Amano, H. Murakami, K. Nomiya, J. Chem. Soc. Dalton Trans. (2007) 3646.
[313] J.E. Huheey, E.A. Keiter, R.L. Keiter, Inorganic Chemistry: Principals of structure and Reactivity, fourth ed., Harper Collins College, Publishers, New York, 1993, 292.
[314] I.G. Santos, A. Hagenbach, U. Abram, Dalton Trans. (2004) 677.
[315] A. Sreekanth, H.-K. Fun, M.R.P. Kurup, Inorg. Chem. Commun. 7 (2004) 1250.
[316] A. Castinieras, D.X. West, J. Mol. Struct. 604 (2002) 113.
[317] X. Li, X.-G. Cui, X.-G. Liu, X.-F. Li, Acta. Crystallogr. Sect. E: Struct. Rep. Online 60 (2004) m307.
[318] C.-J. Fang, C.-Y. Duan, C. He, G. Han, Q.-J. Meng, New J. Chem. 24 (2000) 697.
[319] H. Liang, B. Liu, R.-X. Hu, K.-B. Yu, J. Indian Chem. Soc. 77 (2000) 486.
[320] J.S. Casas, M.V. Castano, E.E. Castellano, J. Ellena, M.S. Garcia-Tasende, A. Gato, A. Sanchez, L.M. Sanjuan, J. Sordo, Inorg. Chem. 41 (2002) 1550.
[321] N.C. Kasuga, K. Sekino, M. Ishikawa, A. Honda, M. Yokoyama, S. Nakano, N. Shimada, C. Koumu, K. Nomiya, J. Inorg. Biochem. 96 (2003) 298.
[322] N.C. Kasuga, Y. Hara, C. Koumo, K. Sekino, N. Nomiya, Acta Crstallogr. Sect. C: Cryst. Struct. Commun. 55 (1999) 1264.
[323] M.B. Ferrari, G.G. Fava, C. Pelizzi, P. Tarasconi, J. Chem. Soc. Dalton Trans. (1992) 2153.
[324] E. Bermejo, A. Castinieras, R. Dominguez, R. Carballo, C. Maichle-Mossmer, J. Strahle, A.E. Liberta, D.X. West, Z. Anorg. Allg. Chem. 626 (2000) 878.
[325] E. Bermejo, R. Carballo, A. Castinieras, R. Domniguez, C. Maichle-Mossmer, J. Strahle, D.X. West, Polyhedron 18 (1999) 3695.
[326] D. Kovala-Demertzi, P.N. Yadav, J. Wiecek, S. Shoulika, T. Varadinova, M.A. Demertzis, J. Inorg. Biochem. 100 (2006) 1558.
[327] T. Bal-Demirci, Polyhedron 27 (2008) 440.
[328] M.C. Rodriguez-Arguelles, L.P. Battaglia, M.B. Ferrari, G.G. Fava, C. Pellizi, G. Pelosi, J. Chem. Soc. Dalton Trans. (1995) 2297.
[329] E. Labisbal, A. Sousa, A. Castineiras, A. Garcia-Vazquez, J. Romero, D.X. West, Polyhedron 19 (2000) 1255.
[330] X.G. Cui, Q.-P. Hu, Chin. J. Struct. Chem. 13 (1994) 340.
[331] L. Bresolin, R.A. Burrow, M. Horner, E. Bermejo, A. Castineiras, Polyhedron 16 (1997) 3947.
[332] E. Labisbal, A. Castineiras, C.A. Brown, D.X. West, Z. Naturforsch B: Chem. Sci. 56 (2001) 229.
[333] M.L. Duran, A. Sousa, J. Romero, A. Castineiras, E. Bermejo, D.X. West, Inorg. Chim. Acta 294 (1999) 79.
[334] G.F. de Sousa, D.X. West, C.A. Brown, J.K. Swearingen, V. Valdes-Martinez, R.A. Toscano, S. Hernandez-Ortega, M. Horner, A.J. Bortoluzzi, Polyhedron 19 (2000) 841.
[335] C.-J. Fang, C.-Y. Duan, C. He, Q.-J. Meng, Chem. Commun. (2000) 1187.
[336] A. Bino, N. Cohen, Inorg. Chim. Acta 210 (1993) 11.
[337] A. Castineiras, R. Carballo, T. Perez, Polyhedron 20 (2001) 441.
[338] Y.-P. Tian, C.-Y. Duan, C.-Y. Zhao, X.-Z. You, T.C.W. Mak, Z.-Y. Zhang, Inorg. Chem. 36 (1997) 1247.
[339] C.-Y. Duan, Y.-P. Tian, C.-Y. Zhao, X.-Z. You, T.C.W. Mak, Polyhedron 16 (1997) 2857.
[340] J.-L. Ma, J.-Y. Wu, Y.-P. Tian, C.-Y. Zhao, Chin. J. Struct. Chem. 19 (2000) 239.
[341] Y.-P. Tian, W.-T. Yu, M.-H. Jiang, S.S.S. Raj, P. Yang, H.-K. Fun, Acta Crystallogr. Sect. C: Struct. Commun. 55 (1999) 1639.
[342] E. Bermejo, A. Castineiras, R. Dominguez, R. Carballo, C. Maichle-Mossmer, J. Straehle, D.X. West, Z. Anorg. Allg. Chem. 625 (1999) 961.
[343] J.S. Casas, M.V. Castano, M.S. Garcia-Tasende, I. Martinez-Santamarta, J. Sordo, E.E. Castellano, J. Zukerman-Schpector, J. Chem. Res. 324 (1992) 2626.
[344] E. Labisbal, A. Sousa, A. Castineiras, J.A. Garcia-Vazquez, J. Romero, G.A. Bain, D.X. West, Z. Naturforsch B: Chem. Sci. 55 (2000) 162.
[345] S. Kotte, L. Stalzig, R. Wonnemann, B. Krebs, A. Stainer, Z. Anorg. Allg. Chem. 626 (2000) 1575.
[346] E. Lopez-Torres, M.A. Mendiola, J. Rodriguez-Procopio, M.T. Sevilla, E. Colacio, J.M. Moreno, I. Sobrados, Inorg. Chim. Acta 323 (2001) 130.
[347] M.A. Ali, A.H. Mirza, W.B. Ejau, P.V. Bernhardt, Polyhedron 25 (2006) 3337.
[348] J.S. Casas, E.E. Castellano, M.S. Garcia-Tasende, A. Sanchez, J. Sordo, J. Zukerman-Schpector, Z. Anorg. Allg. Chem. 825 (1997) 825.
[349] X.G. Cui, Q.-P. Hu, Chin. Chem. Lett. 5 (1994) 893.
[350] T.S. Lobana, Rekha, A. Castineiras, Inorg. Chem. Comm. 8 (2005) 1094.
[351] T.S. Lobana, A. Sanchez, J.S. Casas, M.S. Garcia-Tasende, J. Sordo, Inorg. Chim. Acta 267 (1998) 169.
[352] T.S. Lobana, A. Sanchez, J.S. Casas, A. Castineiras, J. Sordo, M.S. Garcia-Tasende, Polyhedron 17 (1998) 3701.
[353] Y. Kang, N. Yang, S.O. Kang, J. Ko, C.-H. Lee, Y.-H. Lee, Organometallics 16 (1997) 5522.
[354] R. Benn, B. Rufinsky, H. Lehmkhul, E. Janssen, C. Kruger, Angew. Chem., Int. Ed. Engl. 10 (1983) 779.
[355] Z. Jiang, L.V. Interrante, D. Kwon, F.S. Tham, R. Kullnig, Inorg. Chem. 03 (1991) 995.
[356] J.S. Casas, E.E. Castellano, M. Macias, M.C. Rodriguez-Arguelles, A. Sanchez, J. Sordo, J. Chem. Soc. Dalton Trans. (1993) 353.
[357] J.S. Casas, E.E. Castellano, M.S. Garcia-Tasende, A. Sanchez, J. Sordo, M.J. Vidarte, Polyhedron 17 (1998) 2249.
[358] S.W. Ng, V.K. Das, B.W. Skelton, A.H. White, J. Organomet. Chem. 377 (1989) 211.
[359] G.F. de Sousa, V.M. Deflon, E. Niquet, J. Mol. Struct. 667 (2004) 17.
[360] S.-G. Teoh, S.-H. Ang, H.-K. Fun, C.-W. Ong, J. Organomet. Chem. 580 (1999) 17.
[361] L. Labib, T.E. Khalil, M.F. Iskander, L.S. Refaat, Polyhedron 15 (1996) 349.
[362] J.S. Casas, A. Castineiras, M.C. Rodriguez-Arguelles, A. Sanchez, J. Sordo, A. Vazquez-Lopez, E.M. Vazquez-Lopez, J. Chem. Soc. Dalton Trans. (2000) 2267.
[363] G.F. de Sousa, R.H.P. Francisco, M.T. do, P. Gambardella, R.H. de, A. Santos, A. Abras, J. Braz. Chem. Soc. 12 (2001) 722.
[364] S.W. Ng, V.G.K. Das, B.S. Luo, T.C.W. Mak, Z. Kristallogr. 209 (1994) 961.
[365] J.S. Casas, A. Sanchez, J. Sordo, A. Vazquez-Lopez, E.E. Castellano, J. Zukerman-Schpector, M.C. Rodriguez-Arguelles, U. Russo, Inorg. Chim. Acta 216 (1994) 169.
[366] A.P. Rebolledo, G.M. de Lima, L.N. Gambi, N.L. Speziali, D.F. Maia, C.B. Pinheiro, J.D. Ardisson, M.E. Cortes, H. Beraldo, Appl. Organomet. Chem. 17 (2003) 945.
[367] A.P. Rebolledo, G.M. de Lima, N.L. Speziali, O.E. Piro, E.E. Castellano, J.D. Ardisson, H. Beraldo, J. Organomet. Chem. 691 (2006) 3919.
[368] G.F. de Sousa, L.C.C. Manso, E.S. Lang, C.C. Gatto, B. Mahieu, J. Mol. Struct. 826 (2007) 185.

[369] A. Perez-Rebolledo, J.D. Ayala, G.M. de Lima, N. Marchim, G. Bombieri, C.L. Zani, E.M. Souza-Fagundes, H. Beraldo, Eur. J. Med. Chem. 40 (2005) 467.
[370] R.S. Barbieri, H.O. Beraldo, C.A.L. Filgueiras, A. Abras, J.F. Nixon, P.B. Hitchock, Inorg. Chim. Acta 206 (1993) 169.
[371] R.H.P. Francisco, M.T.P. Gamberdella, G.F. de Sousa, J. Chem. Crystall. 34 (2004) 39.
[372] G.F. deSousa, L.S. Lang, L.C.C. Manso, V.M. Deflon, C.A.L. Filgueiras, E. Niquet, J. Mol. Struct. 753 (2005) 22.
[373] G.F. de Sousa, L.S. Lang, L.C.C. Manso, V.M. Deflon, C.A.L. Filgueiras, E. Niquet, J. Mol. Struct. 753 (2005) 22.
[374] M.R. Bermejo, R. Pedrido, M.I. Fernandez, A.M. Gonzalez-Noya, M. Maneiro, M.J. Rodriguez, M.J. Romero, M. Vazquez, Inorg. Chem. Commun. 7 (2004) 4.
[375] G.F. de Sousa, V.M. Deflon, E. Niquet, A. Abras, J. Braz. Chem. Soc. 12 (2001) 493.
[376] G.F. de Sousa, J. Valdes-Martinez, G.E. Perez, R.A. Toscano, A. Abras, C.A.L. Filgueiras, J. Braz. Chem. Soc. 13 (2002) 559.
[377] I.F. Burshtein, N.V. Gerbeleu, O.A. Bologa, A.Y. Kon, T.I. Malinovskii, Organomet. Chem. 3 (1990) 1162.
[378] A. Castineiras, R. Domniguez, L. Bresolin, J. Bordinhao, A.J. Bortoluzzi, M. Horner, Z. Natureforsch B: Chem. Sci. 56 (2001) 517.
[379] (a) U. Abram, E.S. Lang, E. Bonfada, Z. Anorg. Allg. Chem. 628 (2002) 1873;
(b) H. Beraldo, D. Gambino, Min. Rev. Med. Chem. 4 (2004) 31.
[380] D.W. McPherson, G. Umbricht, F.F. Knapp Jr., J. Lablled Compd. Radiopharm. 28 (2006) 877.
[381] P.J. Kostyniak, S.M. Nakeeb, E.M. Schopp, A.E. Maccubbin, E.K. John, M.A. Green, H.F. Kung, J. Appl. Toxicol. 10 (2006) 417.
[382] P. McQuade, K.E. Martin, T.C. Castle, M.T. Went, P.J. Blower, M.J. Welch, J.S. Lewis, Nucl. Med. Biol. 32 (2005) 147.
[383] R.K. Mahajan, T.P.S. Walia, Sumanjit, T.S. Lobana, Anal. Sci. 22 (2006) 389.
[384] K.J. Reddy, J.R. Kumar, C. Ramachandraiah, T. Thriveni, A.V. Reddy, Food. Chem. 101 (2007) 585.
[385] S.E. Ghazy, R.M. El-Shazly, M.S. El-Shahawi, G.A.A. Al-Hazmi, A.A. El-Asmy, J. Iranian Chem. Soc. 3 (2006) 140.
[386] (a) B.K. Reddy, J.R. Kumar, K.J. Reddy, L.S. Sarma, A.V. Reddy, Anal. Sci. 19 (2003) 423;
(b) B.K. Reddy, K.J. Reddy, J.R. Kumar, A.K. Kumar, A.V. Reddy, Anal. Sci. 20 (2004) 925.
[387] M.A. Aki, M.E. Khalifa, S.E. Ghazy, M.M. Hassanien, Anal. Sci. 18 (2002) 1235.
[388] M. Colilla, M.A. Mendiola, J.R. Procopio, M.T. Sevilla, Electroanalysis 17 (2005) 933.
[389] K.S. Abou-El-Sherbini, G.A.E. Mostafa, M.M. Hassanein, Anal. Sci. 19 (2003) 1269.
[390] A. Varghese, A.M.A. Khadar, Ind. J. Chem. Tech. 13 (2006) 470.
[391] L.S. Sarma, J.R. Kumar, C.J. Kumar, A.V. Reddy, Anal. Lett. 36 (2003) 605.
[392] A.V. Reddy, G.S. Reddy, Y.K. Reddy, J. Radioanal. Nucl. Chem. 103 (1986) 167.
[393] D.D.N. Singh, M.M. Singh, R.S. Chaudhary, C.V. Agarwal, J. App. Electrochem. 10 (1980) 587.
[394] S. Banerjee, S. Basu, Radiochim. Acta 91 (2003) 97.
[395] M. Ali AKL, A.A. El-Asmy, W.M. Yossef, Anal. Sci. 21 (2005) 1325.
[396] K.H. Reddy, K.G. Reddy, D.V. Reddy, Microchim. Acta 86 (1985) 319.
[397] F. Salinae, J. Carlos, J. Sanchez, T.G. Diaz, Anal. Chem. 58 (1986) 824.
[398] L.S. Sarma, J.R. Kumar, K.J. Reddy, A.K. Kumar, A.V. Reddy, Anal. Sci. 18 (2002) 1257.
[399] D. Perez-Bendito, F. Pino-Perez, Microchim. Acta 65 (1976) 613.
[400] M.T. Aguillar, J.M.C. Pavon, Microchim. Acta 68 (1977) 631.
[401] M.E. Vazquez-Diaz, J.C. Sanchez, M.C. Mochan, A.G. Perez, Analyst 119 (1994) 1571.
[402] S. Huszal, J. Kowalska, M. Krzeminska, J. Golimowski, Electroanalysis 17 (2004) 299.
[403] B. Asci, G. Alpdogan, S. Sungur, Anal. Lett. 39 (2006) 997.
[404] (a) R.K. Mahajan, I. Kaur, T.S. Lobana, Talanta 59 (2003) 101;
(b) R.K. Mahajan, R. Kaur, T.S. Lobana, Ind. J. Chem. 45A (2006) 639.
[405] R.K. Mahajan, T.P.S. Walia, Sumanjit, T.S. Lobana, Talanta 67 (2005) 755.